**Dissertation submitted to the
Combined Faculties for Natural Sciences and for Mathematics
of the Ruperto-Carola University of Heidelberg, Germany**

for the degree of Doctor of Natural Science

Presented by

Diplom-Biologist Verena Marx

Born in: Saarlouis

Oral-examination:

Molecular alterations of AMPA receptors and their effects on hippocampus dependent tasks

Referees: **Prof. Dr. P. H. Seeburg**
PD Dr. S. Urban

Hiermit erkläre ich, dass ich die vorliegende Dissertation selbst verfasst und mich dabei keiner anderen Mittel als der von mir ausdrücklich bezeichneten Quellen und Hilfen bedient habe. Des Weiteren erkläre ich, dass ich an keiner anderen Stelle ein Prüfungsverfahren beantragt oder die Dissertation in dieser oder einer anderen Form bereits anderweitig als Prüfungsarbeit verwendet oder einer anderen Fakultät als Dissertation vorgelegt habe.

Heidelberg, den 01.10.2006

Acknowledgements

Good help is hard to find, I am sincerely grateful to those who gave it when I needed it the most:

Peter H. Seeburg

David Bannerman

Nick Rawlins

Tansu Celikel

All the people I worked with during my time at MPI and at the Department for Experimental Psychology, University of Oxford.

The people in my student accommodation in Oxford I hang out with.

All my friends, who supported me during my time as PhD student. Especially, Iris Loew, Elfi Spieler, Wannan Tang, Sabrina Laudenklos, Thomas Löschmann, Holger Fritz, Peter Bell.

Annette Herold, Laura Hasenkamp and Uschi Bergmann who provided help in different ways.

My family, alive or deceased, for providing emotional security and financial support.

Summary

I investigated the role of C-terminal domain modifications in GluR-A mediated behavioral function using several hippocampus dependent behavioral tasks, ranging from neophobia to spatial reference memory, in a variety of genetically modified mice. Studies using GluR-A knock-out (GluR-A$^{-/-}$) mice showed that GluR-A containing AMPA receptors are required for working memory, strengthened by those findings that expression of a transgenic GluR-A subunit in the forebrain of GluR-A$^{-/-}$ mice partially rescues this memory deficit. In a spatial reference memory task GluR-A$^{-/-}$ mice learn as good as wild types. These results suggest that the GluR-A subunit is differentially involved in memory formations, and its lack in the dorsal hippocampus alters the mnemonic ability of the animals. Understanding the mechanisms by which GluR-A contributes to encoding sensory information in time, requires targeted alteration of the C-terminal domain of the GluR-A subunit. With the help of genetically engineered mice I studied three positions within the C-terminal domain, where phosphorylation of the subunit and interaction with the PDZ binding proteins take place. These lines expressed either an altered or a wild type transgenic GluR-A subunit in GluR-A$^{-/-}$ mice. In SA mice, the transgenetically expressed GluR-A had substitutions of serine against alanine at the phosphorylation sites S831 and S845. TG mice carried a transgene for a GluR-A subunit where the last C-terminal amino acid was deleted, which resulted in interruption of the PDZ interaction domain with the post-synaptic density proteins. The third line expressed transgenically the wild type GluR-A subunit and served as a control line. After determining the contribution of different parts of the C-terminal domain to GluR-A dependent function, I studied the mice lacking GluR-B (GluR-B$^{\Delta Fb}$) or both subunits (GluR-A$^{-/-}$/B$^{\Delta Fb}$) in hippocampal tasks. In contrast to the GluR-A deletion the GluR-B deletion was aimed to be restricted to the forebrain. GluR-A$^{-/-}$/B$^{\Delta Fb}$ mice were used to study synergistic effects of GluR-A and GluR-B deletion in the hippocampal dependent tasks. In a last group of experiments, I questioned the specificity of the hippocampal phenotypes to the AMPA receptor function using mice engineered to express Homer1a constitutively in the neocortex. The results of the studies presented in this thesis showed that hippocampal contributions to the expression of the emotional responses, emotional and motor learning as well as spatial working and reference memory are modulated by glutamatergic neurotransmission and molecular modifications of the GluR-A subunit. These findings help to identify the molecules and processes by which the hippocampus administrates its functions.

Zusammenfassung

In dieser Doktorarbeit untersuchte ich, welche Rolle die c-terminalen Modifikationen in den GluR-A-vermittelten Funktionen spielen, indem ich einer Reihe genetisch veränderter Mäuse mehrere hippokampusabhängige verhaltensbezogene Aufgaben stellte, die von Neuphobie bis zum räumlichen Referenzgedächtnis reichten. Die Annahme, dass GluR-A-haltige AMPA-Rezeptoren für das Arbeitsgedächtnis benötigt werden, haben Studien an Mäusen mit einem GluR-A-Knock-out (GluR-A$^{-/-}$) gezeigt. Dies wurde weiterhin dadurch bestärkt, dass die Expression einer transgenen GluR-A-Untereinheit im Vorderhirn von GluR-A$^{-/-}$ Mäusen das Gedächtnisdefizit teilweise wieder aufheben kann. In einer Aufgabenstellung für das räumliche Referenzgedächtnis lernen GluR-A$^{-/-}$-Mäuse genauso gut wie ihre Wildtypgegenstücke. Diese Ergebnisse zeigen an, dass die GluR-A-Untereinheit in unterschiedlicher Weise an der Gedächtnisbildung beteiligt ist und dass ihr Fehlen im dorsalen Hippokampus die mnemonischen Fähigkeiten des Tieres verändert. Um die Mechanismen zu verstehen, durch welche die GluR-A-Untereinheit zur Verschlüsselung der sensorischen Information über die Zeit beiträgt, benötigt man gezielte Veränderungen der c-terminalen Domäne dieser Untereinheit. Mit Hilfe genetisch veränderter Mäuse habe ich drei der Orte der c-terminalen Domäne untersucht, an denen Phosphorylierung und Wechselwirkung mit den PDZ-bindenden Proteinen stattfinden. Diese Linien exprimierten entweder eine veränderte oder eine Wildtyp-GluR-A-Untereinheit in GluR-A$^{-/-}$-Mäusen. In SA-Mäusen wurde am transgen exprimierten GluR-A die Aminosäure Serin gegen Alanin an den Phosphorylierungsstellen S831 und S845 ausgetauscht. TG-Mäuse trugen ein Transgen für eine GluR-A-Untereinheit, an der die letzte Aminosäure des C-Terminus (Leucin) entfernt wurde, woraus eine Veränderung der PDZ-Domäne und damit eine Unterbrechung der Wechselwirkung der Untereinheit mit den Proteinen der „post-synaptic density" resultierte. Die dritte Linie exprimierte transgen die Wildtyp-GluR-A-Untereinheit und wurde als Kontrolllinie verwendet. Nachdem ich den Beitrag unterschiedlicher Teile der c-terminalen Domäne zu von GluR-A abhängigen Funktionen untersucht hatte, testete ich Mäuse, denen entweder GluR-A oder GluR-B (GluR-B$^{\Delta Fb}$) oder beide Untereinheiten (GluR-A$^{-/-}$/B$^{\Delta Fb}$) fehlten, durch Aufgabenstellungen, die den Einsatz des Hippokampus erfordern. Im Gegensatz zur GluR-A-Deletion war die Entfernung von GluR-B so angelegt, dass sie nur im Vorderhirn stattfand. GluR-A$^{-/-}$/B$^{\Delta Fb}$-Mäuse entstanden durch Kreuzung der zuvor erwähnten Linien, um die synergetischen Auswirkungen der Deletion beider Untereinheiten auf

hippokampusabhängige Aufgabenstellungen zu untersuchen. In der letzten experimentellen Reihe nutzte ich Mäuse, die kontinuierlich Homer1a im Neokortex exprimierten, um zu hinterfragen, wie spezifisch die Funktionen der AMPA-Rezeptoren für diesen hippocampalen Phänotyp sind. Die Ergebnisse dieser Studien, die hier in dieser Doktorarbeit präsentiert werden, zeigten, dass der Beitrag des Hippokampus zum Ausdruck von Emotionen, zum emotionalen und motorischen Lernen genauso wie zur Funktion des Arbeitsgedächtnisses und des Referenzgedächtnisses durch glutamataktivierte neuronale Übertragung und molekulare Veränderungen der GluR-A-Untereinheit gesteuert wird. Diese Erkenntnisse helfen bei der Identifizierung der Moleküle und Prozesse, derer sich der Hippokampus bedient, um seine Funktionen auszuüben.

Table of contents **Page**

List of figures and tables   **Page**

1. Preface

Patient EC approached her kids thinking "when did you grow this fast" one day in 1992. Doctors found out that not remembering her children's recent years was only one of the symptoms of her extensive retrograde memory loss. She did not remember that she is bilingual and speaks Spanish, did not recall her birthplace, her education and had no knowledge of her husband before the onset of the memory problems. Neither did she have any recollection of what happened when during the last two years, between the time that she witnessed a physical abuse of her sister-in-law and the morning she spontaneously started to suffer from partial memory loss (Case#7, Kritchevsky et al, 2004).

Patient EC suffered from retrograde functional amnesia, also known as "hysterical amnesia" or "psychogenic amnesia", a condition that is often caused by depression, anxiety, post-traumatic stress or other emotionally challenging situations. Although these cases are uncommon, they suggest that systems for emotions and memories are linked. Studies suggest that medial temporal lobe and most importantly, the hippocampus is the structure where this interaction occurs. Understanding the cellular and molecular mechanisms of hippocampal function will therefore be instrumental in helping Patient EC to enjoy the memories of kids growing older.

2. Introduction

2.1. The hippocampus

The hippocampus, a part of the limbic system, is located in the temporal lobe of the human brain. Since the 16th century anatomist Aranzi named the structure. Until the famous patient HM, this organ was believed to take a role in encoding smell, although early in 1900s the Russian scientist Bekhterev suggested hippocampus as a structure, taking role in memory formation.

Today, it is widely accepted that the hippocampus has an essential role in the formation of new memories about experienced events, also called episodic memory. Together with the other structures in the medial temporal memory system, it is also responsible for acquisition of memories explicitly verbalized (declarative memory). Damage in hippocampus results in deficit in forming new memories (anterograde amnesia) and alters the recollection of previously learned information (retrograde amnesia) as in the case of patient EC. The Hippocampus, however, is not the sole memory system responsible for learning. After hippocampal lesions people can still learn how to play an instrument, suggesting that memory systems encoding procedural learning are independent from this structure (for further details on the roles of hippocampus, see below).

The hippocampus of rats and mice has attracted attention as a model to understand the mechanisms of hippocampal function in behavior. The rodent hippocampal formation consists of dentate gyrus including hilus, CA1-CA3 fields and subiculum. The CA1 and CA3 fields are considered hippocampus proper (Figure 1).
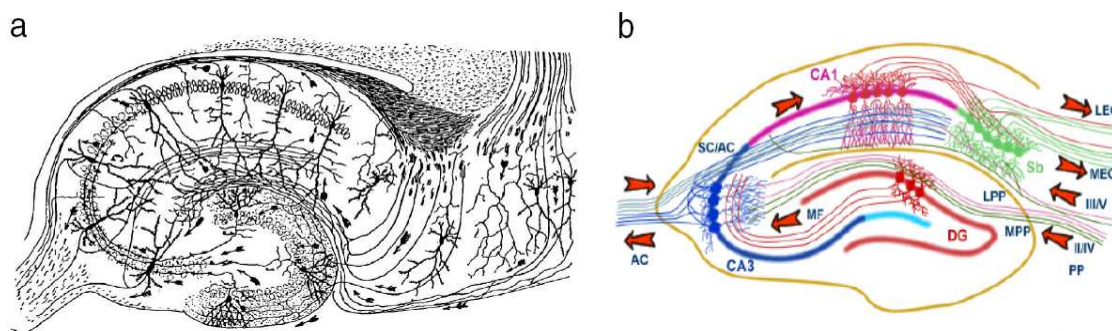
Figure 1. Anatomy of and connectivity within hippocampus. (a) Cellular anatomy and projections of hippocampus as originally depicted by Santiago Ramon y Cajal (1911). (b) Input-output relationship of the hippocampal cells (see text for the details). Legends; EC=entorhinal cortex, LEC=lateral entorhinal cortex, MEC=medial entorhinal cortex, II-V= layers of entorhinal cortex, DG=dentate gyrus, Sb=subiculum, SC=Schaffer collaterals, AC=association commissural pathway, PP=Perforant pathway, LPP=Lateral perforant pathway, MPP=Medial perforant pathway, MF=Mossy fibers. Adapted from www.bris.ac.uk/Depts/Synaptic/info/pathway/figs/hippocampus.gif

The connections into and within hippocampus are unidirectional and create a closed-loop network which originates mainly in the entorhinal cortex. The information flow into the hippocampus is maintained by predominantly perforant path. Within the hippocampus, however, the information flows through mossy fiber and Schaffer collateral pathways (Amaral and Witter, 1989).

Perforant path (PP) starts principally in the entorhinal cortical layers of II/III and to a lesser extent from layers IV/V. Not all of these projections target the same structures within the hippocampus (Figure 1). Axons from layers II/IV, for example, project to the dentate gyrus (DG) granule cells and pyramidal cells of the CA3 region (Dolorfo and Amaral, 1998a). Axons originated at the layers III/V target the CA1 pyramidal cells and the subiculum. The perforant path is further segregated into lateral (LPP) and medial pathways (MPP), according to the origin of the fibers. Lateral entorhinal cortex (LEC) axons constitute the LPP and medial entorhinal cortex (MEC) axons the MPP (Figure 1).

Mossy fiber (MF) path includes the axons of granule cells in the DG targeting pyramidal cells in the CA3 region. MF projections establish strong and reliable synapses with the excitatory neurons of the CA3 and are the main input to these cells.

The other within hippocampus projection is the Schaffer Collateral/Associational Commissural Pathway. This path includes axons of CA3 cells within the ipsilateral (Schaffer collateral) or contralateral (commissural fibers or associational commissural path) hippocampus region projecting onto the cells of the CA1. These axons constitute the principal input of the CA1 pyramidal cells. Once the information reaches to CA1 and processed herein, the output from hippocampus is carried via subiculum (Sb) into the EC with topographical projections both at the CA1 to Sb and Sb to EC into the lateral and medial entorhinal cortex (Dolorfo and Amaral, 1998b).

2.1.1. Roles of hippocampus

As mentioned before, hippocampus is most frequently associated with the acquisition of new memories especially in the episodic and semantic memory domains. However attractive the role of hippocampus in memory formation is, lesion and pharmacological inactivation studies suggest that this structure has also non-mnemonic functions.

One of the early examples of such a function of hippocampus is its role in establishing a cognitive map of the environment around us (O'Keefe and Nadel, 1978). Original studies in rats have shown that both excitatory and inhibitory neurons in the hippocampus have spatial firing fields, so called place cells. These cells fire action potentials only when the animal is

within a spatial location and their activity might depend on direction of travel and the head position in space. Considering that different cells have mostly non-overlapping place fields, by looking at the firing of the place cells alone the brain might be able to encode the space. This spatial component of the hippocampal neuronal activity not only nominated hippocampus as a structure creating the neural representation of the layout of the environment (the cognitive map) but also suggested that it might contribute to path finding during exploration and navigation of the space around us. This function is furthermore supported by the fact that the brain needs to integrate sensory information across space and time in order to create a representation of location within a particular space throughout time. Hippocampus, indeed, seems to be an ideal location for such an association. First of all it receives highly processed sensory information from sensory modalities allowing it to process multi modal information. Moreover with the spatially restricted firing (place) fields and hippocampal contribution to acquisition of episodic information it might allow integration of incoming sensory stimuli in a spatiotemporally organized manner. Once the sensory information is encoded and its neural representation is established, the brain needs to regulate the behavior of the organism according to this incoming information. Hippocampus is thought to have a role also in this aspect of animal behavior, suggested by studies, which show that hippocampal lesions result in behavioral disinhibition, reduced anxiety and an inability to express "fear" response upon conditioned sensory stimuli (reviewed in Bannerman et al, 2004).

2.1.2. Functional differentiation of hippocampus

Many roles of hippocampus in animal behavior and differential input/output relationships of hippocampal neurons raise the possibility that hippocampus might not be a functionally homogeneous structure.

Hippocampus is elongated in the dorso-ventral axis. The dorsal part receives most of its inputs from sensory areas via association cortex-perirhinal cortex-entorhinal cortex path (Burwell and Amaral, 1998a-b, Dolorfo and Amaral, 1998a-b). Ventral part, however, has reciprocal connections with the medial and lateral amygdala, bed nucleus stria terminalis and other hypothalamic-pituitary-adrenal axis structures as well as the prefrontal cortex (Van Groen and Wyss, 1990; Petrovich et al, 2001). Lesion studies targeting selectively dorsal and ventral parts of the hippocampus showed that indeed these subsections have different roles. Animals with dorsal hippocampus lesions for example are unable to learn spatial working memory as well as spatial reference memory tasks, although the animals with ventral

hippocampus lesions are virtually unimpaired in these tasks (Moser et al, 1993 and 1998). After ventral hippocampal lesions, however, animals display reduced anxiety and in tasks which require sensory information to be associated with a conditioned freezing response, they fail to acquire and/or express the associations (McNish et al, 1997; Good and Honey, 1997; Richmond et al, 1999). These results argue that functions of the hippocampus are distributed in the dorsoventral axis. While the dorsal half has a role in spatial learning and memory, the ventral half contributes to induction of anxiety related behaviors.

2.2. Glutamate receptors

L-Glutamate, or glutamate in short, is the major excitatory neurotransmitter in the mammalian brain and activates ligand gated ion channels (Ionotropic glutamate receptors) as well as G-protein coupled (metabotropic) glutamate receptors (Figure 2).
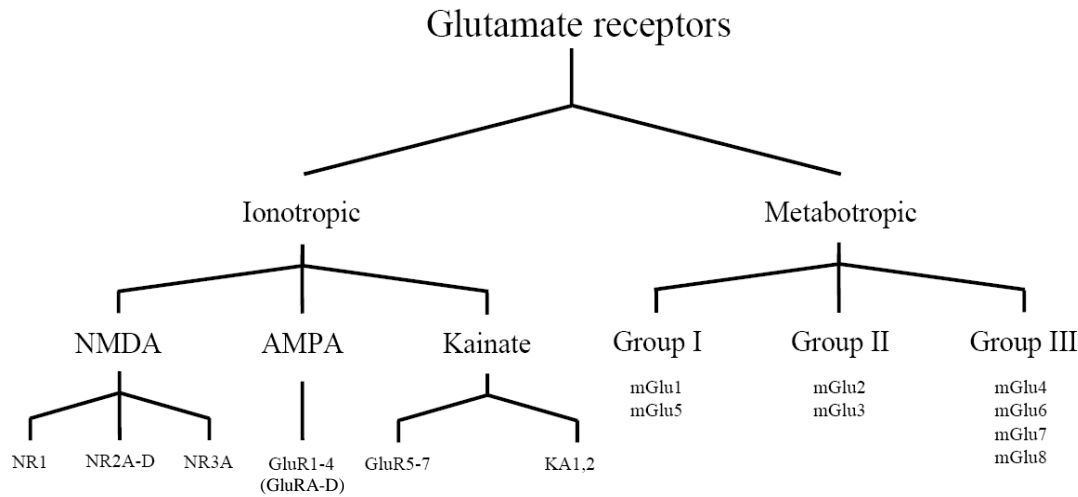
Figure 2. Classification of the glutamate receptors and receptor subunit composition.

The principal function of glutamate receptors is thought to be regulating intracellular ionic, predominantly Ca^{2+}, concentration and in turn modulate neural excitability, genomic expression and plasticity. These functions of the glutamate at the postsynaptic neuron are achieved with two distinct families (ionotropic and metabotropic) of receptors activated sequentially upon glutamate release from the excitatory presynaptic neuron. Upon release, the neurotransmitter mediated activation is first observed in ionotropic glutamate channels and results in "activation" of the neuron before slowly acting metabotropic glutamate receptors initiate their action on modulating neurotransmitter release and plasticity (see below).

2.2.1. Classification, structure and distribution of ionotropic glutamate receptors

Ionotropic glutamate receptors are widely distributed in the mammalian central nervous system and mediate the principal fast synaptic transmission in the brain. Upon glutamate binding, these receptors alter their conformations allowing ion influx into the postsynaptic cell (see for example Figure 3). Such activation results in rapid depolarization of the postsynaptic cell membrane by an exchange of primarily Ca^{2+}, Na^+ and K^+ between the extra cellular and intracellular space.
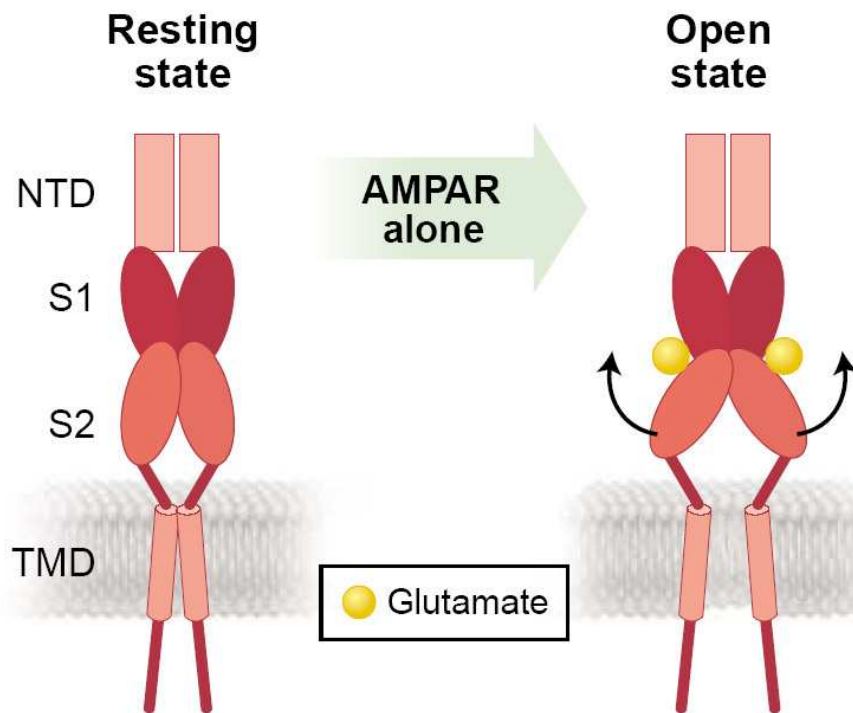
Figure 3. A schematic representation of AMPA receptor mediated ion influx into the postsynaptic neuron. AMPA receptors are tetramers and consist of four domains. Ligand binding pockets (S1-S2) link the N-terminal domain (NTD) to the transmembrane domains (TMD), which is tailed by an intracellular carboxyl-terminal domain that carries phosphorylation sites. During the resting state glutamate is not bound to the S1-S2 domains and the transmembrane subdomains are physically close to each other, creating an impearmeable ion channel. Upon glutamate release from the presynaptic neuron, S1-S2 domains' high affinity binding sites bind glutamate and close onto the S1 domain. During this transformation, TMD subdomains are moved apart and ion influx into the postsynaptic cell is initiated. Modified from Nicoll et al, 2006.

Not each receptor has high affinity to all of the ions. For example, while NMDA receptors have high affinity to Ca^{2+} and lower affinity to Na^+ and K^+, AMPA and kainate receptors have higher affinity for Na^+ then Ca^{2+}. Inactivation of the ionotropic glutamate receptors is achieved either in the presence of previously bound glutamate through receptor desensitization or after glutamate unbound (deactivation).

Ionotropic glutamate receptors are classified into three subtypes according to the ligand that they bind. For example, N-methyl-D-aspartate (NMDA) receptors require both glutamate and glycine for activation. Alternatively, these receptors can also bind NMDA for transformation into the open channel configuration. Non-NMDA channels of the ionotropic glutamate receptors include 2-amino-3-(3-hydroxy-5-methylisoxazol-4-yl) propionic acid (AMPA) and kainate activated channels.

Independent from the subtype specification of the ionotropic glutamate receptors, they are encoded by six or more gene families defined by sequence homology. A single gene

family encodes the four subunits of the AMPA receptors, although two and three gene families encode kainate and NMDA receptors, respectively. All ionotropic receptors are multimeric structures that are composed of homomeric or heteromeric assembly of multiple subunits (Figure 2). Although the distribution and density of the ionotropic glutamate receptors (iGluRs) and their subtypes change significantly across neural structures, the subunit stoichiometry of these receptors is constant. AMPA receptors, for example, are tetrameric structures organized from GluR A-D (GluR 1-4) subunits. NMDA receptors, on the other hand, display an enriched subunit variation including NR1, NR2A-D, and NR3A in the form of a pentameric or tetrameric structure, which is composed of two or three NR1 and two NR2 subunits. Kainate receptors, like AMPA receptors are tetrameric structures, made of five subunits: GluR 5-7 and KA 1-2. During development, some of the receptors might share subunits, as in δ1 inclusion in AMPA and kainate receptors, but only to exchange these receptors later in development.

The rich subunit variability together with alternative splicing of subunits results in a large variability of glutamate receptors in the peripheral (Table 1) and central nervous system (Table 2) (reviewed in Wisden et al, 2000).

Spinal Cord	*Retina*
Motor Neuron	Retinal OFF-bipolar cell
	GluR-A
GluR-B$_{i,o}$	GluR-B
GluR-C$_{i,o}$	
GluR-D$_i$	
KA1	
	KA2
	GluR5
	GluR6
	GluR7
δ1 (low)	
NR1	NR1
NR2A	
NR2B (low)	
	NR2C
NR2D (low)	
NR3A(low)	

Table 1. Expression of glutamate receptor subunits in the peripheral nervous system. i and o are the flip and flop splice forms of AMPA receptors, respectively. Modified from Wisden et al (2000).

For example, GluR-A mRNAs are most abundant in hippocampus, amygdala and cerebellar Bergmann glia while GluR-B mRNA is universally expressed throughout the brain with strong expression in cerebellar granule cells, neocortex and the hippocampus. GluR-C expression is highest in the neocortex and hippocampus although as in the GluR-A and GluR-B subunits there is minimal or no expression in the thalamic areas. The only AMPA subunit expressed strongly in the thalamic region is the GluR-D whose mRNA is also strongly expressed in the cerebellum. All AMPA subunits, however, are prominently expressed in the olfactory bulb and medial habenula (Boulter et al, 1990; Keinanen et al, 1990).

Hippocampus			*Cerebellum*			*Caudate putamen*	
Dentate granule	CA1 pyramidal	CA3 pyramidal	Purkinje cell	Granule cell	Bergmann glia	Medium spiny neuron	Cholinergic interneuron
$\text{GluR-A}_{i,o}$ ↓	GluR-A_o GluR-A_i ↓	GluR-A_i GluR-A_o	GluR-A_o		GluR-A_i	$\text{GluR-A}_{i,o}$	GluR-A
$\text{GluR-B}_{i,o}$	GluR-B_o GluR-B_i ↓	GluR-B_i GluR-B_o ↓	$\text{GluR-B}_{i,o}$	GluR-B_i		$\text{GluR-B}_{i,o}$	
$\text{GluR-C}_{i,o}$	$\text{GluR-C}_{i,o}$	GluR-C_i	GluR-C_i			GluR-C_i ↓	
GluR-D_o	GluR-D_o			GluR-D_o	GluR-D_i	GluR-D_o ↓	GluR-D
KA1		KA1	KA1	KA2		KA2	KA2
KA2	KA2	KA2	GluR5				
GluR6	GluR6	GluR6		GluR6		GluR6	GluR6
GluR7						GluR7	
δ1 ↓	δ1 ↓	δ1 ↓	δ2				
NR1	NR1	NR1	NR1	NR1	NR1	NR1	NR1
NR2A	NR2A	NR2A		NR2A		NR2A	
NR2B	NR2B	NR2B			NR2B	NR2B	NR2B
				NR2C			
NR2D ↓							NR2D
	NR3A ↓						

Table 2. Expression of glutamate receptor subunits in the central nervous system. i and o are the flip and flop splice forms of AMPA receptors, respectively. Modified from Wisden et al (2000). Downward arrow signifies lower level of expression.

Kainate receptor subunit expression, after development, is characterized by high level of KA1 in hippocampal CA3 pyramidal and dentate granule cells (Werner et al, 1991) and lower expression in glia cells, corpus callosum and cerebellar white matter (Wisden and Seeburg, 1993) as well as a ubiquitous expression of KA2 throughout the brain (Herb et al, 1992). GluR5 mRNA, however, is widely expressed in Purkinje cells, the cingulate cortex,

piriform cortex and in a numerous subcortical areas including septal, thalamic, amygdaloid and hypothalamic nuclei (Bettler et al, 1990; Wisden and Seeburg, 1993; Bahn et al, 1994). GluR6 expression is high in cerebellar granule cells and only moderate in hippocampus and caudate putamen (Bettler et al, 1990; Wisden and Seeburg, 1993; Bahn et al, 1994). GluR7 gene expression is predominantly restricted to the cerebellar stellate/basket cells, deep layers of the cerebral cortex and reticular thalamic nuclei populated by inhibitory neurons (Bettler et al, 1992; Lomeli et al, 1992; Wisden and Seeburg, 1993; Bahn et al, 1994).

NMDA receptor distribution is characterized by a brain wide expression of NR1 mRNA, which is peaked in the hippocampus, olfactory bulbs, cerebral and cerebellar cortices (Monyer et al, 1992, 1994). NR1 and NR2A heteromers are the most commonly found NMDA receptors and these heteromers are particularly expressed at high levels in areas NR2A mRNA is abundant. These areas include, hippocampus, neocortex, olfactory bulb and cerebellar granule cells but not subcortical areas (Monyer et al, 1994; Nase et al, 1999). NR2B mRNA expression, on the other hand, is modulated during development. Early in postnatal development, expression in the entire brain is up-regulated (Monyer et al, 1994) only to be down regulated later in the adulthood. In the adult animals, NR2B is mainly restricted in hippocampus, olfactory bulb and to a lesser extent in striatum and thalamic areas (Monyer et al, 1992, 1994). NR2C is weakly expressed in the cerebrum, although it's widely expressed cerebellum (Standaert et al, 1996, 1999). NR2D, a subunit specific for inhibitory neurons, is expressed, albeit weakly, in subcortical areas including globus pallidus, thalamus and brain stem (Monyer et al, 1994; Standaert et al, 1996, 1999)

2.2.2. Classification, structure and distribution of metabotropic glutamate receptors

Presynaptically released glutamate binds onto not only ionotropic glutamate receptors but also G-protein coupled, slowly acting metabotropic glutamate receptors (mGluR). This family of receptors consists of eight single polypeptide chain with 7 transmembrane domain motif, an extracellular N-terminus and intracellular C-terminus where these receptors are linked to numerous synaptic and cytosolic targets including but not limited to NMDA receptors and smooth endoplasmic reticulum through SHANK-GKAP-PSD95 and Homer1, respectively.

mGluRs are subdivided into three groups based on sequence similarity, pharmacology and intracellular signalling mechanisms (Figure 2). Group I mGluR receptors are coupled to phospholipase C (PLC) and intracellular calcium signaling while group II and group III receptors inhibit adenylyl cyclase cascades.

Different from iGluRs, mGluRs are located both in presynaptic and postsynaptic neurons and widely expressed throughout the brain (Figure 4).
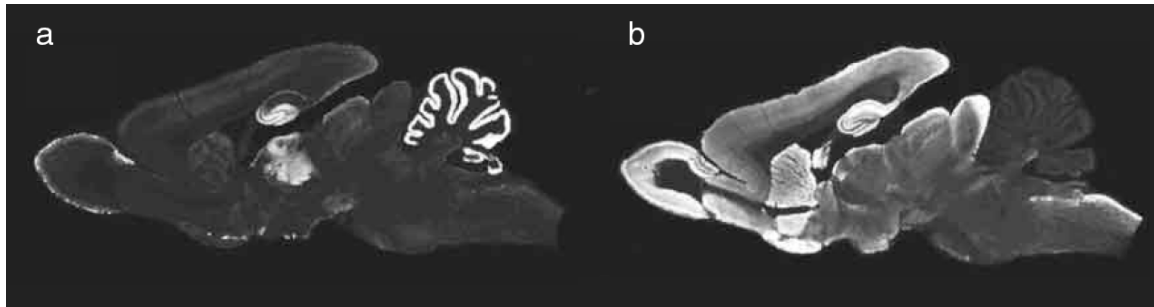
Figure 4. mGluRs are widely distributed in the brain. An example of mGluR distribution from the Group I receptors (a, mGluR1 and b, mGluR5). Further details are in the text. Modified from Shigemoto and Mizuno, 2000.

The individual subtypes of mGluRs are differentially distributed in the brain although certain subtypes have overlapping expression. Studies using *in situ* hybridization (Pin et al, 1992, Shigemoto et al, 1992) and immunocytochemistry (Martin et al, 1992) have shown that mGlu-Group I receptors are widely expressed in the brain. mGluR1, one of the two receptors in this group of mGluR, is expressed (albeit to a smaller extent compared to mGluR5) particularly in hippocampus excluding CA1 cells but including dentate gyrus granule cells, CA4 cells, CA2–CA3 pyramidal cells, cerebellar Purkinje cells, thalamic nuclei as well as at the surface of the olfactory bulb by mitral and tufted cells and lateral septum. This receptor is exclusively expressed in neurons and localized postsynaptically (Martin et al, 1992). Expression of mGluR5, the higher expressing mGlu-Group I receptors, is prominent in the cerebral cortex and in the entire hippocampus with a particularly strong expression in CA1 pyramidal cells (Figure 4). Additionally lateral septum, internal granule layer of the olfactory bulb, anterior olfactory nucleus, striatum, and nucleus accumbens display high degree of mGluR5 distribution (Abe et al, 1992).

Among the adenylate-cyclase-inhibiting receptors, the distribution of mGluR2 is more restricted than that of the Group I mGluRs. *In situ* hybridization studies showed the most prominent expression in of mGluR2 is restricted to Golgi cells of the cerebellum, mitral cells of the accessory olfactory bulbs, and pyramidal neurons of the entorhinal cortex and parasubicular cortex, as well as to the dentate gyrus of hippocampus (Ohishi et al, 1993). It has been suggested that mGluR2 may serve as a presynaptic receptor in the cortico-striatal glutamate projection (Ohishi et al, 1993). The other member of the Group II mGluRs is the mGluR3 and it is more widely distributed compared to mGluR2. Its mRNA is prominently

expressed in neurons of the cerebral cortex, dentate gyrus as well as in a number of subcortical areas including thalamic reticular nucleus, caudate putamen and supraoptic nucleus (Tanabe et al, 1993). Different from the mGluR2, these receptors are not neuron specific, also found in glia cells (Tanabe et al, 1993).

The final subgroup of mGluRs (Group III) is characterized by presynaptic localization and distinct patterns of expression of its receptors (Koerner et al, 1981; Thomsen et al 1992). mGluR4, for example, is most prominently expressed in cerebellar granule cells, the olfactory bulb (especially in the internal granule layer), and entorhinal cortex as well as in subcortical nuclei like thalamus and lateral septum. Although they express in hippocampus, their expression level is weak compared to structures mentioned above with a particular loci of expression in dentate gyrus and CA3 (Kristensen et al, 1993, Tanabe et al, 1993).

The diverse localization and subclasses of mGluRs coincides with their functional diversity including not only inhibition of ionic currents, especially calcium and potassium, but also activation of potassium, calcium and non specific cationic channels (reviewed in Anwyl, 1999). The role of mGluRs in modulating the ionic flux in and out of the cell allows them to mediate slow excitatory potentials, inhibition of transmitter release via presynaptic mechanisms and potentiation of AMPA and NMDA synaptic responses result in an interplay between the ionotropic and metabotropic glutamate receptors in activity, function and plasticity of the neurons in the nervous system.

2.3. Linking hippocampal function with its molecular components

One of the ultimate goals of neuroscience is to link the molecules within a cell to the function of a given area in the brain. Considering the importance of hippocampus in cognitive and non-cognitive components of the behavior (see the section on hippocampus above) and considering the critical involvement of the glutamate receptors in numerous cellular functions, most notably in neural excitability and plasticity (see the section on glutamate receptors above), significant interest has been centered at the glutamate contribution for generating behavior especially in hippocampus dependent paradigms (Reisel et al, 2002; Bannerman et al, 2003, 2004; Schmitt et al, 2003; Schmitt et al, 2005 but also see Zamanillo et al, 1999).

Among the glutamate activated receptors GluR-A containing AMPA receptors are believed to play a critical role in hippocampal function. They are expressed in hippocampus during and after development. Like the other AMPA receptors, GluR-A containing receptors are required for cationic ion transfer into the postsynaptic hippocampal neurons to depolarize the membrane to initiate further ion exchange through voltage gated ion channels and other iGluRs. Except the dense expression of GluR-D in inhibitory neurons in hippocampus, GluR-A subunits are the most widely expressed subunits in excitatory and inhibitory neurons of the hippocampus (Figure 5).
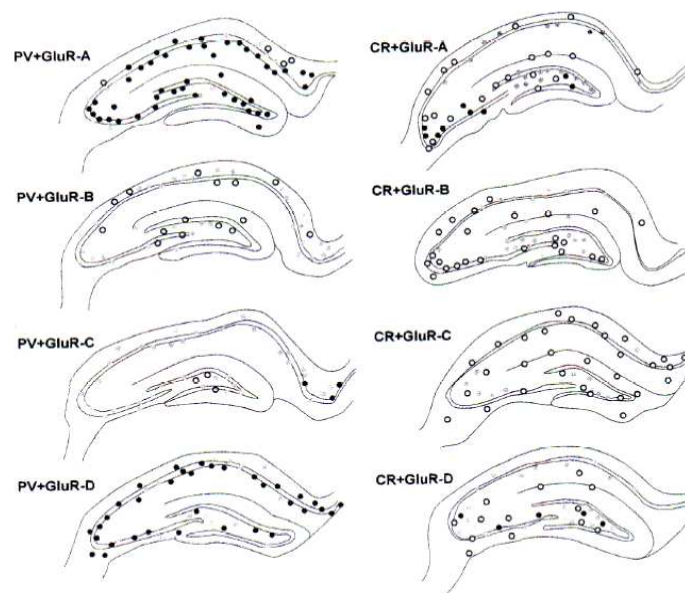
Figure 5. Distribution of AMPA receptor subunits in the hippocampus. Schematic drawings represent the expression level of GluR-A (top) to GluR-D (bottom) using non-radioactive in situ hybridization and immunocytochemistry. Each dot represents one cell at a given location. Color codes: black, strongly positive; grey, moderate or lightly labeled; white, negative. Adapted from (Catania et al, 1998).

Functional studies on the GluR-A knock-out (GluR-A$^{-/-}$) mice (Reisel et al, 2002; Bannerman et al, 2003, 2004) and knock-out animals expressing an copy of the GluR-A subunit (Schmitt et al, 2005) have supported the hypothesis that this subunit is critically involved in generation of behavior. However the mechanisms of GluR-A contribution to behavior are yet unknown but likely to include phosphorylation of the subunit, binding onto post-synaptic density proteins for inclusion into the synapse as well as modulating intracellular Ca^{2+} dynamics and glutamate receptor localization within the synapse.

I have studied these mechanisms in several lines of knock-outs (GluR-A$^{-/-}$, GluR-B$^{\Delta Fb}$, GluR-A$^{-/-}$/B$^{\Delta Fb}$) as well as transgenic mice expressing an copy of the GluR-A gene with mutations at the phosphorylation sites for αCaMKII, PKA, PKC (SA) or at the PDZ

interaction domain (TG) in addition to mice constitutively expressing Homer1a (see Figure 6) using mnemonic and non-mnemonic paradigms designed to address the contribution of hippocampus to behavior.
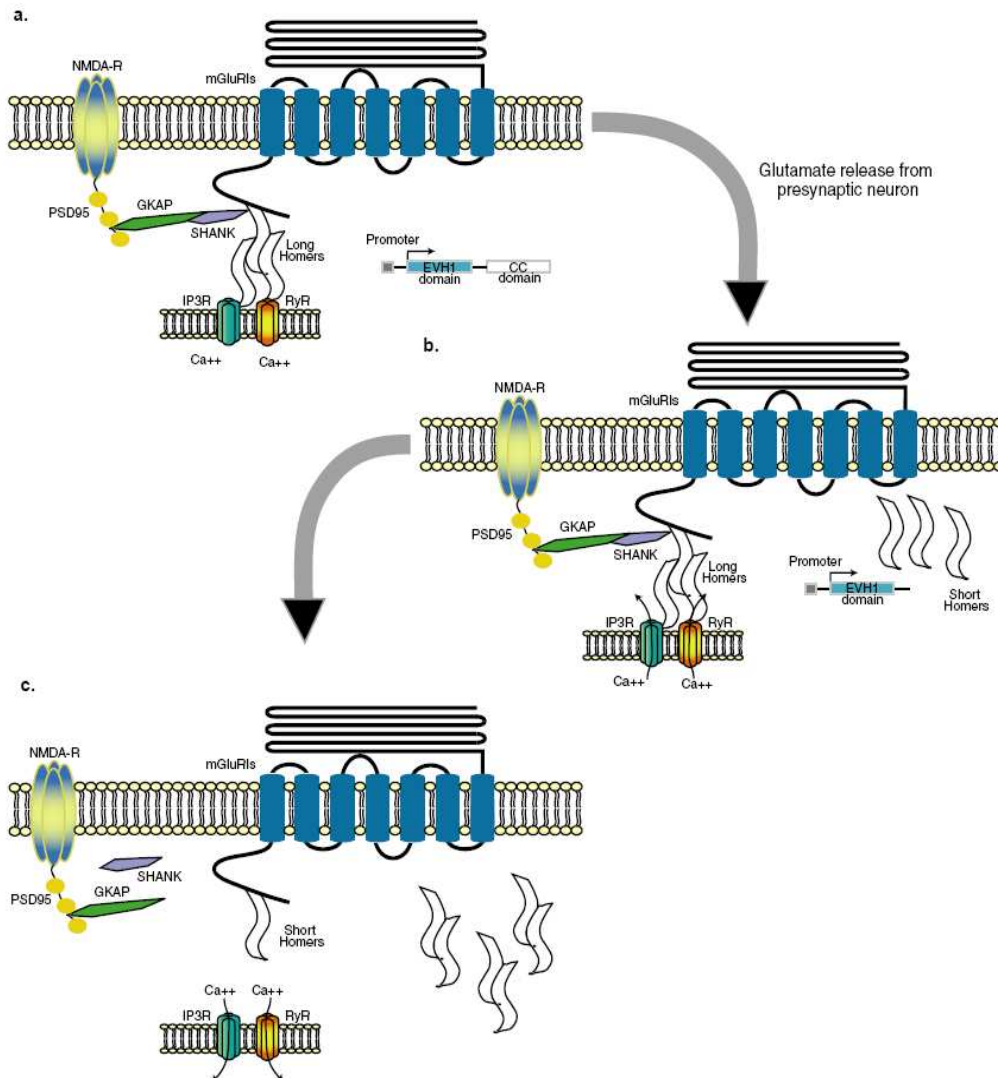
Figure 6. A postsynaptic intracellular molecule to mediate glutamate receptor function. Homer family proteins are attractive models as a mechanism by which glutamate receptors control cellular function through calcium dynamics. This family has three genes (Homer1, Homer2 and Homer3) that are expressed in excitatory cells of the brain, especially in hippocampus. Among the three genes, Homer1 gives rise to two alternative splices, Homer1a and Ania-3. These alternative isoforms (short homers) are expressed as a function of synaptic activation and they lack CCH binding domain that allows the Homer proteins to bind to smooth endoplasmic reticulum calcium release pores, RyR and IP3Rs. Long Homers, on the other hand, bind to both PSD proteins via EVH binding site and RyR and IP3Rs via CCH domain to create a physical link between the synaptic receptors and intracellular calcium stores. (a) Long Homers are expressed constitutively and bind to synaptic targets during low intracellular calcium conditions. They not only bridge receptors with calcium channels but also take a role in synaptic clustering of the receptors. (b) Upon synaptic stimulation and increased intracellular Ca^{2+} concentration, short Homer isoforms are expressed. Because these forms are alternative splices

of the Homer1, expression of the short isoforms depresses the production of the long isoforms. Short isoforms compete with the residual long isoforms in the cytosol to bind onto the EVH domain of the PSD proteins. (c) Once short Homer binds onto these receptors, they disconnect the receptors from each other and the calcium release pores of the ER. During this time, Ca^{2+} ions influx into the calcium stores and complete the refilling of the stores with Ca^{2+}.

3. Material and Methods

The present chapter describes the molecular methods used to engineer mice, the apparatus and procedures for the behavioural tests. All variations from the information provided below are described in the methods section of the individual chapters.

3.1. Subjects

Adult mice from both sexes used in the experiments described here were originally engineered in the Department of Molecular Neurobiology at the Max-Planck Institute for Medical Research (MPImF, Heidelberg, Germany) and bred at Charles River (Sulzfeld, Germany), ZTL (Heidelberg, Germany) and Progen (Heidelberg, Germany).

In total seven lines, excluding the control mice, of genetically engineered mice were used in the current series of experiments (Figure 7).

3.1.1 Complete GluR-A knock-outs (GluR-A$^{-/-}$)

Mice lacking GluR-A containing AMPA receptors were generated by Zamanillo and colleagues as described (Zamanillo et al, 1999). In short, embryonic stem cells were electroporated with a targeting vector which contained parts of the GluR-A gene's introns 10 and 11 as well as the exon 11 (Figure 7a). The targeting vector had additionally included a neo selection marker which was inserted into the intron 11 and a loxP recognition site in the upstream of exon 10. The electroporated stem cell yielded 5 lines of mutants which lacked the expression of GluR-A subunit of the AMPA-type glutamate receptors.

Contribution of the C-terminal domain of GluR-A subunit to behavioural phenotype was studied in three lines of mice engineered to express a mutated version of the GluR-A subunit in the GluR-A$^{-/-}$ background. Transgenic mice were engineered by injecting the vector DNA into the pronucleus. Transgenic mice expressing a mutated or non-mutated version of the GluR-A subunit were bred with mice carrying the tTA transgene and with GluR-A$^{-/-}$ mice to generate mice expressing the gene of interest in a GluR-A$^{-/-}$ background.

In order to control for the specificity of the behavioural phenotypes to be described to the GluR-A function, an additional line of transgenic mice expressing Homer1a were used. These mice were created by crossing the mouse line expressing transgenic Homer1a with mice expressing tTA.

This expression system was based on conditional expression of the transgene by a bi-directional promoter with tetO operator (Figure 7b). The promoter was activated binding of tTA on the tetO operator. tTA was expressed under the control of the αCaMKII promoter and therefore the expression of the transgene was restricted to neocortical excitatory neurons after the embryonic development. Upon tTA expression and binding onto tetO, expression in one direction resulted in a GFP fusion protein of GluR-A. In the other direction, the promoter controlled the expression of the reporter gene nlacZ (Figure 7b).
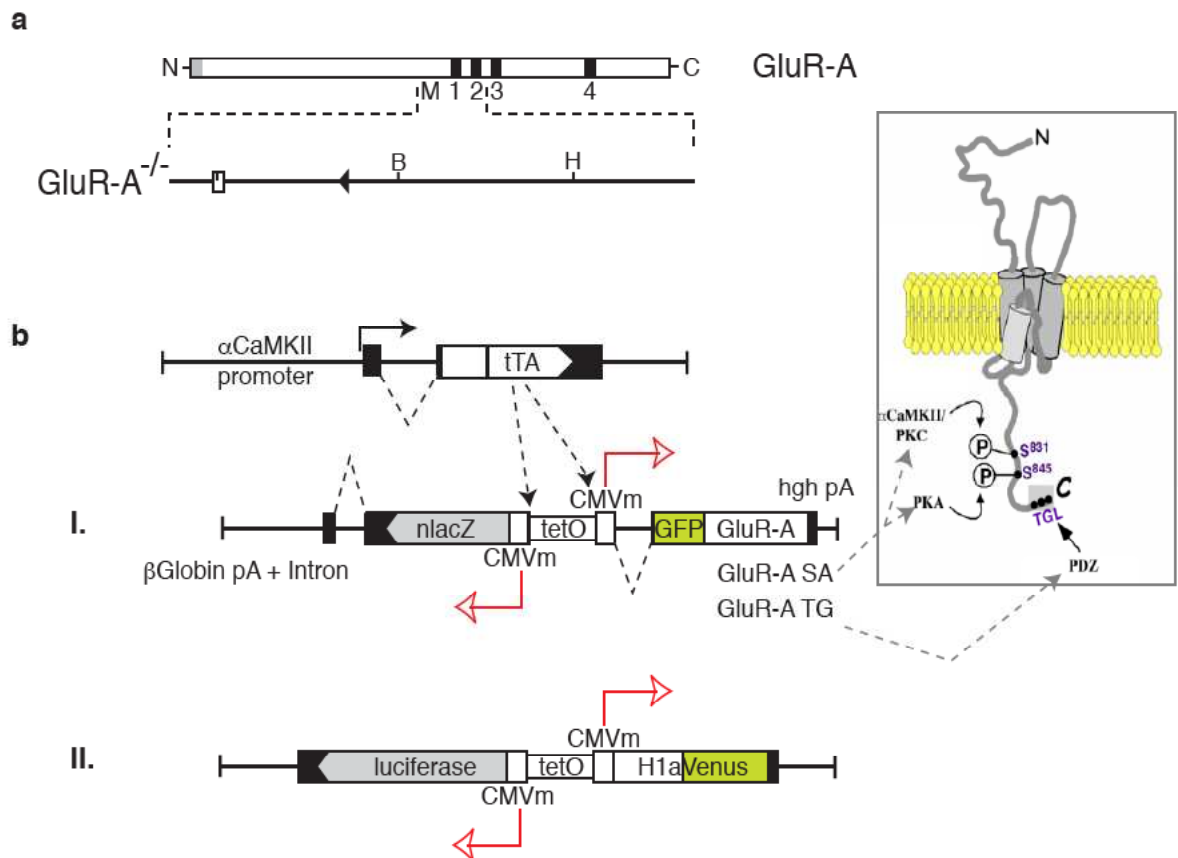
Figure 7. Schematic description of regulation of gene expression.
(a) Global knock-out of GluR-A (after Zamanillo et al, 1999). (b) Tetracycline dependent expression of engineered genes. αCaMKII promoter driven expression of tTA results in tTA binding to the Tet operator (tetO) sequences adjacent to cytomegalovirus (CMV) promoters. Transcription of a reporter gene (I:nlacZ and II:luciferase) and the gene of interest (I: GluR-A, GluR-A SA or GluR-A TG GFP fusion protein and II: Homer1aVenus) are controlled by a bidirectional transcription unit (After Mack et al, 2001; Celikel et al, submitted). The inset (Layer, 2003) shows a schematic drawing of the GluR-A subunit. N-terminus is in the extracellular space. Close to the C-terminus in cytoplasm, a PDZ interaction domain is located. GluR-A TG mice express a transgene with a point mutation for this interaction side. GluR-A SA mice have double mutations for the phosphorylation domains of the GluR-A for the αCaMKII/PKC and PKA. Grey dotted lines leading into the inset indicate the localisation of the point mutations sites for the GluR-A SA and GluR-A TG.

3.1.2. GluR-A$^{-/-}$ mice expressing a transgenic GFP-tagged GluR-A subunit (A1.1)

A naïve version of the subunit without any mutations was expressed in a GluR-A$^{-/-}$ background.   This genotype served as a control line.

3.1.3. GluR-A$^{-/-}$ mice expressing a transgenic GFP-tagged GluR-A subunit with an amino acid (leucine) deletion at the PDZ interaction domain (TG)

Mice expressing a mutated version in which the GluR-A subunit carried a single amino acid deletion at the PDZ-domain interaction locus. At the C-terminus of the GluR-A subunit, the final 3 amino acid residues (TGL) constitute the PDZ interaction domain. This domain is involved in trafficking of synaptic proteins and modulates the size and strength of the post-synaptic density (Kim and Sheng, 2004). The PDZ interaction domain of the GluR-A subunit is believed to be necessary for activity dependent modification of the synaptic distribution of AMPA receptors (El-Husseini et al, 2002; Colledge et al, 2003).
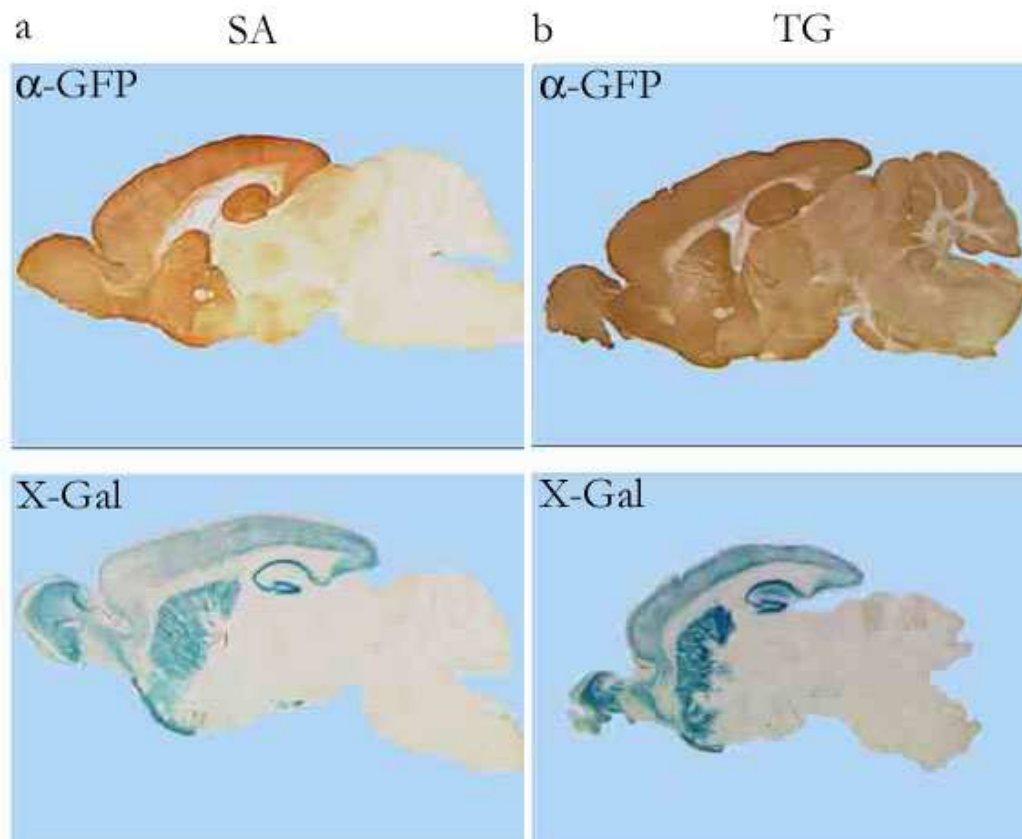
Figure 8. Expression of the GluR-A transgene in the SA and TG lines. Both transgenes express the mutated copy of the GluR-A under the control of a bi-directional promoter. While one direction controls the expression of the GluR-A/GFP fusion construct, the other allows a reporter gene to be expressed.   In figurines, top panels show the immunohistochemical stainings with antibody raised against α-GFP and bottom panels show reported gene, ß-gal, expression. (a) GluR-A$^{-/-}$ mice expressing an exogenous copy of the GluR-A with mutations at S831 and S845 residues (SA). (b) GluR-A$^{-/-}$ mice expressing an exogenous copy of the

GluR-A with an amino acid (leucine) deletion at the PDZ interaction domain (TG) (Adapted from Layer, 2003).

3.1.4. GluR-A$^{-/-}$ mice expressing a transgenic GFP-tagged GluR-A subunit with mutations at S831 and S845 (SA).

SA mice expressed the GluR-A subunit with mutations in the phosphorylation sites S831 and S845 (Figure 7b). S831 is phosphorylated by αCaMKII as well as PKC (Figure 7 inset), while S831 phosphorylation by PKC is shown to modulate synaptic plasticity (Lee et al, 2000), αCaMKII mediated phosphorylation of this residue potentiates GluR-A current (Barria et al, 1997). The second residue mutated in this line of mice is the S845. Electrophysiological experiments showed that dephosphorylation of this residue is involved in the long-term synaptic depression (Lee et al, 2000) and modulates the GluR-A mediated AMPA currents (Wang et al, 2005).

The level of the protein expression in the brain tissue was variable across these three transgenes (Figure 9).
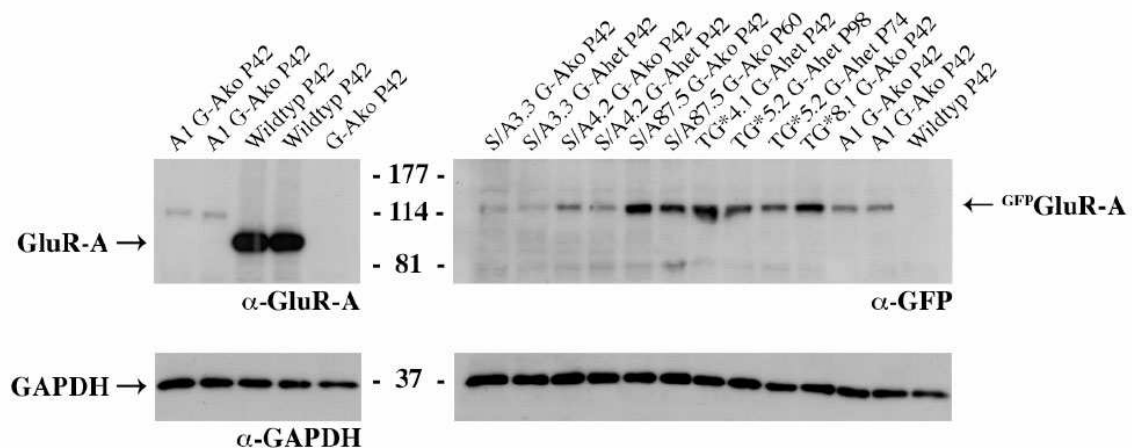
Figure 9. Amount of protein in brain extracts of the transgenes. Extracts from the transgenic animals were run in the western blot analysis using ^{GFP}GluR-A and GluR-A antibody to recognize GFP fusion protein with GluR-A (transgenes) and native GluR-A subunit in the brain, respectively. Among the transgenes examined in the current study, expression of the transgenes in the SA (S/A 87.5) and TG (TG*8.1) mice were more prominent then the expression in the A1 mice (Layer, 2003).

As quantified before (Layer, 2003), the level of protein expression across transgenes varies with the construct most likely due to random insertion of the gene into the host genome. Among the three transgenes studies, the SA and TG transgenic mice had the highest expression level with 11% of the GluR-A protein in the wild type. A1 transgene expression, however, was limited to a mere 6% in the adult hippocampus (Figure 10)
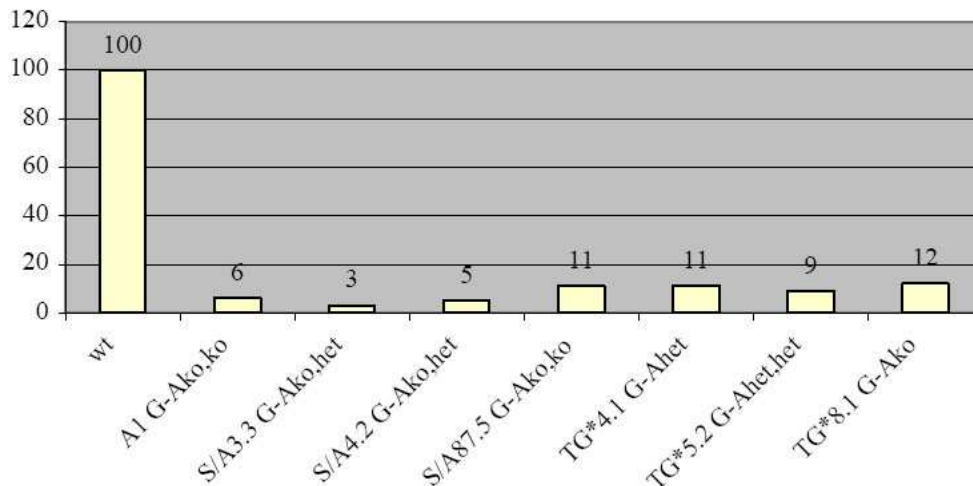
Figure 10. Quantification of the protein expression in adult hippocampi. Hippocampal extracts were run in the western blot and quantification of the protein expression was calculated across genotypes (n=2/genotype) before normalizing the values to the amount of native GluR-A expression in the wild types. (Layer, 2003).

3.1.5. Conditional GluR-B knock-outs (GluR-B$^{\Delta Fb}$)

Conditional GluR-B expression was achieved as described by Shimshek and colleagues (Shimshek et al, 2006). In short, a vector including the exons 10-12 of mouse GluR-B gene flanked by loxP recognition loci was inserted in embryonic stem cells. After confirmation of the successful targeting, stem cells were injected into C57BL/6 blastocysts. Chimeric animals were then bred with native C57BL/6 mice for generating offsprings with GluR-B^{2lox} allele (Shimshek et al, 2006). The resultant mice were bred with mice expressing Cre under a αCaMKII promoter, which restricts the Cre expression to the neocortex. This resulted in a forebrain specific GluR-B knock-out.

3.1.6. Complete GluR-A and conditional GluR-B knock-outs (GluR-A$^{-/-}$/B$^{\Delta Fb}$)

To question if there are synergistic interactions between AMPA receptor subunits, I bred GluR-A$^{-/-}$ and GluR-B$^{\Delta Fb}$ mice to generate GluR-A$^{-/-}$/B$^{\Delta Fb}$ double knock-outs. These knock-outs carried the gene expression characteristics for the GluR-A and GluR-B subunits in the founder lines. The offsprings lacked the GluR-A containing AMPA receptors in the entire brain and GluR-B containing AMPA receptors only in the neocortex after the early development.

3.1.7. Mice expressing a copy of Homer1a constitutively in the neocortex (Homer1a)

The last line of mice used in the current set of experiments expressed the Homer1a transgene in neocortical neurons constitutively (Celikel et al, submitted). The Homer1a expressing mice were generated by crossing tTA expressing (under the control of αCaMKII promoter) mice with animals carrying the bi-directional transgene with Homer1a-Venus fusion gene and luciferase reporter gene (Figure 7). Latter were obtained by pronucleus injection. As previously mentioned, in those lines where transgene expression is regulated by tTA expression under the control of αCaMKII promoter, the transgene expression should have been restricted to the neocortex and did not start until the embryonic development of the organism is completed. Therefore the effect of the Homer1a transgene expression was restricted to post-embryonic development.

All genetically engineered animals and control mice were back-crossed to C57BL6 several times before they were run in experiments. Before and after animals received their respective behavioural protocols, each animal was genotyped and only mice with the right genotype were included in the final analysis of behaviour. Where applicable, results from each gender are presented separately for the behavioural experiments.

Upon delivery adult mice were housed individually and maintained on a 12-hour light/dark cycle. All behavioural testing were performed during the light phase.

Animals had *ad libitum* access to food except during training and testing on appetitive motivated tasks. On such tasks, they were kept on a restricted feeding schedule aiming to keep their weight at the 85%-80% of their free-feeding weight after correcting the body weight according to Body Score Procedure (see below) throughout the behavioural testing. Body Score Procedure is used to estimate the ideal free-feeding weight of the animal under healthy food conditions. Obese animals were put on a diet until they reached normal body conditions and only then their free-feeding weight was calculated. Animals had continuous access to water at all times except during short epochs when they were run on experiments. Experiments took place in the Department of Psychology at the University of Oxford (UK) and at the MPImF (Germany). All experiments were performed in accordance with UK Animals Scientific Procedures Act 1986 as well as the animal welfare guidelines of the Max-Planck Society.

3.2. Biochemical Material and Methods

3.2.1. Antibodies

Mouse Monoclonal Anti-GluR1; Santa Cruz

Mouse Monoclonal Anti-ß-Actin, Clone AC-15 A5441; Sigma

Rabbit Anti-ß-Galactosidase; 55976 ICN

Peroxidase-conjugated Goat Anti-Rabbit IgG (H+L), 111-035-144; Dianova

Peroxidase-conjugated Goat Anti-Mouse IgG (H+L), 115-035-100; Dianova

3.2.2. Preparation of protein out of the mouse brain

The preparation procedure was done on 4°C and proteinase inhibitors (Complete, EDTA-free, Roche Diagnostics) were added in the utilised solutions. Hippocampi, Cortex and Cerebellum were dissociated and homogenised in 25 mM HEPES pH 7.4. This was followed by spinning at 2000 rpm for 5min. The determination of the protein concentration was done after Bradford.

3.2.3. Western blotting

After the determination of the protein concentration of the protein preparation, 10-20µg of this protein denaturated in SDS loading buffer for 5 min by 95°C and were separated by a SDS-polyacrylamide gel electrophoresis (10-12% polyacrylamide, Mini-Protean 3, Bio-Rad). The transfer of the proteins took place for about 18 hours onto a nitrocellulosis membrane (Protran BA 85, Schleicher und Schuell; Mini Trans-Blot, Bio-Rad). Membranes were blocked by blocking buffer (0.1% Tween 20, 10% skimmed milk powder in TBS pH 7.5) for two to three hours and washed in washing buffer (0.1% Tween 20 in PBS pH 7.5). Incubation with the specific primary antibodies occurred in 0.1% Tween 20 in PBS pH 7.5 for two hours by room temperature or by 4°C over night. In order to detect the specific antibody binding, horseradish-peroxidase labelled secondary antibodies were used, which can binde the previously used primary antibodies. The membrane was incubated with the solution of the secondary antibody in TBS pH 7.5 for 45-60 minutes and after washing inTBS pH 7.5 three times for 10 minutes detected with the help of chemiluminescence (ECL plus, Amersham-Pharmacia).

3.2.4. Tissue sectioning by vibratome

Mice were either sedated by Isoflurane and perfused intracardiacally first with PBS pH 7.4 and afterwards with 4% PFA/PBS, or sedated, and killed. The brain was removed,

postfixated for 1 h on 4°C, washed in PBS, embedded in agarose and cut with the vibratome (100 µm) (Leica VT1000S) and stored at 4°C.

3.2.5. Immunohistologic investigations of brain slices

Brain slices (100 µm) cut by a vibratome were incubated for 10 minutes in 0.5% H_2O/PBS and washed in PBS (2 x 10 min). Permeabilisation took place in buffer 1 (0.3% Triton X-100, 1% bovinal serum albumin (BSA), 2% normal goat serum in PBS) for 30 minutes. Afterwards slices were incubated in the specific primary antibody for about 15 hours, washed in buffer 2 (0,3% BSA, 0,1% TritonX-100 in PBS) 2 x 10 minutes, incubated with peroxidase tagged secondary-antibody for 1 h, washed in buffer 1 (1 x 10 minutes) and in buffer 2 (2 x 10 minutes). The stain reaction was developed by 20 mg Diamonobenzidine (3.3´Diaminobenzidine Hydrochloride, Sigma), solved in 50 ml HEPES (20 mM, pH 7.6) and stopped in PBS. The colored slices were washed in 10 mM Tris pH 7.5 and transferred onto object slides. After drying they were put into Xylol and embedded in Eukitt (Langenbrink).

3.3. General animal handling prior to behavioural testing

Mice were taken out of their cage by the tail and placed on the experimenter's arm wearing a lab coat. This was done until the mice were used to the experimenter and to the fact that they were taken out of the cage. Wearing the same lab coat is helpful for the habituation, because the mouse smell on the lab coat decreases the anxiety.

Before starting to train animals in appetitive motivated tasks (like T-Maze and Y-maze) mice were habituated to the condensed milk (diluted in water; 50/50 (w/w)) first in their home cages, then in an open field. Habituation to the condensed milk in the open field aimed to motivate the animals to explore the environment for food reward. To do so, mice were placed in an open field for five minutes two times a day on two consecutive days with two containers filled with diluted condensed milk placed in random locations within the open field.

3.4. Descriptions of behavioural paradigms
3.4.1. Nesting

From rodents to birds, it has been shown that intact hippocampus is required for creating complex nests (i.e. Antonawich et al, 1997; Abbott et al, 1999; Deacon et al, 2002). Lesions or scrapie infection of hippocampus, but not of medial prefrontal cortex, impairs successful nesting. To quantify the nesting complexity, mice were housed over night in

individual cages with 5X5 cm squares of pressed white cotton (Nestlet, Datesand Ltd., Manchester UK) as nesting material. Nest construction was scored the following morning according to the scoring scheme below:

1. no nesting
2. some craters in bedding
3. nestlet mostly shredded but no identifiable nest site
4. an identifiable but flat nest
5. nestlets pulled to pieces and closed roof formed, covering the mouse completely

Higher scores in this task associate with intact hippocampal processing.

3.4.2. Accelerating rotarod

Apparatus

Two different apparatuses were used for the accelerating rotarod experiments. The first one, located at the Department of Pharmacology of the University of Oxford, was composed of a 3cm diameter, 4.5 cm long knurled rod, which was perpendicularly flanked on both sides by 30 cm diameter grey flanges. The rod was installed 17 cm above the base of the apparatus. Speed and acceleration of the moveable rod were electronically controlled by manual switches. The second apparatus (Acceler Rota-Rod 7650), located at the Max-Planck Institute for Medical Research, was bought from Ugo Basile. This apparatus was used for testing WT / GluR-A$^{-/-}$ / SA mice. It consisted of five 3 cm diameter drums, suitably machined to provide grip. Six flanges divide the drums, enabling five mice to be on the treadmill simultaneously. The rotation starts at 4 rpm and goes up to 40 rpm.

Procedure

Each mouse was held by the tail and allowed to grasp the rod, which was rotating at a speed of 4 rpm. If it was still on the rod after 10 seconds, the rotation of the rod was gradually accelerated until it reached either 20 or 40 rpm. If the mouse fell off the rod before the rod reached a speed above 10 rpm, it was given another chance to succeed at a speed of >10 rpm. Mice were tested three times across three consecutive days (Apparatus 1) or three times a day for eight consecutive days (Apparatus 2). For each animal tested, I quantified as standardized variable, the speed at which the mouse fell off (Apparatus 1). For those mice run on the second apparatus, latency to fall was recorded.

3.4.3. Horizontal bar

Apparatus

The apparatus consisted of a 0.2 cm thick and 38 cm long metal bar, which was held 49 cm above a cushioned surface to reduce the impact of a probable fall.

Procedure

The mouse was held by the tail and raised over the bar so that it could grasp it at the central point with its forepaws only. The tail was released and a timer, registering the time in seconds' resolution, was started simultaneously. The latency to fall was recorded and categorized as described below. If the mouse reached one of the end supports of the bar, it was left there for 30s before the session was concluded. Performance was then scored as follows: falling off between 0 and 5s = 1; 6 and 10 s = 2; 11 and 20 s = 3; 21 and 30 s = 4, holding on for 30 s or reaching one of the end supports = 5.

3.4.4 Neophobia

Neophobia is classically described as the tendency of an animal to avoid or retreat from an unfamiliar object or situation. Hippocampal lesions and AMPA receptor binding studies in rodent hippocampus showed that glutamate activitation in hippocampus correlates with the neophobic behaviour (Miller et al, 1986; Maren et al, 1994).

Apparatus

The testing was done on a black wooden T-Maze with transparent walls made out of plexiglas. The testing area was restricted to a part of the left arm.

Procedure

The well was filled with a solution of 50% sweetened condensed milk. All mice were food deprived for one night before testing. During testing mice were individually placed onto the T-Maze facing away from the well. The latency to drink was measured. If the mouse did not drink after 2 minutes, it was re-tested after 2 minutes interval in its home cage. This was repeated until drinking occurred or cut-off point of 15 minutes in the testing apparatus was reached.

3.4.5. Black-white-alley

Rodents prefer dark places where they are at less risk of predators. Every new environment, however, is best explored to check out sources of food and escape routes from predators. Therefore there is a potential conflict between the need to explore and to hide. What the animal finally does is partly determined by its affective state: more anxious animals will tend to stay hidden and won't explore. Factors such as past experience and hippocampal dysfunctions will also influence the behaviour of the animal. The black-white-alley is a laboratory model that allows us to quantify the presumed affective state in such situations.

Apparatus

Two wooden alleys were used (120 x 9 x 29 cm). One half was painted in black, the other half white. Between the two halves, there was a small piece of vertical wire mesh (approx. 1cm high) designed to separate the two halves.

Procedure

The mouse was placed onto the black-white-alley for a 2 minutes testing trial. It was placed at the closed end of the black or white alley, facing the end wall. Recorded parameters were: latencies to enter (all four paws) into the opposite half, total time spent in the black half, number of crossings of the barrier, the number of faecal boli.

3.4.6 Light-dark-box

The light-dark- box task is based on the same ethologically behavioral features of mice like the black-white-alley.

Apparatus

The apparatus consisted of an open white compartment 30 x 20 x 20 cm joined by a 3 x 3 cm opening to a dark box (painted black with a lid) 15 x 20 x 20 cm. The aversiveness of the white compartment was increased by additional illumination, a lamp (60 W) placed 45 cm above the center of the floor.

Protocol

The mouse was placed in the middle of the light side facing away from the opening. The latency to cross (all four feet) to the dark side, time spent on the dark side (all four feet) and the number of transitions through the opening were measured for the 5 minutes test

duration. Number of faecal boli was recorded.

3.4.7. Successive alleys

Successive alleys paradigm is similar to the black-white-alley with one difference that there are multiple alleys with putatively increasing anxiogenic character.

Apparatus

The apparatus consisted of four wooden alleys connected to form a linear track. Each alley was 25 cm long. Alley #1 had 25 cm high walls, is 8.5 cm wide and painted in black. A 0.5 cm step down lead to alley #2 which, was also 8.5 cm wide, but had 1.3 cm high walls and was grey. A 1.0 cm step down lead to white coloured alley #3, which was 3.5 cm wide, had 0.8 cm high walls. A 0.4 cm step lead down to the last alley #4, which is also white, 1.2 cm wide ground was surrounded with 0.2 cm high walls. The apparatus was elevated by anchoring the back of alley #1 to a stand, 50 cm high. The open end of alley 1 was >10 cm away from the stand to prevent mice trying to climb on to it. Beddings were placed under alleys #3 and #4 to reduce the impact of a possible fall off the alleys.

Procedure

A mouse was placed at the closed end of alley #1 facing the wall. Timers were started for the quantification of 1) the overall length of the test and latency to enter arms; 2) the time spent in alley #1. When the mouse placed all 4 feet onto the next alley, it was considered to have entered it. Total time spent in each alley is recorded, as are number of entries (both forward and backward), number of faecal boli occurred during the test, which lasted 5 minutes. If a mouse fell off the apparatus, the clock was stopped and the animal was replaced on the alley from which it fell, facing alley #1. All urine and faeces were removed between animals and the apparatus was cleaned and dried.

3.4.8. Forced (Porsolt) swimming test

As outlined before, one of the functions of the hippocampus is to contribute to the emotional states of animals. Lesion studies in rodents showed that removal of the ventral hippocampus alters the degree of anxiety measured in behaviour (Nadel, 1968; Moser and Moser, 1998; Bannerman et al, 2002; Bannerman et al, 2004). One of the well-established measurements of the chronic stress is the forced swimming test (Ramboz et al, 1998; Poleszak et al, 2005; Black, 2005; Hinojasa et al, 2006) and has been used in this study to quantify the

contribution of the glutamatergic transmission to expression of dorsal hippocampal function.

Apparatus

Forced swimming test was administered by placing mice into a swimming pool filled with warm (25°C) water. The pool used in the current study was 30 cm in diameter and height and was made of white plastic. One third of the pool was filled in with water to ensure that once the animals are in the pool, they could not support their posture by simply touching the pool surface with their hindlimbs and/or tail. A camera placed 140 cm above the surface of the pool recorded the swimming session. Data analyses were performed from these images. All experiments were performed under white light at 200 lux.

Procedure

Forced swimming test included two sessions with an interval of 24 hours. Both sessions were administered similarly except the duration of the session (Session 1, 15 min and Session 2, 10 minutes.). At the start of a session, each animal was placed at the center of pool and left alone for swimming during the rest of the session. Upon completion of the session, animals were placed into a "dry-box" placed under a red, heating lamp.

3.4.9. Open field

In order to measure overall motor activity, mice were tested in an open field.

Apparatus

All the mice were run in the same wooden arena measuring 60x60x30 (h) cm, painted in black except the white colored ground.

Procedure

Mice were placed in a corner of an open field and allowed to run around freely for a duration of 6 minutes while their motor activity was monitored using a video camera placed 2 m above the center of the arena. Statistics of the motor activity was calculated, using previously published computerized data acquisition system (Shimshek et al, 2006).

3.4.10 T-maze

The Hippocampus has been traditionally referred to as a structure, which creates a cognitive map of the environment. Establishment of such a cognitive map requires

hippocampus to process information in a spatiotemporally distributed manner. What happened when this particular event happened can be encoded only if the neural structure responsible to encode the information can associate spatially and temporally dispersed inputs to create a composite representation of the sensory information.

The role of hippocampus in integrating information across time and space has been studied in several paradigms including Morris water maze, hole board test, radial arm maze, T-maze, Y-maze, modified open field and many others. I have studied the role of excitatory transmission in several of these (see below) paradigms starting with T-maze.

T-maze is a working memory task during which the subject needs to remember its choice in the previous run in order to successfully complete the training and find the food on the maze. The success of the animal depends on its ability to maintain its choices over time. On this task, animals perform similarly when they are run with or without extensive spatial cues available to solve the task, suggesting that this task predominantly measures working memory capabilities of the subjects.

Apparatus

The T-maze apparatus was a wooden elevated (150 cm) apparatus consisting out of three arms that were connected in the form of a T. Start arm (47x10 cm) and two identical goal arms (35x10 cm) were surrounded by a 10 cm high wall. A metal food well was located 3 cm from the end of each goal arm. Bait, 50% diluted (in water) sweetened condensed milk as described above, was used to reward the animal for the successful choices in the task.

Procedure

Every trial of the training included two runs, sample run and choice run. On a given trial an animal was put into the starting arm, while one of the two arms was closed with a wooden block (sample run). The closed arm served as the target arm where the animal would receive food reward upon successful completion of the choice run. The identity of the sample arm for each trial was determined by random sequences, a different one for each mouse and each session. The maximum number of consecutive identical arms was two, as a precaution against temporary position habits developing. After animal was directed to sample arm and allowed to drink the milk during the first run, a 5-10 second delay was given before the mouse was required to choose one of the two accessible arms during the choice run. If the animal chose the arm, which was not visited in the sample run ('successful alternation'), it was baited. Number of correct choices was recorded and learning in the task was described as

the increased number of correct choices over the course of the training.

Eight trials were run in a daily session, each one of a squad of approximately ten mice. After all mice finished one trial the first mouse started the next round of the next trial.

3.4.11 Y-maze

While T-maze measures the ability of animals to preserve information in the working memory across time, Y-maze training quantifies if an animal can integrate spatial sensory cues in the environment with the task requirements. Y-maze learning is hippocampus dependent and requires the mice to use allocentric (i.e. in respect to other landmarks in the environment) spatial information to locate the target arm. Lesion of the dorsal hippocampus impairs acquisition and retrieval of the associative spatial reference memory on the Y-maze.

Apparatus

The Y-maze was made out of black painted wood. The central polygonal area was 14 cm in diameter. The arms attached (50 x 9 cm) were surrounded by a 0.5 cm high wall. A metal food well was located 5 cm from the distal end of each arm. Two of the three arms were assigned as the start arm and the other one was the target arm. The identity of the start arm was randomized for each trial with the exception that the maximum number of consecutive identical arms was two. Ten trials were run in a daily session. As on the T-maze, animals were run in the task sequentially.

Procedure

The apparatus was placed in a room with several extra maze cues. The goal arm was always at the same position and baited with condensed milk (as described). Mice were placed at distal end of the start arm, facing arms junction. The identity of the start arm for each trial was determined by random sequences, a different one for each mouse and each session (with equal numbers of left and right starts per session). The maximum number of consecutive identical arms was two, as a precaution against temporary position habits developing. The maze was rotated clockwise or anticlockwise direction between trials, to exclude that the mice identify the correct goal arm by olfactory, visual or tactile cues unique to a particular arm. The mouse was allowed to run and to enter arms until it found the milk during the first two days. When it had finished the milk, it was returned to the home cage. Later it was removed immediately after entering the wrong arm. Number of correct choices was recorded. As correct choice was conceived when the mouse entered directly the baited arm.

To ensure that the mice did not pick the correct arm just by smelling the milk, the milk was filled into the well after they have entered the correct arm during the last block. Mice received 10 trials a day, 90 trials in total during the acquisition, five sessions during the retrieval and one in the new room.

3.5. Statistical evaluation of the behavioral data

All statistical analyses are performed on the raw data and when possible parametric tests are preferred over nonparametric ones. For those experiments require quantification of significant difference between more than 2 experimental groups a multi-way analysis of variance was run after tests on normality and equal variance were performed. In the case of failure in these comparisons, appropriate nonparametric statistical test was performed. When parametric tests are performed, the values are specified as the mean ± standard error of the mean (SEM) of the raw data when specified in the text. For those data sets where nonparametric statistical tests used for significance assignment, values are specified as median and inter quartile range (IQR). For pairwise comparisons, P value was corrected for multiple comparisons of the same data set. Significance of the normality, equal variance and the group comparisons together with the test performed are given where appropriate.

Summary of statistical information on the comparisons are given next to the tests performed. The statistics reported are:

Degrees of freedom=Degrees of freedom represent the number of observations and variables in the regression equation. Its calculation depends on the number of elements in the comparisons. For example, if three experimental groups were to be compared for statistical difference, degree of freedom of this comparison would be 3-1=2.

Difference of means=Difference of means is a measure to quantify the spread of the data of the groups to be compared. If the difference of means is smaller than the variance within a group, it is concluded that the groups come from the same population and are not independent. The likelihood of the statistical independence increases, the larger this value is.

Equal variance test=Analysis of variance comparisons assume that the groups compared are sampled from a distribution with the same variance. This test is run together with the normality Test (see below) before ANOVA tests are performed.

F value=F value is the ratio between estimated populations variance between groups and variance within groups. This value is used to quantify the overlap in the raw data for the groups compared. If the value is 1, then the variance across groups is as large as the variance within a group, therefore it is concluded that there is no statistical difference between the

groups. As the value gets larger, the likelihood of statistical difference increases.

Normality Test= Tests on analysis of variance require that the data groups compared include "outliers" (data points which are away from the rest of the distribution) are normally distributed. Together with the equal variance test, normality test are run prior to analysis of variance comparisons.

P value=P value is described as the probability of falsely rejecting the null hypothesis that the two groups compared are coming from independent populations. As this value approaches to zero likelihood of Type I errors (false positives) decreases.

T value=T value is a measurement for the shape (slope) of distributions. T is most frequently used to compare the two distributions without relying on their mean values.

H value=Equal to F value in nonparametric tests.

Q value= Measurement of distance between individual distributions.

Difference of ranks=In those nonparametric tasks where experimental groups are compared after reordering individual subjects in each group, difference of ranks represent the mean difference of the ranked data across the groups.

4. Results

In this series of experiments questioning the molecular basis of hippocampal function, more than ten experimental paradigms have been utilized to study GluR-A$^{-/-}$, A1, TG, SA, GluR-B$^{\Delta Fb}$, GluR-A$^{-/-}$/B$^{\Delta Fb}$ and Homer1a mutants together with their respective controls in hippocampal paradigms.

4.1. Expression pattern and level in different mouse lines

Among the genotypes studied, modification of the gene expression using embryonic stem cell technology resulted in a more complete alteration of the protein expression in the genetically altered animals. In GluR-A$^{-/-}$ mice, for example, the GluR-A AMPA receptor subunit was completely missing in the brain (Zamanillo et al, 1999; also see Figure 11).
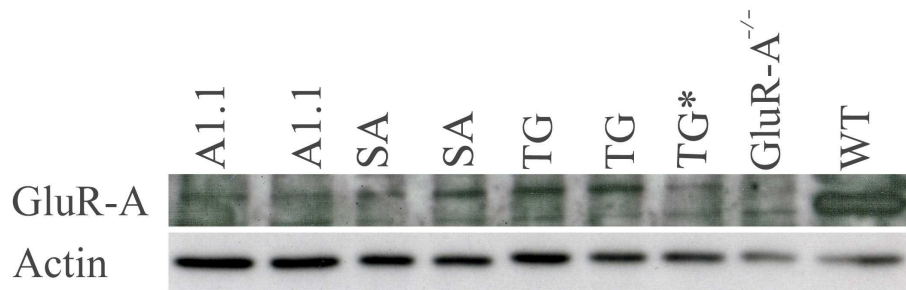
Figure 11. Detection of GluR-A expression across the genotypes studied. Standardized Western Blot analysis with monoclonal anti GluR-A antibody and ß-actin antibody and a load size of 20 μg sample/lane. Descriptions of the genotypes are as detailed in the materials and methods part. Asterisk denotes no-tTA-control. The band in the lane labelled TG* shows that there is also an expresson of the transgene if no tTA is present. This indicates that the promoter is ´leaky´.

Creation of the mutants through transgene expression resulted in a more heterogeneous expression pattern for both, AMPA variants and β-gal proteins (Figure 11, 12).
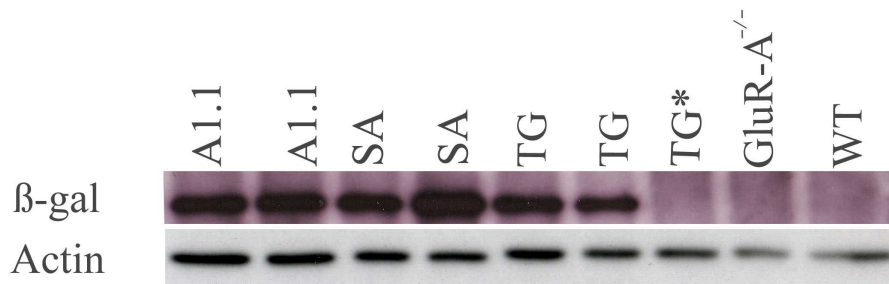
Figure 12. Detection of ß-gal expression across the genotypes studied. Standardized Western Blot analysis with polyclonal ß-gal anti antibody and ß-actin antibody and a load size of 20μg sample/lane. Descriptions of the genotypes are as detailed in the materials and methods part. Asterisk denotes a no-tTA-control. In the lane labelled TG* no band is visible, which shows that there is no expression of the transgene in the absence of tTA.

Western blot analysis and immunohistochemical brain slice stainings showed that the transgenic GluR-A subunit with a point mutation in the PDZ domain was expressed even in the absence of the activator tTA transgene (Figure 11). Although SA mice showed no sign of expression without tTA (Figure 13)

Figure 13. Quantification of GluR-A expression across the genotypes studied. Amount of the GluR-A in hippocampal extracts was quantified using standardized Western Blot analysis with monoclonal anti GluR-A antibody and a load size of 20 µg sample/lane. Descriptions of the genotypes are as detailed in the materials and methods. Asterisk denotes a no-tTA-control. The quantification of the protein in each lane was performed after subtracting the light intensity for the β-actin and GluR-A bands from the background and correcting the GluR-A value to the intensity of the β-actin. The results of this quantification showed that among the three transgenic lines TG expressed the highest. The extent of the expression of the transgene in A1.1 mice was only ~57% of the expression in TG mice, and the expression in SA mice was about 90% of that in TG animals.

Such leaky expression of the protein products was specific to the GFP-tagged side of the bidirectional promoter. In the TG mice, the ß-gal expression depended on the activator transgene (Figures 12, 14)
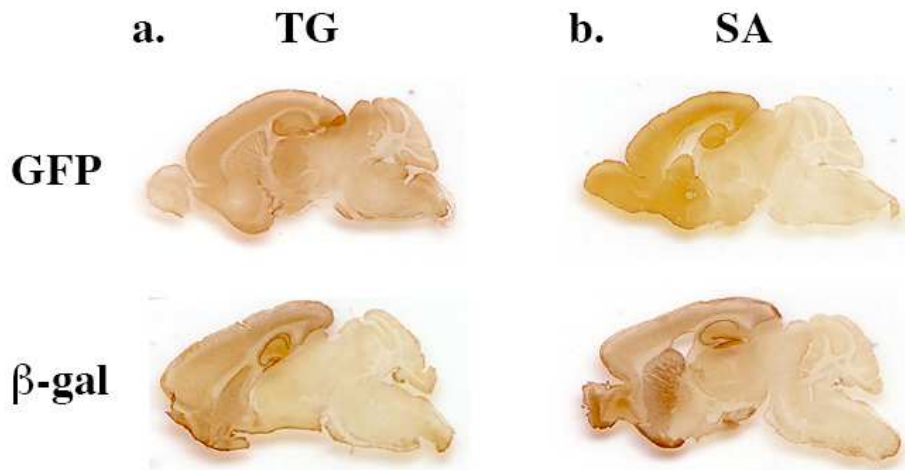
Figure 14. Expression of the transgene in TG mice, TG mice missing tTA and SA mice. While one direction controls the expression of the GluR-A/GFP fusion construct, the other allows a reporter gene to be expressed. All of these mice express a mutated transgenic GluR-A subunit. The other directon of the transgene is only expressed in mice which contain the tTA activator transgene.
a) shows the immunohistochemical stainings with antibody raised against GFP (upper pannel) and ß-gal (lower pannel). The GFP staining is done on a brain slice of a TG mouse without the tTA transgene. b) shows the immunohistochemical stainings of SA mice GFP (upper pannel) and ß-gal (lower panel).

In order to confirm the differential expression of the proteins across the transgenes, I studied SA, TG and A1.1 expression levels in adult hippocampal extracts. The results showed that TG has the strongest expression of the transgene which is 1.1 folds higher than the expression of the mutant GluR-A subunits in SA and 1.8 folds stronger than in A1.1 (Table3).

	SA (lane2)	SA (lane3)	TG (lane6)	TG (lane7)	A1.1 (lane8)
GluR-A	63.44	68.66	91.32	70.83	41.12
Actin (**normalized**)	1.119	1.099	1	1.113	1.118
ratio	70.99	75.46	91.32	70.83	45.97
mean	73.225		81.075		45.97
% of TG	90.32		100		56.7

Table 3. Quantification of the expression levels of the different GluR-A subunits. Table shows mean values of the luminance of GluR-A band minus the background (first row); actin band minus back ground before normalizing it to the weakest band across genotypes (second row); normalized (after intensity of the actin band) amount of GluR-A (third row); Actin serves as a standard; mean values of the animals of the same genotypes (fourth row), percentage of luminance in comparision to TG (fifth row). Luminance values normalized to TG. Measurements are from the western blot (Figure 13) in Adobe photoshop.

4.2. Behavioral results

Behavioral results of these experiments are presented in five sections:

In the first section (WT | GluR-A$^{-/-}$ | TG), animals lacking GluR-A containing AMPA receptors from the entire brain (GluR-A$^{-/-}$), animals which express a copy of the GluR-A with a point mutation at the PDZ-interaction domain on the GluR-A$^{-/-}$ background (TG) and wild type (WT) control animals either littermates or from the same strain (C57BL6) were studied (Figure 8).

In the second section (WT | GluR-A$^{-/-}$ | SA), as in the first one WT, GluR- A$^{-/-}$ and GluR-A$^{-/-}$ mice expressing a mutated transgenic GluR-A subunit were studied (Figure 8), but this time the point mutations were at the phosphorylation sites S831A and S845A (SA).

In the third section (WT | GluR-B$^{\Delta Fb}$), animals lacking GluR-B subunits from the forebrain (GluR-B$^{\Delta Fb}$) are studied in respect to control mice.

In the next section (WT | GluR-A$^{-/-}$/B$^{\Delta Fb}$), the effect of double mutations, GluR-A$^{-/-}$ with GluR-B$^{\Delta Fb}$,was studied with WT mice as control animals.

In the last section (WT | Homer1a), an immediate early gene which has tight links with synaptic glutamate receptors as well as intracellular calcium stores has been studied with WT mice as cotrol animals.

4.2.1. WT | GluR-A$^{-/-}$ | TG

4.2.1.1. Nesting

Considering that the ability to construct complex nests is inhibited by hippocampal lesions and scrapie infection of the hippocampus, but not by medial prefrontal cortex lesions, characterization of the nest structure should allow us to predict a possible hippocampal dysfunction in the animals' home cage environment. As explained before (see Materials and Methods), to do so, mice were placed in a fresh cage over night with nesting material. The next morning nest construction was evaluated for the quality and scored between 0 (worst) to 5 (best).

According to the rating scale all WT mice reached the highest score of 5±5-5 (median and IQR). GluR-A$^{-/-}$ mice scored 1.75±1.25-2.75 and TG mice were in between WT and GluR-A$^{-/-}$ animals with a score of 4.5±2.5-5 (Figure 15). The three genotypes differed significantly from each other (normality test, $P<0.05$; Kruskal-Wallis on ranks, $H(2)=11.385$, $P=0.003$). To visualize the statistical differences between groups pairwise multiple comparisons (Dunn's Method) was performed. These analysis revealed a significant difference between WT and GluR-A$^{-/-}$ mice with respect to the nest construction, but no significant difference between TG and GluR-A$^{-/-}$ or TG and WT mice.

These results support that the hippocampal function is disturbed in GluR-A$^{-/-}$ mice as suggested before[9]. Additionally, we now report that impairment in nest construction after GluR-A deletion can be partially rescued in TG mice.
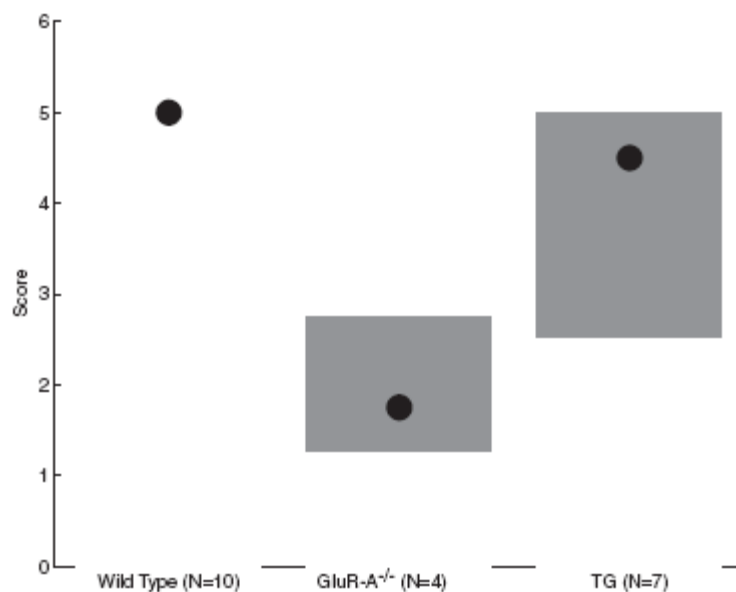
Figure 15. Ability to construct complex nests requires GluR-A. Figure depicts median nesting scores (median and IQR).

Accelerating rotarod and horizontal bar were conducted in order to exclude that the differences that might occur during the tests are because of motor impairment or muscle weakness of one of the groups.

4.2.1.2. Accelerating rotarod

It is known that GluR-A$^{-/-}$ males are strongly impaired in this task (Bannerman et al, 2004). This is consistent with the results shown in my experiments where GluR-A$^{-/-}$, WT, TG and SA mice were tested on the accelerating rotarod. As explained before, one of the variables studied in this paradigm is the slowest speed that the animals fail to keep up with the accelerating rotarod. To measure this variable, each mouse was held by the tail and allowed to grasp the rod, which was rotating at a speed of 4rpm. After 10 seconds the rotation of the rod was gradually accelerated and speed at fall from the rod was recorded. This was repeated three times

WT and TG mice improved in performance while GluR-A$^{-/-}$ did not when they were trained in the apparatus two more times for one trial. However these changes did not reach a statistically significant difference in the mean values among the different levels of session ($F(2)=1.778$, $P=0.184$). Therefore the tendency observed could just be due to overall random sampling variability. Neither was there a statistically significant interaction between genotype and session ($F(4) =1.889$, $P = 0,134$). Normality test failed ($P<0.05$) and equal variance test passed ($P=0.886$).

Compairing the least square means of genotype reveled that GluR-A$^{-/-}$ mice fell off at a lower speed (8.425 ± 1.56 (mean$\pm$SEM)), indicating impaired motor coordination relative to WT 17.377 ± 0.986 and TG (15.257 ± 1.179) mice ($F(2) = 11.811$, $P < 0.001$). Latter seem to rescue the phenotype of the GluR-A$^{-/-}$ mice, considering the fact that they do perform the task just slightly worse than mice with endogenous GluR-A expression (Figure 16). All pairwise multiple comparisons procedures (Holm-Sidak method, overall significance level before correction for multiple comparisons=0.05) revealed a significant difference for WT versus GluR-A$^{-/-}$ ($t=4.851$) and TG versus GluR-A$^{-/-}$ ($t=3.494$), but not for WT versus TG ($t=1.379$).
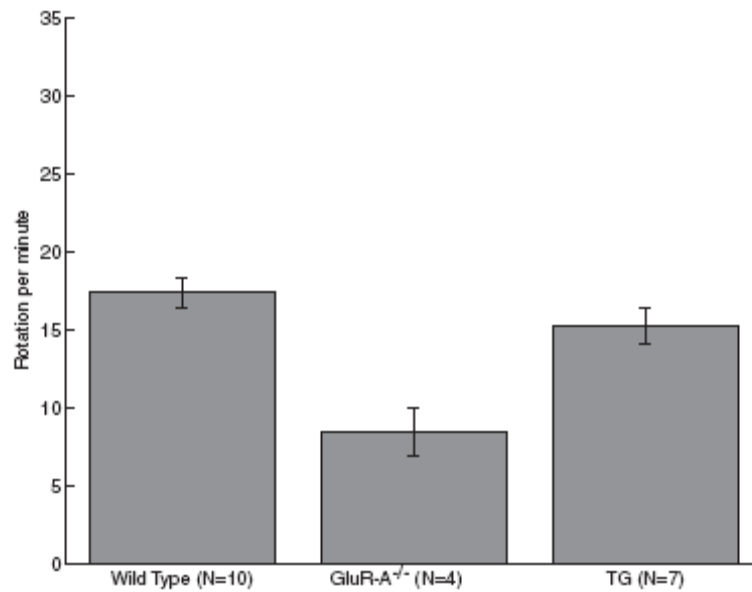
Figure 16. Rotarod performance is altered upon GluR-A deletion. Figure depicts the speed of accelerating rotarod at which animals of the three genotypes fell off the rod as least square means for genotype. Values are in mean±SEM).

In order to exclude that the differences seen in the rotarod task are just because of muscle weakness or weight differences (see Table 4) of the mutants the weights were compared and mice underwent a muscle test (Horizontal bar, see below).

Genotype	N	Mean	Std Dev	SEM
TG	7	26.91	2.124	0.803
WT	10	30.086	1.354	0.428
GluR-A$^{-/-}$	4	27.532	1.686	0.843

Table 4. Weight distribution across genotypes.

A One Way ANOVA (normality test P=0.289, equal variance test=0.098) showed that the weight differences among the investigated groups are greater than would be expected by chance (Table 1); there is a statistically significant difference (F(2)=8.042, P= 0.003). In order to isolate which groups differ from each other an all pairwise multiple comparison procedure (Holm-Sidak method, overall significance level before correcting for multiple comparisons= 0.05) was conducted and displayed a significant difference for WT versus TG (T=3.788, P=0.00135) and WT versus GluR-A$^{-/-}$ (T=2.537, P=0.0207), but not for GluR-A$^{-/-}$ versus TG (T=0.584, P=0.567). These results show that independent from the nature of the genetic manipulations, mutant mice compared to WT mice were smaller in size.

However, the small size of the mutants were highly unlikely to contribute to the difference between the WT and GluR-A$^{-/-}$ animals, considering the fact that although TG mice are as small as GluR-A$^{-/-}$ mice, their performance on the accelerating rotarod is statistically comparable to that of WT mice.

4.2.1.3. Horizontal bar

In order to exclude the possibility that the differences in motor coordination are due to an impairment of the muscle strength the horizontal bar task was conducted.

In this task, each mouse is directed to hold onto an elevated bar oriented in a horizontal position and the latency to fall off the bar was recorded.

Referring to a scoring scale described before (see Materials and Methods), the animals did not differ in their performance on the horizontal bar (Figure 17). They did not differ significantly in the amount of time spent on this apparatus, although, there was a slight tendency for the GluR-A$^{-/-}$ mice to fall off earlier (normality test failed ($P<0.050$), Kruskal-Wallis One Way ANOVA on Ranks, $H(2)=2.237$, $P=0.327$). This result was in contrast to Bannerman and colleagues (2004), who found a significant difference between the GluR-A$^{-/-}$ and WT animals with a larger group of mice.
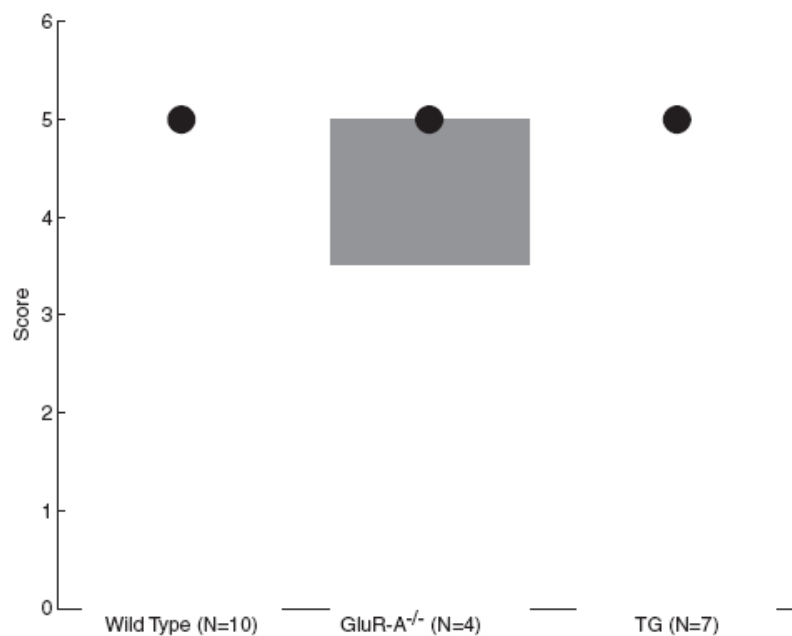
Figure 17. Horizontal bar performance is independent from the GluR-A. Figure shows median scores achieved on the horizontal bar (median and IQR).

These results show that the mutant mice were unlikely to be too weak or obese and that the difference seen is not a consequence of the weight differences. If there was an influence this would be the overweight of the WT mice. However, those perform the best in every task and reach the maximum score on the horizontal bar.

Considering the weight difference between the genotypes, I applied a body score scheme at the start of food deprivation, before animals were trained in appetitive motivated task, in order to exclude differences of motivations due to body weight.

A number of ethologically based tests of anxiety were conducted to describe the role of glutamate receptors in emotions. These included neophobia, black-white-alley, light-dark-box and successive alleys.

4.2.1.4. Neophobia

In food neophobia tasks rats with ventral hippocampal lesions consume unfamiliar food faster than controls, which is widely interpreted as the reduction in the level of anxiety following the lesions. These results are supported with a series of positive control experiments, which studied the same phenomena, but after amygdaloid lesions, a protocol known to increase the fear/anxiety response (McHugh et al, 2004).

We adopted this task to study anxiety across the genotypes of interest. The testing was done on a black wooden T-maze with transparent walls out of plexiglas with a well used to present the food (50% sweetened condensed milk) positioned at the end (see Materials and Method for further details). The mouse was placed onto the T-Maze facing away from the well. The latency to drink from the first sniff was recorded.

TG mice spent more time, compared to WT and GluR-A$^{-/-}$ mice, to start eating the food after having approached it (sniffing at the milk) for the first time (Figure 18). In contrast to the Bannerman et al (2004) study on GluR-A$^{-/-}$ mice, here, GluR-A$^{-/-}$ and WT mice do not differ from each other. This difference could be explained either by the small number of animals available for this study, or because of the different protocols used in this test. Nevertheless, the results of the test show an increased anxiety for these transgenic mice.

The parametric statistical analysis of neophobia failed to satisfy the assumption required for One Way ANOVA. Normality Test failed ($P<0.050$). Therefore, a Kruskal-Wallis One Way Analysis of Variance on Ranks was conducted and it revealed a statistically significant difference across the genotypes ($H(2) =11.911$, $P = 0.003$) (TG $=230\pm56.75$-353.25 (median and IQR), WT$=0\pm0$, GluR-A$^{-/-}=0\pm0$).

To isolate the group or groups that differ from the others a multiple comparison proce-dure was conducted. Results of these analyses showed a significant difference for TG vs GluR-A$^{-/-}$ (diff of ranks=9.714, Q=2.498, P<0.05) and WT (diff of ranks=8.114, Q=0.436, P<0.05), but not for WT vs GluR-A$^{-/-}$ (diff of ranks=1.6, Q=0.436, P>=0.05).
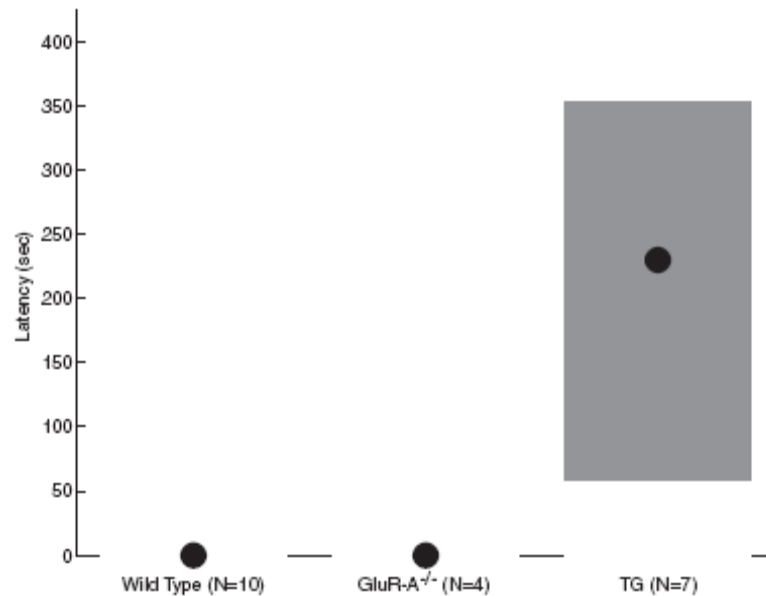
Figure 18. **Neophobia to eat unfamiliar food is not affected after GluR-A deletion.** Figure shows medians of latency to drink (median and IQR).

4.2.1.5. Black-white-alley

This test is based on the fact that animals prefer dark colours over bright ones and dark environments over well lit ones, possibly due to reduced likelihood of being detected by predators in darkness. Their drive to explore the environment in order to find food and a partner on the one hand and on the other hand the anxiety to be exposed in a bright area, where they can be detected by predators, put them into the dilemma to choose between exploration and hiding.

The black-white-alley is a laboratory model that allows us to quantify the presumed affective state in such situations. Its principle is very similar to the light-dark-box (see separate protocol). In short, the mouse was first transferred onto the white alley of the black-white-alley for a 2 minutes testing trial. Latencies to enter into the opposite half, total time spent in the black half, number of crossings of the barrier and the number of faecal boli were recorded.

Latency to enter the dark compartment

There is a clear tendency for knockout mice to enter the black compartment later than WT and TG animals (Figure 19). Nevertheless, there is a not significant difference between any of the three groups. This finding is consistent with Bannerman et al (2004) for GluR-A$^{-/-}$ mice in respect to WT, who found a difference only for females, suggesting that knockouts were more anxious.

Data analysis revealed no difference between the groups with respect to their latencies to cross from the black to the white alley. Normality test (P=0.091) and equal variance test (P=0.840) passed. An One Way ANOVA revealed no statistically significant difference between the mean values of the three groups (F(2)=0.443, P=0.649) (Figure 19). (TG=35.571±13.091, WT=40.8 ±11.16, GluR-A$^{-/-}$=57.333 ±11.865 (Means ± SEM).
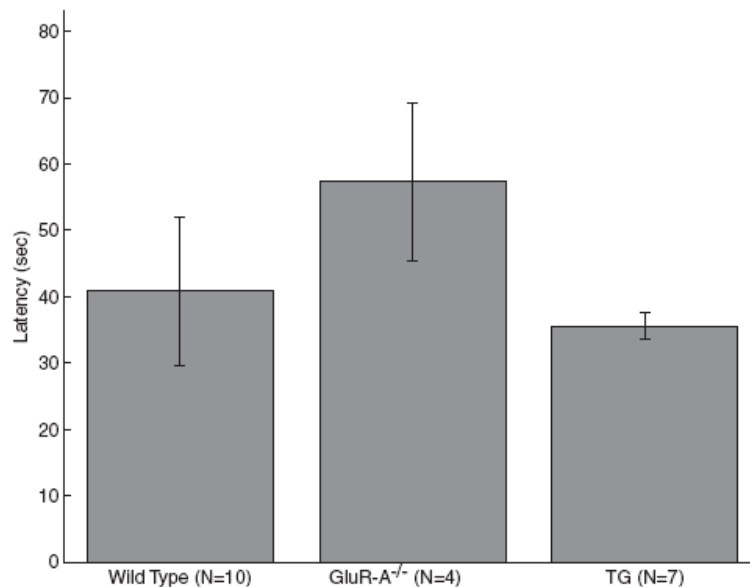
Figure 19. Anxiety level of the mice on the black-white-alley paradigm did not differ between genotypes as studied by the latency to enter the black compartment. Values are median and IQR.

Time spent in the black compartment

In terms of time spent in the black compartment, WT and TG mice had the tendency to explore the dark arena more than GluR-A$^{-/-}$ mice (Figure 20). The data did not fulfil the requirements of a One Way analysis of variance (The normality test failed (P < 0.050)). A Kruskal-Wallis on Ranks was conducted. The differences in the median values among the treatment groups are not great enough to exclude the possibility that the difference is due to

random sampling variability; there is not a statistically significant difference (Figure 20; P=0,094)

This finding is consistent with Bannerman and colleagues for GluR-A$^{-/-}$ mice in respect to WT mice. They found a difference only for females, which suggested that GluR-A$^{-/-}$ females are more anxious than WT females (e.g. spent more time in the dark compartment). A gender-based analysis could not be done in the current data set due to lack of mice.
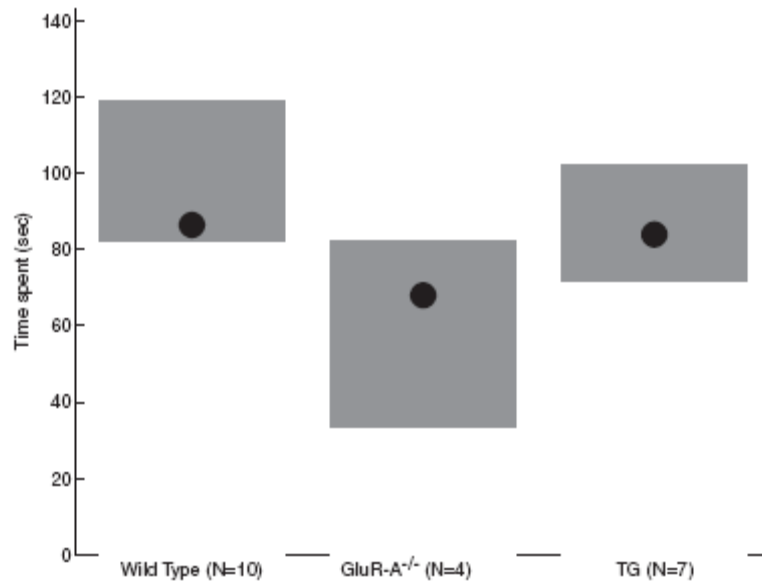
Figure 20. Anxiety level of the mice on the black-white-alley paradigm did not differ between genotypes as studied by the time spent in the black compartment. Values are median and IQR.

Number of boli

The number of boli each mouse left in the apparatus during the task was counted. The data did not satisfy the requirements of ANOVA (normality test passed (P=0.13), but equal variance test failed (P<0.05)). Hence, a Kruskal-Wallis one way ANOVA on ranks was conducted, which did not discover a significant difference between the groups (Figure 21; H(2)=1.314, P=0.518). (TG=1±0-2 (median and IQR); WT=1±1-1; GluR-A$^{-/-}$=0.5±0-1).
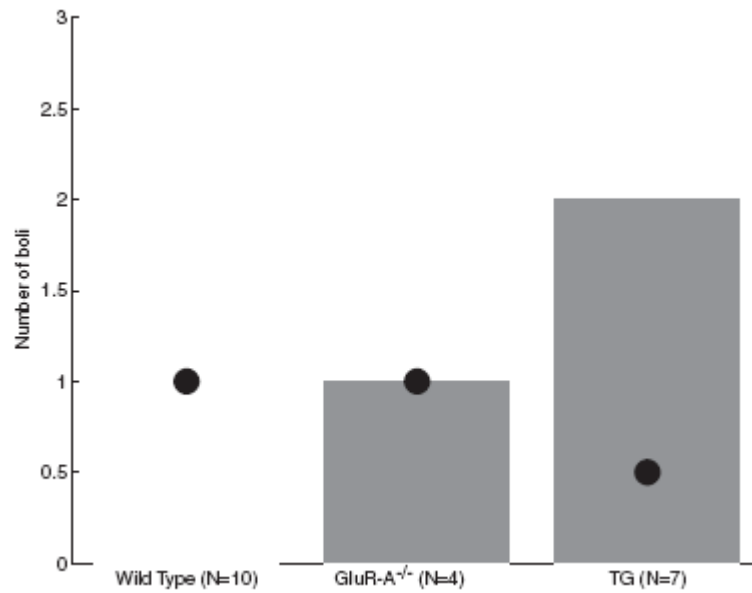
Figure 21. Alterations concerning the GluR-A subunit do not affect the anxiety level of the mice on the black-white-alley paradigm as studied by the number of boli during the course of session. Values are median and IQR.

Numbers of crossings between alleys

TG animals (8.143±2.064) showed a strong tendency to travel between the two alleys more often than WT (4.7±1.033) and GluR-A^{-/-} (5±0.707) mice (Figure 22). Nevertheless, a One Way ANOVA did not find a significant difference ($F(2)=1.693$, $P=0.212$). The normality test ($P=0.225$) and the equal variance test passed ($P=0.079$). The tendency for the TG mice to shuttle more is likely due to general hyperactivity. Considering that in the other measurements of anxiety in this battery of behavioral tasks TG mice were comparable to WT, it is possible to conclude that TG mice showed no anxiety.
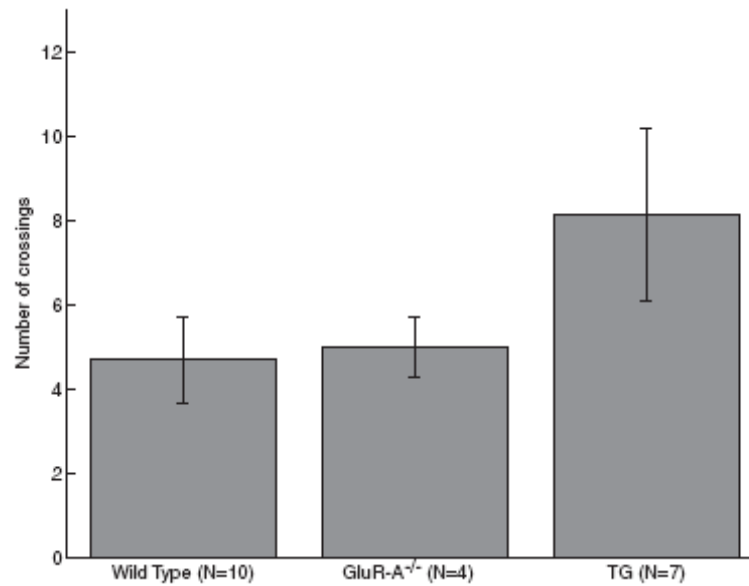
Figure 22. **Number of crossings between the alleys in the black-white-alley task revealed no difference across genotypes, although there was a tendency for the TG mice to shuttle between the alleys more.** Values are mean±SEM.

4.2.1.6. Light-dark-box

This test, like the black-white-alley, is based upon the fact that animals avoid well lit areas and prefer shelters over being exposed on a free field. Lesioning studies on rats showed that rats with ventral hippocampus or amygdala lesions showed less fear/anxiety on this test. They entered the white compartment more readily compared to rats with dorsal hippocampus lesions or sham-operated rats. Hence, this test might be able to discover hippocampal and amygdala impairment (McHugh et al, 2004).

I used this task to confirm the findings coming from the black-white-alley task and questioned if the role of hippocampal formation in expression of emotions is altered following modifications concerning the GluR-A subunit.

The task, as described above, is performed in a box divided into two sections each of which is painted to black (dark) or white (light). After the mouse was placed into either the dark or the light half, latencies to enter into the opposite half, total time spent in the black half, number of crossings of the barrier and the number of faecal boli were recorded.

Start from the dark part

Latency to cross

TG mice entered the light compartment more readily (31.571±7.985) than the other groups (Figure 23; One way ANOVA, F(2)=6.961, P=0.006, normality test: P=0.074, equal variance test P=0.094).
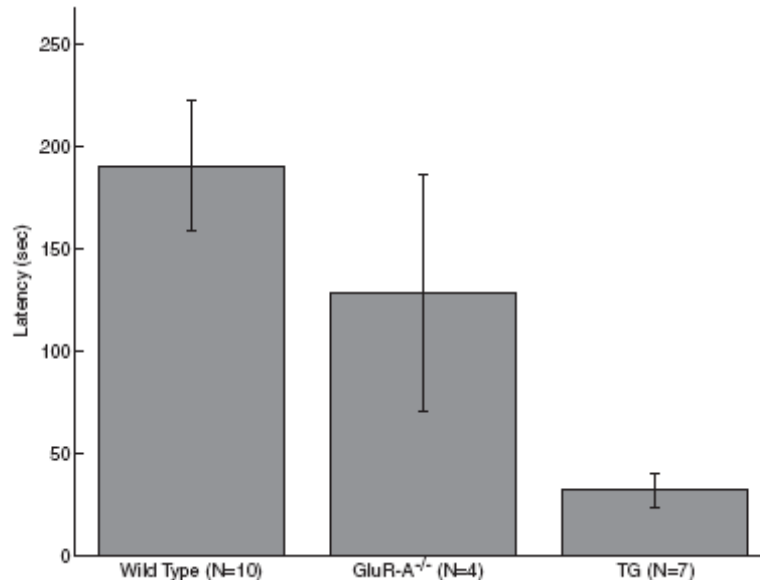
Figure 23. Light-dark-box paradigm (start in the dark compartment) showed that TG mice were less anxious than their WT and GluR-A^{-/-} counterparts. Values are mean±SEM.

Although there was a tendency for the GluR-A^{-/-} animals (128±57.804) to enter earlier than WT mice (190.3±31.867). A pairwise multiple comparison procedure (Holm-Sidak method, overall significance level before the correction for multiple comparisons=0.05) revealed a significant difference only for the groups WT versus TG (t=3.731, P=0.00153), but not for WT versus GluR-A^{-/-} (t=1.782, P=0.0916) and TG versus GluR-A^{-/-} (t=1.22, P=0.238).

Number of crossings

TG (18±7:23.75 (median and IQR)) mice shuttled between the two halves more often than the other groups (Figure 24). But the difference between WT mice (1.3± 0:8) and GluR-A^{-/-} mice (28.5±12.5:34) is the most obvious discrepancy. The normality test failed (P<0.05) so that a Kruskal-Wallis One Way Analysis of Variance on Ranks was conducted, which revealed that the differences in the median values among the treatment groups are greater than would be expected by chance (H(2)=6.935, P=0.031) .

Furthermore, pairwise comparisons (Mann-Whitney Rank sum test) showed that the difference between groups arose from the significantly smaller number of crosses made by

WT compared to TG (P=0.017). This difference might be related with the fact that WT animals do enter the light compartment much later, so that the time that remains for crossing between the compartments is very limited in comparison to GluR-A$^{-/-}$ and TG mice.
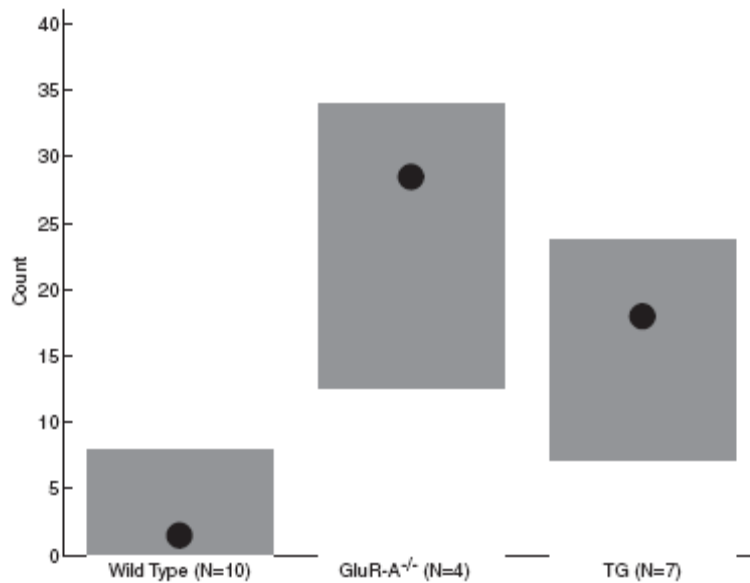
Figure 24. Number of crosses between the two halves of the light-dark-box showed that GluR-A$^{-/-}$ mice are hyperactive compared to WT mice. Values are median and IQR.

Time spent in the dark compartment

Among the three groups WT animals were the ones spent the longest time in the dark compartment (Figure 25). An One Way ANOVA revealed a difference between groups (F(2)=7.59, P=0.004; normality test, P=0.209 and equal variance test, P=0.307) (TG=196.429 ±20.946; WT=277.4±9.481; GluR-A$^{-/-}$=233.75±44.35). To find out which groups differ from each other an all pairwise multiple comparison procedures (Holm-Sidak method) was conducted which revealed only a significant difference between WT and TG mice (difference of means=80.971, T=3.872, P=0.00112). GluR-A$^{-/-}$ versus WT (difference of mean=43.65, T=1.739, P=0.0992) and GluR-A$^{-/-}$ versus TG (difference of mean=37.321, T=1.403, P=0.178) were not significant different.
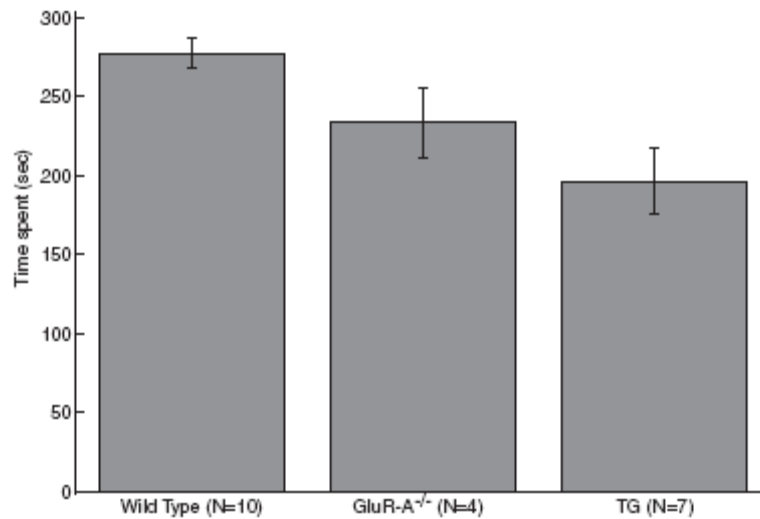
Figure 25. Time spent in the dark compartment in the light-dark-box revealed that mutant mice had the tendency to explore the light section more than WT mice. Values are mean±SEM.

All results considered, TG animals could be less anxious than WT mice (latency to cross is lower and time spent in the dark compartment is less). GluR-A$^{-/-}$ mice show a tendency, in respect to WT counterparts, to be less anxious (latency to cross is lower and time spent in the dark compartment is less). But this is just a tendency and not a significant difference.

Number of boli

The data did not satisfy the requirements of ANOVA (normality test failed ($P<0.05$)). Therefore a Kruskal-Wallis One Way Analysis of Variance on Ranks was conducted, which could not find a significant difference ($H(2)=2.113$, $P=0.348$). (TG=2±0.25-4, median and IQR; WT=0±0-0; GluR-A$^{-/-}$=2±1-2.5).
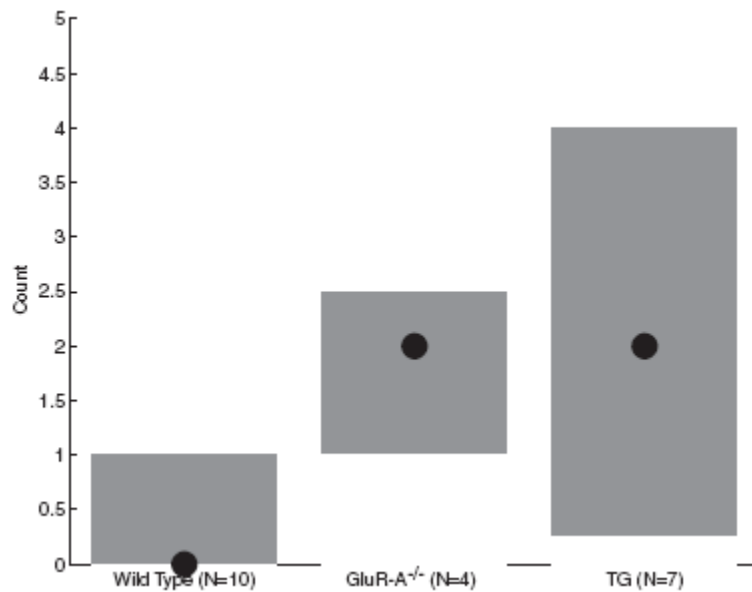
Figure 26. Number of boli, a presumed measure of anxiety, did not differ between experimental groups in the light-dark-box (dark first). Values are median and IQR.

Start from the light part

Latency to enter the black compartment

When the three groups were compared in terms of latency to enter the black compartment, WT mice were the quickest (35.5±27-85; median and IQR) followed by TG (41±16-80) and finally the GluR-A$^{-/-}$ (86±21.25-114.75) mice (Figure 27). However, the differences in the median scores and the spread of the distribution did not reach to statistically significant level. The normality test failed (P<0.05), hence, a Kruskal-Wallis One Way ANOVA on Ranks was conducted, which did not discover a significant effect (H(2)=0.336, P=0.846).
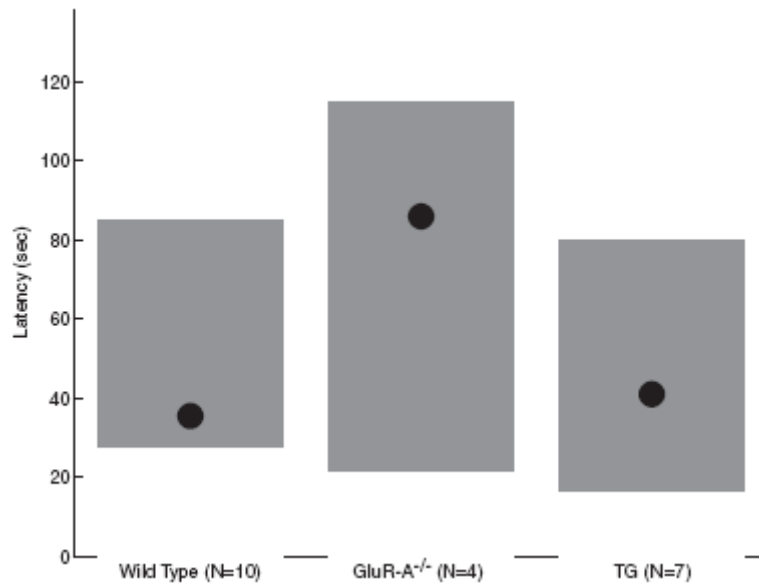
Figure 27. Light-dark-box paradigm (start in the dark compartment) showed that the three groups were statistically comparable with each other. Values are median and IQR.

Number of crossings

Mice were put into the light compartment first and they were let to shuttle between the light and dark sections of the apparatus as before. Although WT animals crossed (5.5±3-11, median and IQR), half as much as TG animals (11±3.5-28.75) and only 41% of the amount GluR-A$^{-/-}$ crossed (13.5±5.5-26.5), this tendency was not significant (Figure 28). The normality test passed (P=0.075) but the equal variance test failed (P<0.05). Thus, a Kruskal-Wallis One Way ANOVA on Ranks was chosen for the data analysis. This test could not exclude the possibility that the difference is due to random sampling variability e.g. no significant difference was discovered (H(2)=1.733, P=0.42).
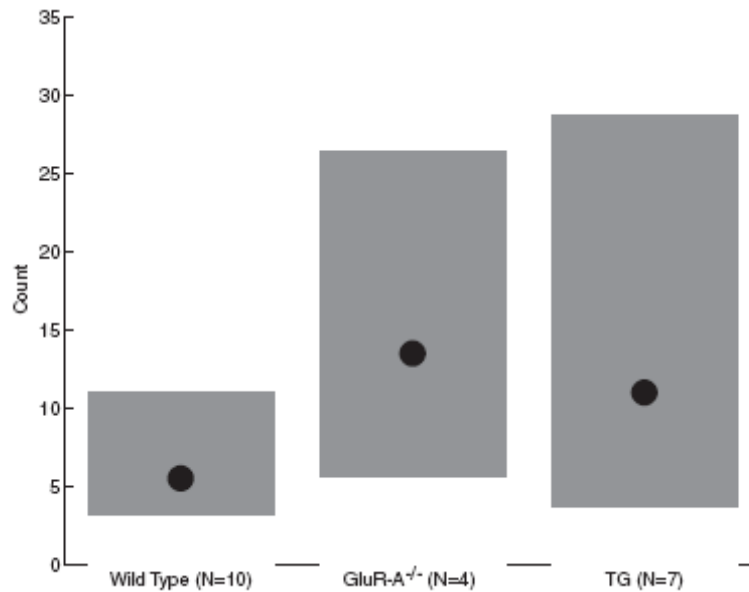
Figure 28. Number of crosses in the light-dark-box paradigm (start in the dark compartment) showed that the mutants were not anxious. Values are median and IQR.

Time spent in the dark compartment

Considering the statistically similar number of crossings between the two halves of the apparatus, it was important to quantify the time spent in the dark compartment. With 226.5± 11.222 sec (mean±SEM), WT mice spent the longest time in the black compartment. TG animals spent just 67% (152±33.101) and GluR-A$^{-/-}$ mice just 59% (133.5±50.5) of the time that WT mice spent there (Figure 29). A One Way ANOVA was conducted (normality test (P=0.224) and equal variance test (P=0.29) passed) which revealed a statistically significant difference for genotypes (F(2)=3.626, P=0.048). Post-hoc all pairwise comparisons showed that the difference for the means of WT versus GluR-A$^{-/-}$ mice was the highest with 93% (t=2.249, P=0.0373) followed by WT versus TG (74.5; t=2.163, P=0.0443) and the smallest difference for TG versus GluR-A$^{-/-}$ (18.5; t=0.422, P=0.678).
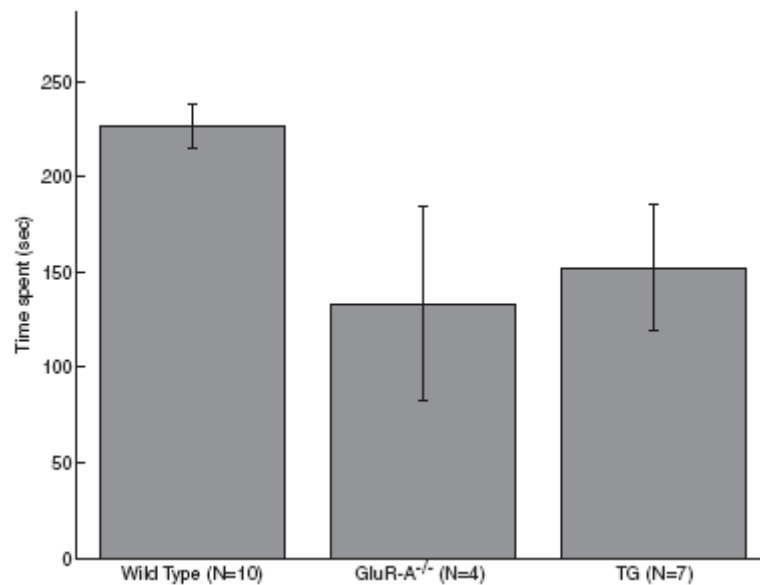
Figure 29. Time spent in the dark compartment in the light-dark-box showed that mutant mice showed the tendency to explore the dark section less than WT mice. Values are mean±SEM.

Number of boli

The number of boli each mouse left in the apparatus during the task was also counted. The data did not satisfy the requirements of an One Way ANOVA (normality test failed, $P<0.05$), hence, a Kruskal-Wallis One Way Analysis of Variance on Ranks was conducted, which did not show a significant difference between the genotypes (Figure 30; $H(2)=5.616$, $P=0.06$). (TG $=2\pm0.5$-6.75 (median and IQR), WT$=0\pm0$-0, GluR-A$^{-/-}=3\pm2$-4.5).
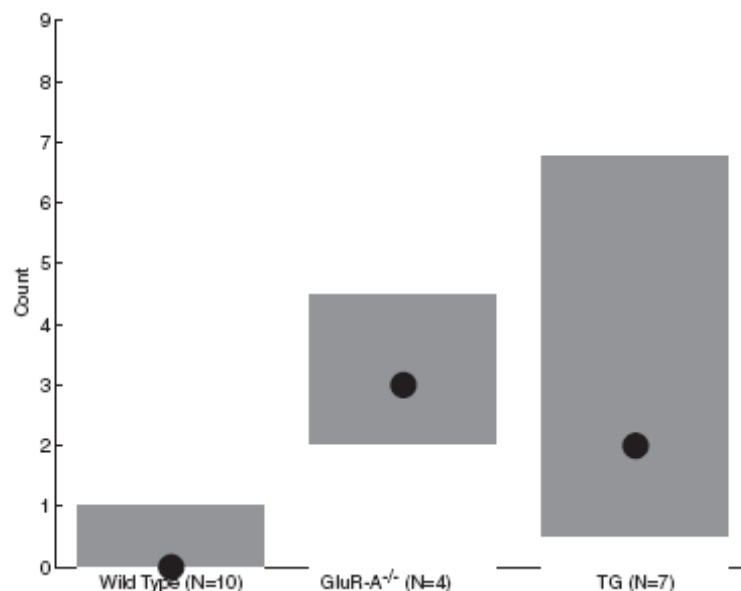
Figure 30. Number of boli did not differ between experimental groups in the light-dark-box. Values are median and IQR.

4.2.1.7. Successive alleys (a further development of the plus maze)

This test is based upon the fact that animals prefer darker areas and colours and also expanded cat-walks over narrow ones. Furthermore their drive to explore the environment in order to find food and a partner and on the other hand the anxiety to be exposed on a small bright area where they can be detected by predators put them into the dilemma to choose between exploration and hiding.

In the successive alleys task, the cat-walks the mice explore are without walls and elevated (as in the plus maze) but get thinner and thinner with every successful completion of the alley exploration. Rats with ventral hippocampal complex-lesions are less anxious, spending less time in the more anxiogenic sections compared to sham-operated controls and rats with lesions of amygdala and dorsal hippocampus lesions. In this task, I studied the latency to enter the first alley and total number of crossings.

Latency to enter the first alley

GluR-A$^{-/-}$ mice took longer to enter the first alley (300±300-300) compared to TG (165±42.5-273.25) and WT (110±70-300) mice (Figure 31). This result implies a tendency for GluR-A$^{-/-}$ mice to be more anxious in this task than WT animals and TG mice. However statistical analyses showed that the trend in the data is not significant. The normality test passed (P = 0.081) but the equal variance test failed. A Kruskal-Wallis One Way Analysis of Variance on Ranks was conducted as a non-parametric test. This could not detect a significant difference between the groups (H(2)=5.041, P=0.080)
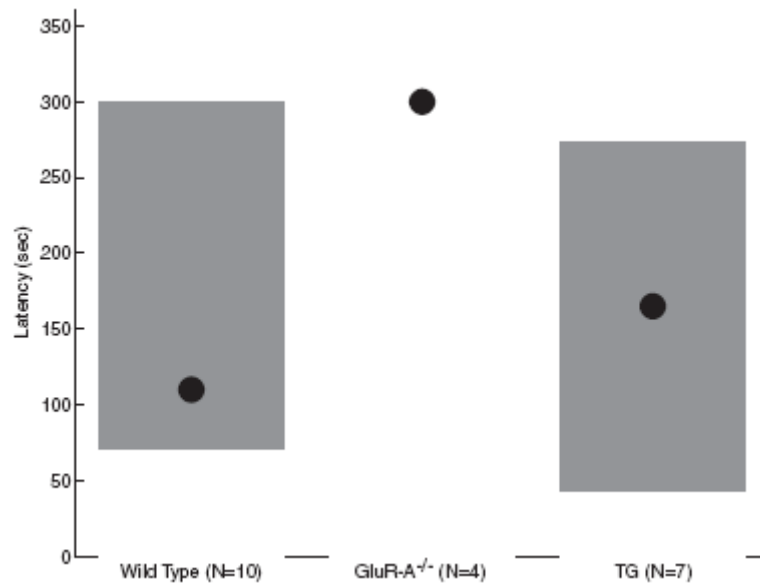
Figure 31. Latency to enter the first alley in the successive alleys did not differ across genotypes. Values are median and IQR.

Number of crossings in total

As previous analyses showed that all GluR-A$^{-/-}$ mice failed to enter the first alley upon initiation of the trial, their number of alley crossing shows a floor effect (0±0-0). However, the results from TG (8±1.5-19) and WT mice (3.5±0-5) show that TG animals crossed alleys more often than WT mice, which suggests they are less anxious or hyperactive. The data across the three groups did not fulfil the requirements of One Way ANOVA due to failed normality test (P<0.050). A Kruskal-Wallis One Way Analysis of Variance on Ranks was, therefore, conducted and revealed a statistically significant difference among the groups (H(2)=6.802, P=0.033). To isolate the groups that differ from one another, an all Pairwise Multiple Comparison Procedure (Dunn's Method) was chosen. The analysis revealed a significant effect only for the TG compared to GluR-A$^{-/-}$ mice, suggesting that GluR-A deletion increases anxiety in this task and transgenic expression of the transgene in TG mice rescues this phenotype (Figure 32).
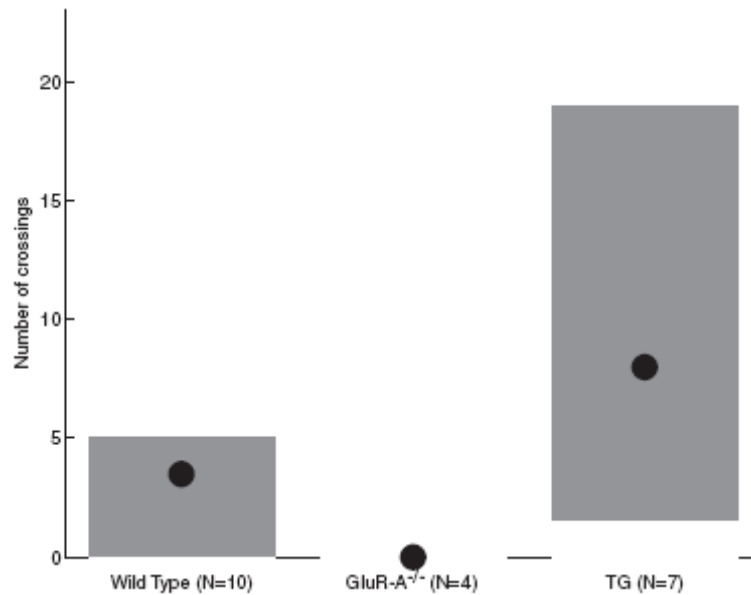
Figure 32. Number of crossings between alleys in the successive alleys task did only differ between TG an GluR-A$^{-/-}$ mice. Values are median and IQR.

4.2.1.8. Forced swimming test

Forced swimming test (FST), also known as Porsolt swimming test, is a standardized rodent model of human depression (Cryan et al, 2005; Petit-Demouliere et al, 2005; Chenu et al, 2006; do-Rego et al, 2006). It is commonly used to test the efficiency of anti depressants and anxiolytic drugs. I used this task to analyze further if the expression of the transgene in the TG mice could rescue the GluR-A deletion mediated behavioral phenotype.

FST is administered in two sessions with an interval of 24 hours. There are multiple factors, like sex of the subject, the depth and temperature of the water, amount of lightning etc., which influence animal behaviour in this task (i.e. Alonso et al, 1991; Petit-Demouliere et al, 2005). Therefore, the subjects were first grouped according to the gender and were tested under identical conditions including water temperature, water height, environment that the pool is placed and the amount of lightning.

There are several variables used to quantify the mobility in the forced swimming test. Among these variables latency to immobility, duration of mobility and distance traveled are widely used and pharmacological validated measurements of the behavioral despair in rodents.

Testing female mice in the PST

Latency to immobility

WT females (N=11) took 98±31 (mean±STD) seconds before they became immobile in the first session of the swimming test. In the second session, administered 24 h later, they reduced the latency to immobility to 39±34 sec (Figure 33, Paired T-test, P<0.0001) confirming the previous observations in the literature supporting the conclusion that learned helplessness acquired during the first session of FST results in reduced latency to immobility. GluR-A deletion significantly altered these statistics (Figure 33). During the first session GluR-A^{-/-} females (N=8) first became immobile after 361±272 sec, which was significantly later than WT mice (T-test, P=0.005). In the second session this pattern continued. GluR-A^{-/-} mice became immobile significantly later than WT mice (WT=39±34 vs GluR-A[-/-]=215±202, T-test, P=0.011). The small reduction in the latency to immobility within GluR-A^{-/-} across the sessions (361±272 sec vs 215±202 sec) was insignificant (Paired-T test, P=0.237).
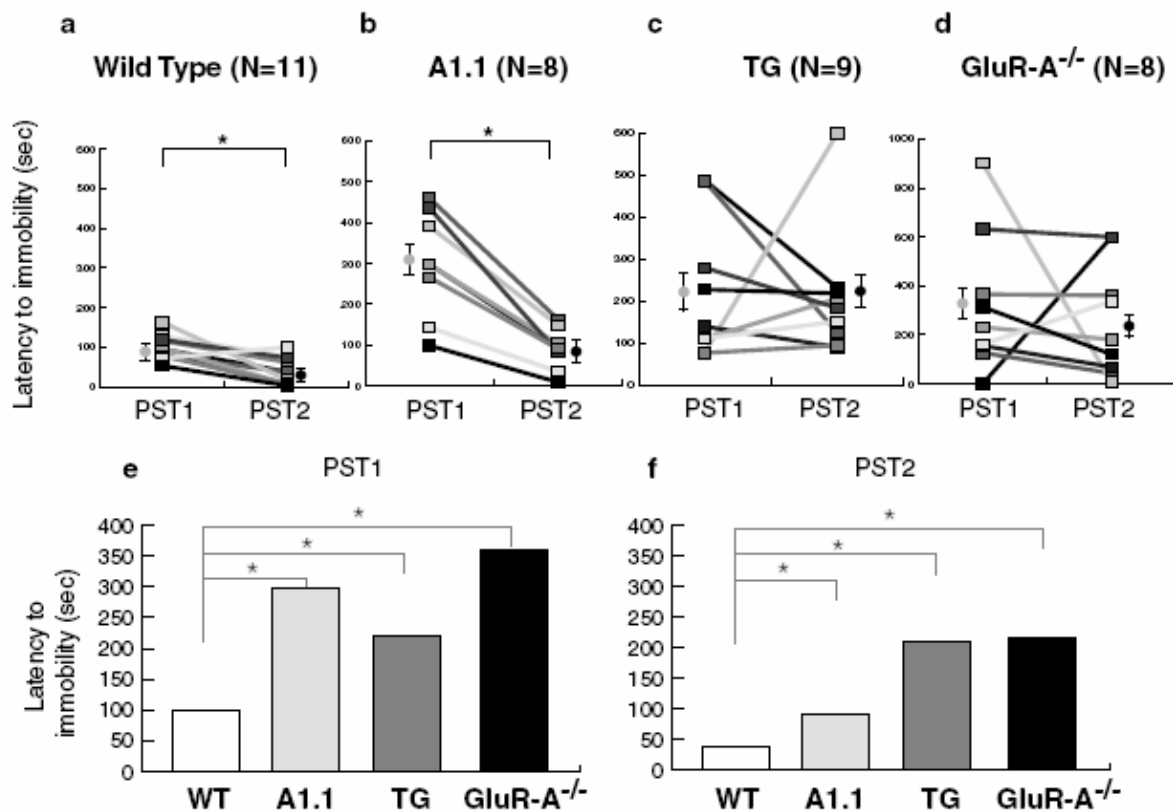
Figure 33. Comparison of the latency to immobility across genotypes and sessions in the forced swimming test. Data are only from female adult mice and values are mean±SEM. Asterisk denotes significance at P<0.05.

Expressing the GluR-A subunit with a point mutation in the PDZ interaction domain on the GluR-A$^{-/-}$ background did not significantly alter these statistics. TG females (N=9) became immobile 221±164 sec after the start of the first session and 211±155 sec after the second session had started (Figure 33). Similar to the GluR-A$^{-/-}$ females, latency to immobility on both sessions were significantly longer than those of WT mice (T-Test, PST1: P=0.025, PST2: P=0.002), however it was indifferent when compared within genotype across sessions (Paired T-test, P=0.9). These latency distributions were, furthermore, statistically indifferent compared to the GluR-A$^{-/-}$ mice (PST1: 221±164 sec vs 361±272 sec, P=0.214 PST2: 211±155 sec vs 215±202 sec, P=0.96). This phenotype was partially rescued in the A1.1 by expressing a transgenic GluR-A subunit in the GluR-A$^{-/-}$ background (Figure 33). A1.1 females (N=8) took 299±130 sec to become immobile in the first swimming test. Compared to WT this represents three fold increased latency to become immobile (T-test, P<0.001). A1.1 mice, nonetheless, were significantly indifferent from GluR-A$^{-/-}$ (T-test, P=0.57) and TG mice (T-test, P=0.3).

Repeating the forced swimming test 24 h later resulted in a significantly earlier onset of immobility in A1.1 animals (90±52, Paired T-test, P<0.001), which was later than in the group of WT mice (T-test, P=0.02) and shorter than TG mice's latency to immobility on this session (T-test, P=0.05). Albeit the tendency for a difference between the GluR-A$^{-/-}$ and A1.1 mice, it failed to reach statistical significance (Figure 33, T-test, P=0.1).

Animals that become immobile earlier are likely to stay immobilized more often therefore travel less distance during the session. This could be easily calculated from the distance traveled within a session.

Distance traveled

This analysis showed that indeed the genotype, which became immobile the earliest (WT), traveled the least distance in the task (Figure 34). WT females traveled 50.1±18.8 m throughout the first session. This was significantly less than distance traveled by the GluR-A$^{-/-}$ (69.9±14.8 m, T-test, P=0.02) and A1.1 mice (67.9±17.2 m, T-test, P<0.05). Although there was a tendency towards more distance traveled by the TG mice (62.2±14.3 m) compared to the WT, this comparison failed to reach statistical difference (Figure 34, WT vs TG, P=0.1286, WT vs A1.1, P<0.13).

Repeating the forced swimming test session a second time revealed a similar pattern of duration of exploration across genotypes. WT females traveled less than GluR-A

(26.14±15.4 m vs 44.25±12.9 m, T-test, P<0.01) and TG mice (43±9 m, T-test, P=0.015). The only difference in this session was that A1.1 mice traveled statistically similar distance to WT mice (32.8±4.83 m, T-test, P=0.25).

When within genotype across session comparisons performed all groups showed statistical reduction in the distance traveled (Figure 34). However, this is due to the difference in the duration of sessions. PST1 takes 15 min and PST2 10 min. Therefore a direct comparison between the two sessions and how the mobility changes across these sessions can only be done after normalizing the distance traveled to the duration of the session.
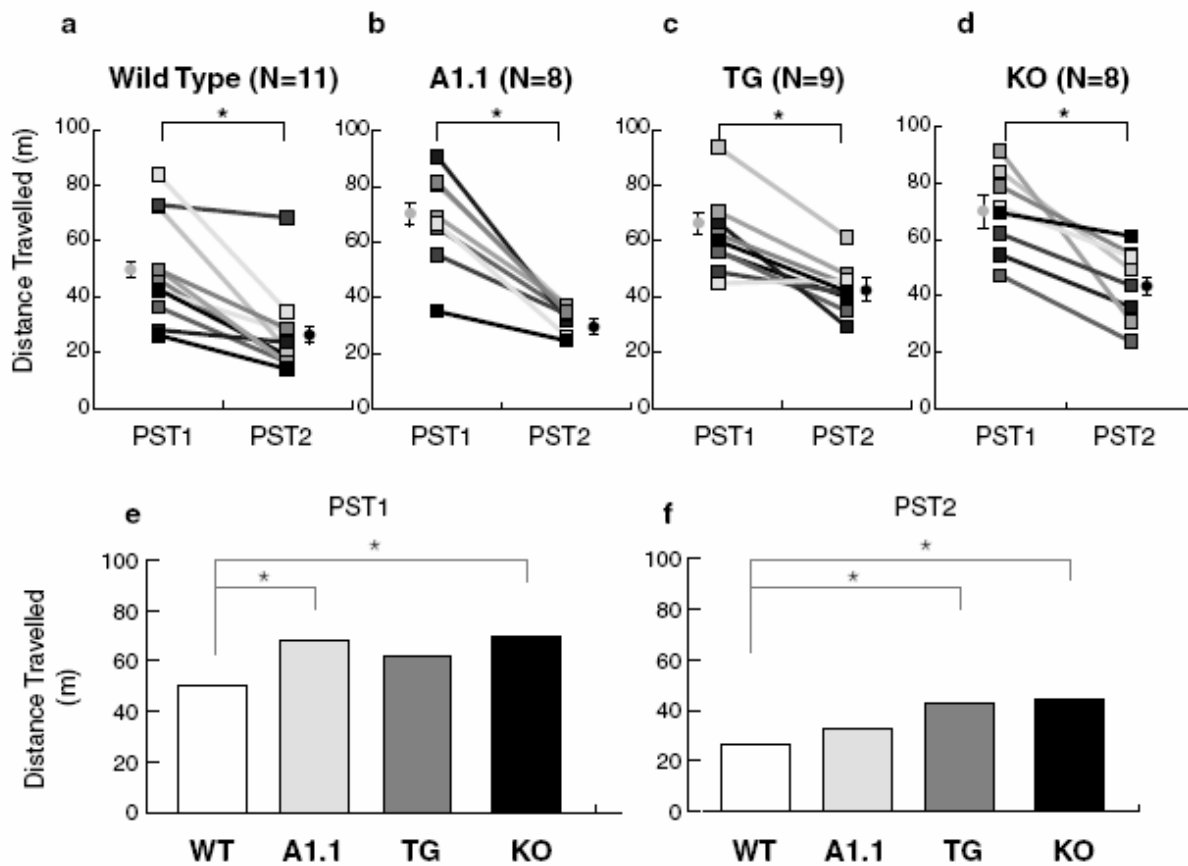
Figure 34. Comparison of distance traveled in the forced swimming test. Data are only from female adult mice and values are mean±SEM. Asterisk denotes significance at P<0.05.

When distance traveled is normalized by the duration of the session, it was found that WT females had the highest probability of immobility across both sessions.

Normalized immobility

In the first session WT mice were immobile on average 45±17% of the time which increased to 57±17% in the second session (Paired T-test, P=0.05). In both sessions WT mice were immobile longer compared to GluR-A$^{-/-}$ (PST1: 25±8, T-test, P=0.007; PST2: 31±16, T-test, P<0.001), TG (PST1: 27±4, T-test, P=0.009; PST2: 26±7, T-test, P<0.005) and to a certain extent compared to A1.1 females (PST1: 32±13, T-test, P=0.08; PST2: 36±9, T-test, P<0.01). None of the genetically engineered lines significantly increased their probability of immobility across the sessions (Figure 35).
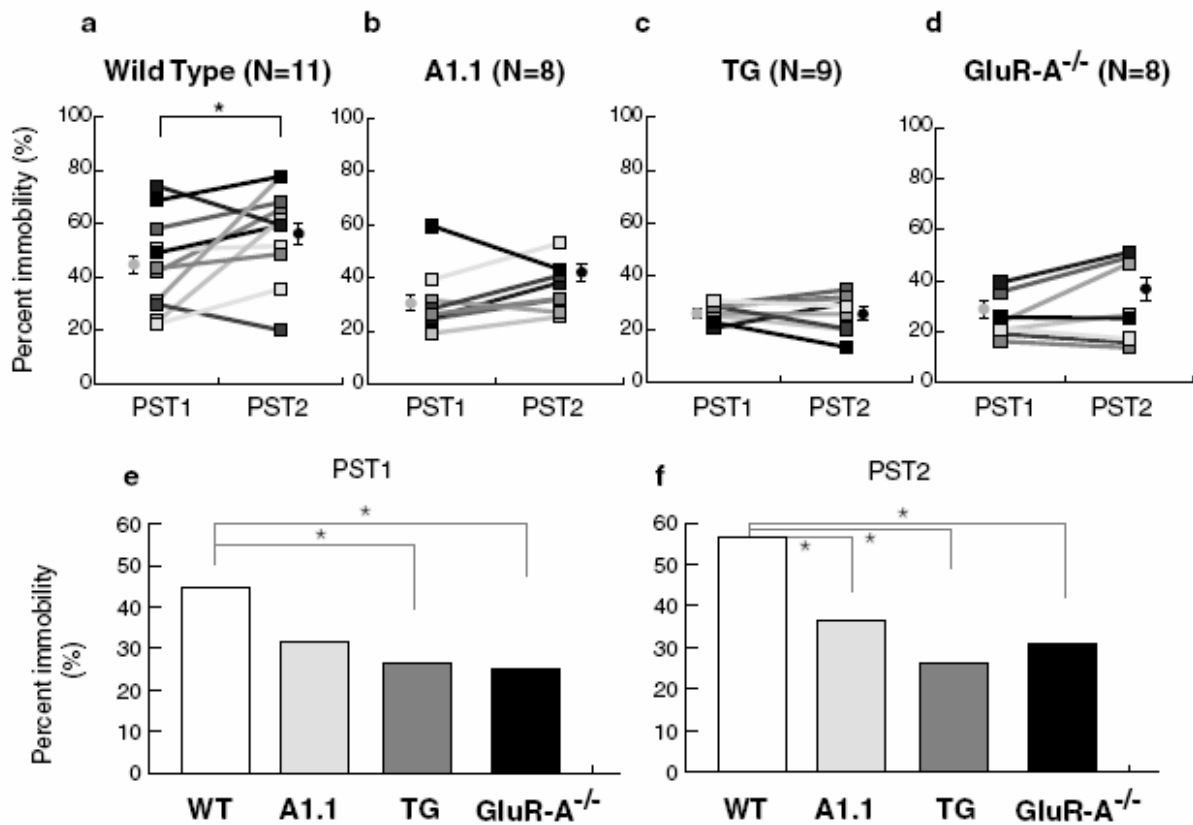
Figure 35. Comparison of the percent immobility across genotypes and sessions in the forced swimming test. Percent immobility is calculated by a ratio between the distance traveled and the duration of the experimental session (PST1: 15 min, PST2: 10 min). a-d individual animals of a certain genotype in PST1 and PST2. e-f mean value of the animals grouped in genotypes for PST1 and PST2. Data are only from female adult mice and values are mean±SEM. Asterisk denotes significance at P<0.05.

Variables studied so far includes latency to immobility, distance traveled and duration of immobility, all of which are influenced by the speed of the animal mobility in the task. Therefore, the maximum swim speed of each animal and the mean of the swim speed for each group is calculated for each session and compared across genotypes and sessions.

72

Maximum swimming speed

Maximum swimming speed achieved by WT and genetically modified animals were comparable in both sessions (Figure 36). During the first session, the groups swam with an average maximum speed of ~5.5 cm/sec, which was distributed across genotypes as follows: WT, 5.4±0.7 cm/sec; GluR-A$^{-/-}$, 5.8±0.4 cm/sec; TG, 5.3±0.5 cm/sec and A1.1, 5.2±0.3 cm/sec. None of the pairwise comparisons show any significant relationship between any of the genotypes studied (Figure 36). The swimming speed distribution in the second session followed a similar trend, albeit a nominal reduction in the WT (4.5±0.7 cm/sec) and A1.1 mice (4.9±0.4 cm/sec). GluR-A$^{-/-}$ (5.9±1.4 cm/sec) and TG (5.4±0.7 cm/sec) females had a slight tendency for faster movement in the second session, although paired T-test within genotypes showed a statistical difference only for WT mice ($P<0.01$).
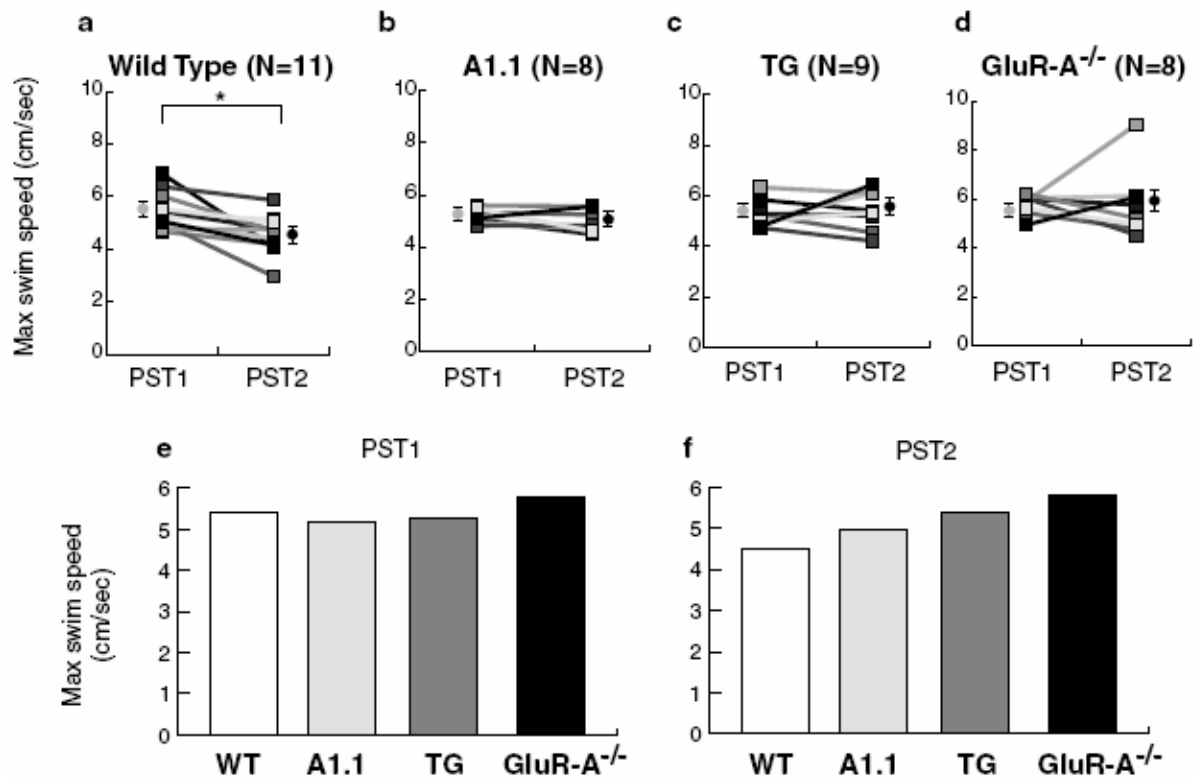
Figure 36. Comparison of the maximum swim speed across genotypes and sessions in the forced swimming test. a-d individual animals of a certain genotype in PST1 and PST2. e-f mean value of the animals grouped in genotypes for PST1 and PST2. Data are only from female adult mice and values are mean±SEM. Asterisk denotes significance at $P<0.05$.

As mentioned previously, males differently respond to the uncontrollable and unpredictable nature of the swimming stress (Alonso et al, 1991). Therefore, it is feasible that expressing the TG construct in males can differentially alter the behavioral phenotype on this task.

Testing male mice in the PST

Latency to immobility

WT males (N=13) took 168±153 (mean±STD) seconds before they became immobile during the first run of the FST (Figure 37). During the second run of the test, 24 h later, they came to the immobile state faster within 79±85 seconds (Paired T-test, P=0.02) suggesting that having a previous forced swimming experience results in an earlier onset of inactivity similar to the one observed in females.

GluR-A$^{-/-}$ males (N=10) had a tendency to become immobile later than the WT mice (240±146 sec vs 168±153 sec) although this difference failed to reach statistical significance (P=0.26). GluR-A$^{-/-}$ mice behaved similar to WT mice in the second run of the swimming test (Figure 37). Compared to the PST1 they became immobile significantly faster (240±146 sec vs 107±62 sec, Paired T-test, P<0.001).

Expressing the PDZ interaction domain mutated GluR-A subunit as a transgene on the GluR-A$^{-/-}$ background, however, resulted in substantial changes (Figure 37). TG males (N=9) became immobile significantly later (362±153 sec) than WT (P<0.01) but not than GluR-A$^{-/-}$ mice (P=0.09). During PST2 the difference between TG mice and other groups became even more apparent as TG mice did not significantly reduce the time they required to become immobile (PST1: 362±153 sec vs PST2: 253±174 sec, Paired T-test, P=0.1) although both WT and GluR-A$^{-/-}$ mice had statistically smaller latency to immobility (see above).

Expressing a copy of the naive GluR-A on the GluR-A$^{-/-}$ background did not alter the behavior of the GluR-A$^{-/-}$ mice. A1.1 males (N=9) became immobile at a statistically similar time course (280±200 sec) to the other groups of mice tested (Figure 37). As for WT and GluR-A$^{-/-}$ males, the latency to immobility was significantly reduced in the second forced swimming test. A1.1 males took only 56±50 sec to become immobile during PST2. Considering the latencies across the other three groups, this result suggests a significantly faster onset of immobility compared to TG (P=0.005) but not WT (P=0.48) and GluR-A$^{-/-}$ (P=0.07) mice.
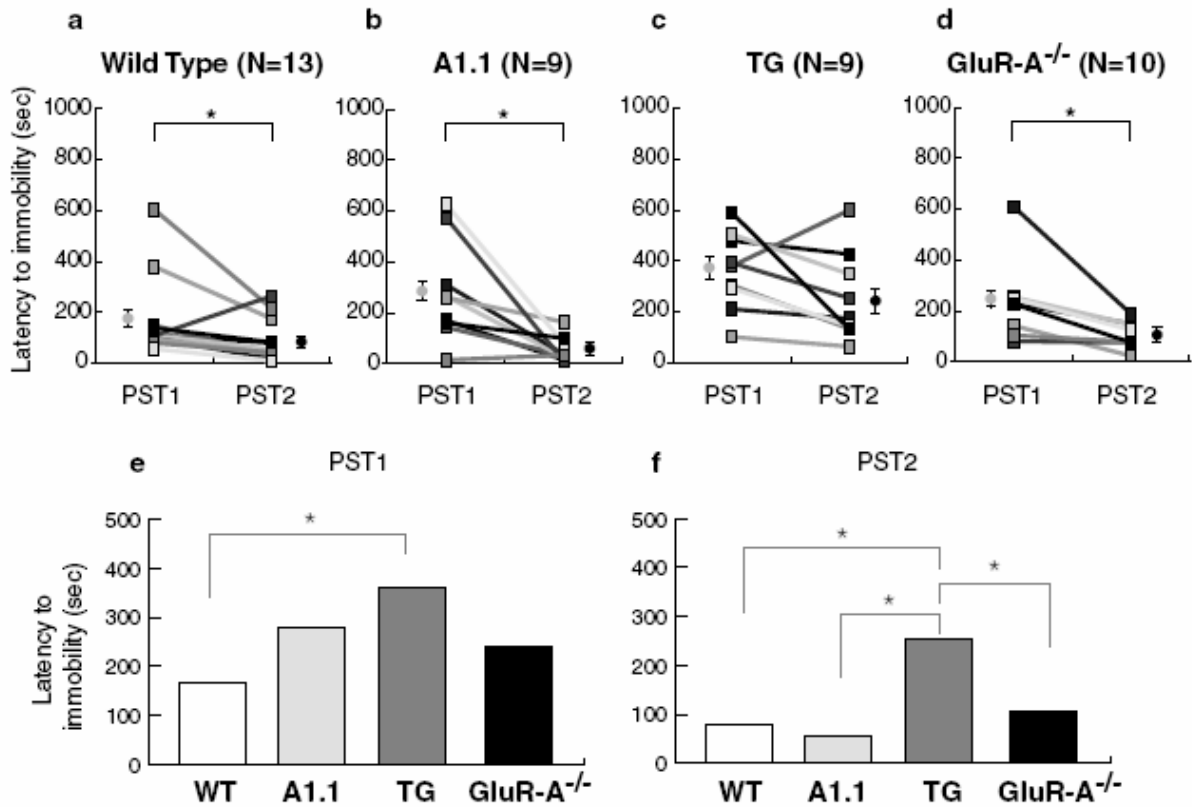
Figure 37. Comparison of the latency to immobility across genotypes and sessions in the forced swimming test. a-d individual animals of a certain genotype in PST1 and PST2. e-f mean value of the animals grouped in genotypes for PST1 and PST2. Data are only from male adult mice and values are mean±SEM. Asterisk denotes significance at P<0.05.

Amount of immobility, quantified as the percent of the time the animal is inactive, is inversely correlated with the latency to immobility. As the animal gets to become immobile later, the duration of immobility gets shorter. Therefore, it was expected from the analysis of latency to immobility that duration of immobility will be higher for WT mice and smaller for TG mice.

Normalized immobility

WT males were immobile 37±10 % of the time during the PST1 (Figure 38). This duration had just a tendency to increase in the second session (41±17%, Paired T-test, P=0.18). GluR-A$^{-/-}$ males displayed more prominent increase in immobility across the sessions (PST1: 29±10% vs PST2: 36±15%, Paired T-test, P=0.03) although in neither session overall activity of the GluR-A$^{-/-}$ males was significantly different from those of WT (PST1: P=0.065; PST2: P=0.414). Expressing the GluR-A subunit with a mutation at the PDZ interaction domain on the GluR-A$^{-/-}$ background, markedly altered these statistics (Figure 38). In the first session, immobility of the TG males was significantly less than for WT (T-test, P<0.001) but not

GluR-A$^{-/-}$ mice (T-test, P=0.077). During the second session, in contrast to the tendency of WT and GluR-A$^{-/-}$, TG mice did not increase the duration of immobility (PST1: 22±4% vs PST2: 21.4±7%, Paired T-test, P=0.765). Their immobility was significantly shorter than the immobility of both WT (T-test, P=0.003) and GluR-A$^{-/-}$ mice (T-test, P=0.02). Expressing a native version of the GluR-A on the GluR-A$^{-/-}$ background did not show the same behavioral phenotype like TG mice displayed (Figure 38). A1.1 males were significantly less mobile compared to the TG mice in the first (22.4±4% vs 31±7%, T-test, P=0.005) and the second session (21±7% vs 44±9), although their mobility was comparable to those of WT and GluR-A$^{-/-}$ mice across both sessions (Figure 38).

Figure 38. Comparison of the percent immobility in the forced swimming test across genotypes and sessions. a-d individual animals of a certain genotype in PST1 and PST2. e-f mean value of the animals grouped in genotypes for PST1 and PST2. As described before, percent immobility is calculated by dividing the distance traveled throughout a session by the duration of the session. Data are only from male adult mice and values are mean±SEM. Asterisk denotes significance at P<0.05.

Onset of immobilization and duration of overall mobility within a session significantly contributes to the distance traveled on this paradigm.

Distance traveled

WT males swam 56.5±12.7 m within the 15 minutes long first session of the forced swimming test. As in the previous measurements GluR-A$^{-/-}$ mice were comparable to the WT mice in terms of the distance traveled within the first session (67.1±21.3 m, T-test, P=0.15). Despite the longer duration of immobility of the GluR-A$^{-/-}$ mice compared to TG (GluR-A$^{-/-}$ 29±10% vs TG=22±4%, P=0.077), the total distance traveled within the session across these two genotypes did not significantly differ (67.1±21.3 m vs 78.9±11 m, T-test, P=0.15). Nonetheless, TG mice traveled significantly more distance compared to the WT mice (56.5±12.7 m vs 78.9±11 m, T-test, P<0.001). Similar results were observed also for the WT and A1.1 comparison (56.5±12.7 m vs 73.6±11.8 m, T-test, P<0.005) but not for those comparisons between A1.1 and GluR-A$^{-/-}$ (67.1±21.3 m vs 73.6±11.8 m, T-test, P=0.43) or TG (78.9±11 m vs 73.6±11.8 m, T-test, P>0.33). The pattern of the observed distance traveled in the second session was mostly comparable to that of the first session. WT and GluR-A$^{-/-}$ mice traveled comparable distances (31.2±12.4 m vs 31.1±21.3 m, T-test, P=0.33) and TG mice swum (46.7±11.9 m) more than WT mice (T-test, P<0.001) but this time A1.1 mice did not (T-test, P>0.1). The only difference in the second session, in respect to the first one, was that A1.1 mice acquired an activity pattern (distance traveled: 33.6±6.3 m) rather comparable to WT animals (T-test, P=0.6) than to the TG like behavioral phenotype (T-test, P<0.01) in terms of distance swum in the first session.
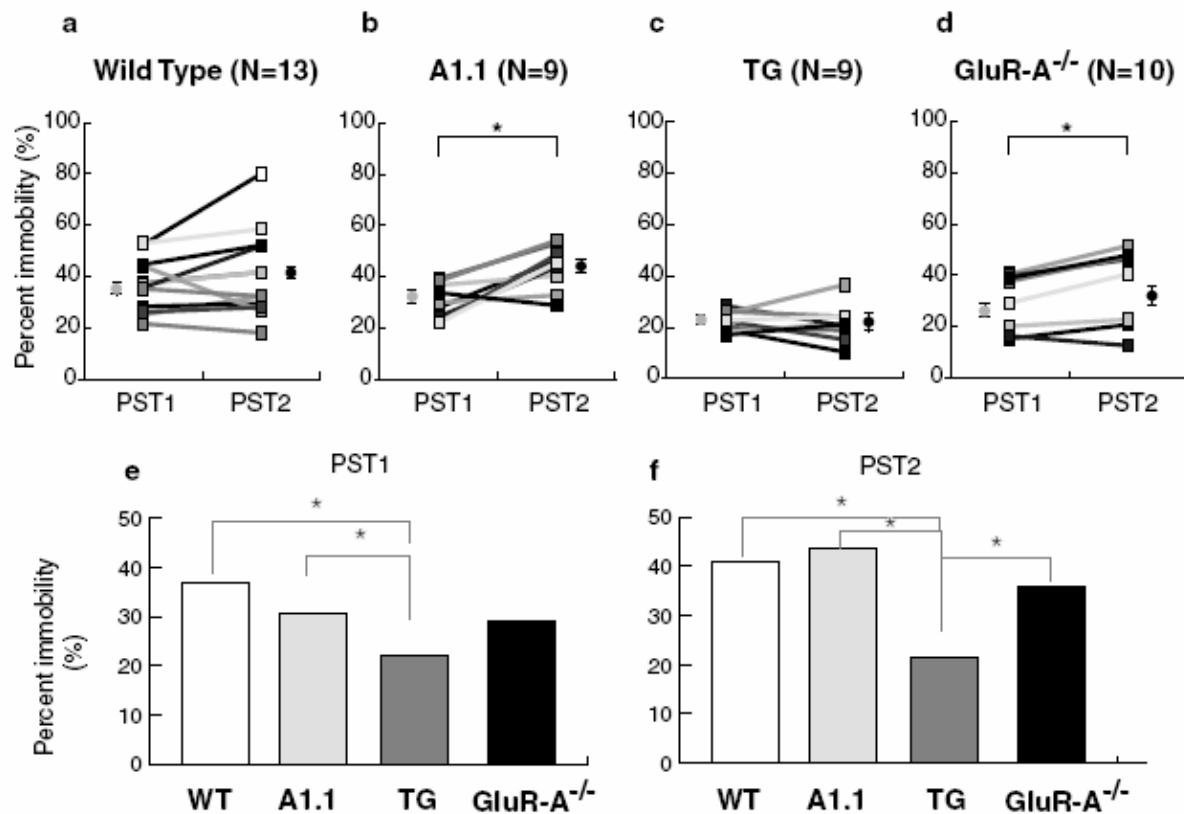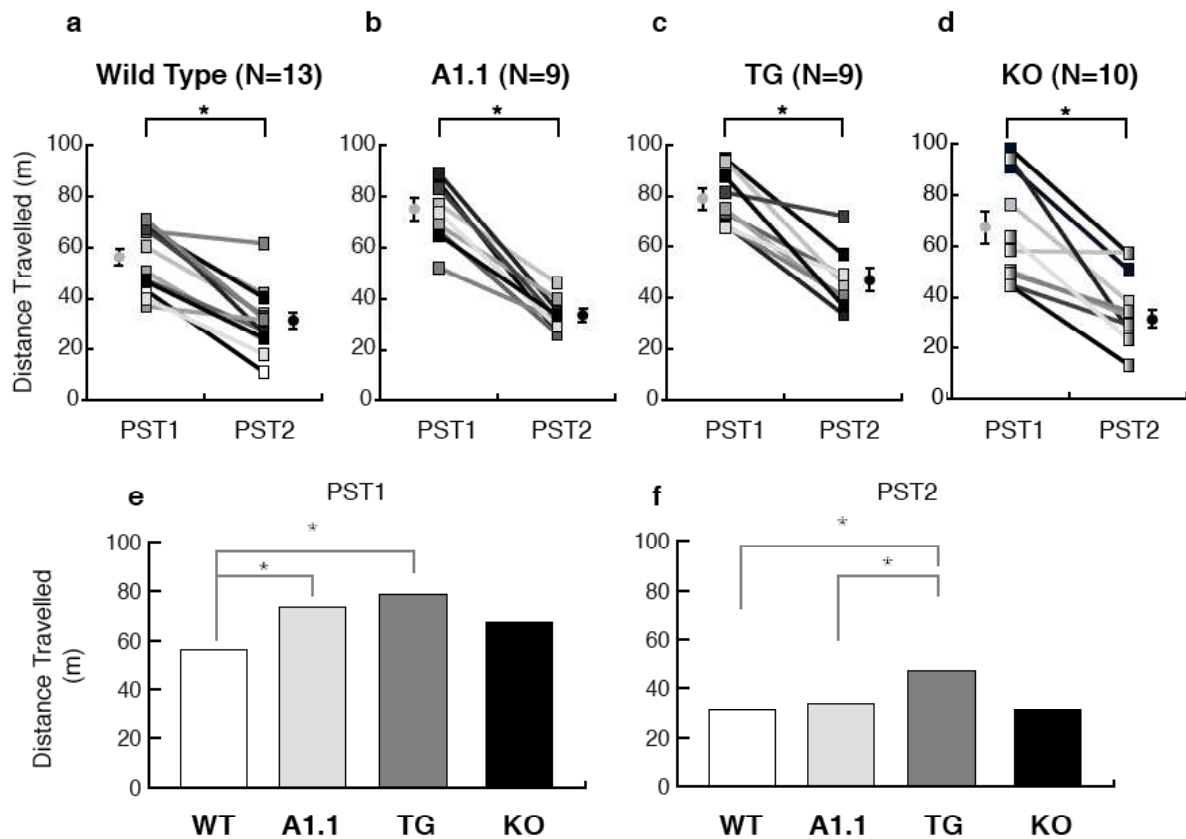
Figure 39. Comparison of the distance traveled across genotypes and sessions in the forced swimming test. a-d individual animals of a certain genotype in PST1 and PST2. e-f mean value of the animals grouped in genotypes for PST1 and PST2. Data are only from male adult mice and values are mean±SEM. Asterisk denotes significance at P<0.05.

The quantification of the distance traveled might have been confounded if the genotypes studied differed in terms of speed of movement. Therefore, the maximum swim speed of each animal and the mean of the swim speed for each group is calculated for each session and compared across genotypes and sessions.

Maximum swim speed

The results showed that there was no significant genotype effect. On average maximum swimming speed across the four genotypes studied varied between 5.5-6.5 cm/sec. WT mice had a tendency of displaying a higher average maximum speed (6.5±4.2 cm/sec) compared to GluR-A$^{-/-}$ (5.6±0.3 cm/sec), TG (5.5±0.5 cm/sec) and A1.1 (5.5±0.4 cm/sec), although none of the pairwise comparisons was significant (Figure 40). Similar lack of difference continued also in the second swimming test. All groups had an average of ~5 cm/sec

maximum speed of movement in the task (WT=5.3±0.6 cm/sec; GluR-A$^{-/-}$=5.6±1.3 cm/sec; TG=5.1±3.4 cm/sec; A1.1=5.1±0.5 cm/sec)
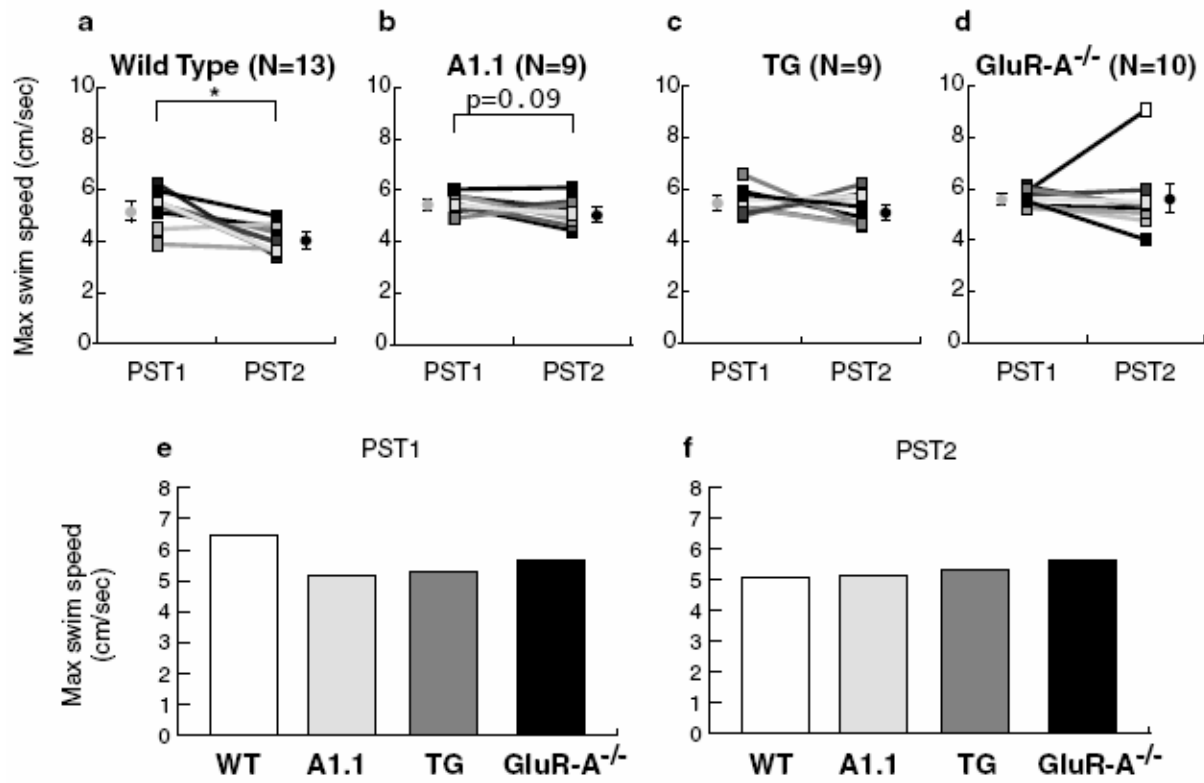
Figure 40. Comparison of the maximum swim speed as a measure of swim speed distribution across genotypes and sessions in the forced swimming test. a-d individual animals of a certain genotype in PST1 and PST2. e-f mean value of the animals grouped in genotypes for PST1 and PST2. Data are only from male adult mice and values are mean±SEM. Asterisk denotes significance at P<0.05.

4.2.1.9. Open field

The results of the forced swimming test suggest that the genetic alterations involving GluR-A containing AMPA receptors result in increased mobility and possibly reduced anxiety. In order to control if these results are confounded by the task, animals were given an open field session and the statistics of animal mobility was quantified. Because the mobile activity of the animal on the open field did not differ across genders, the results are presented after combining the two genders.

WT mice, as in the forced swimming test, were less active than the other three groups of mice studied on the open field task (Figure 41a). Within the 6 minutes long session, WT mice travelled 17.5±2.33 m (mean±STD) while the GluR-A$^{-/-}$ (22.3±5.6, T-test, P=0.002) and

A1.1 (22.8±4.7, T-test, P<0.001) mice explored the environment significantly more than WT animals. TG mice travelled 20.6±8.7 m, statistically similar to the WT mice (T-test, P=0.15).
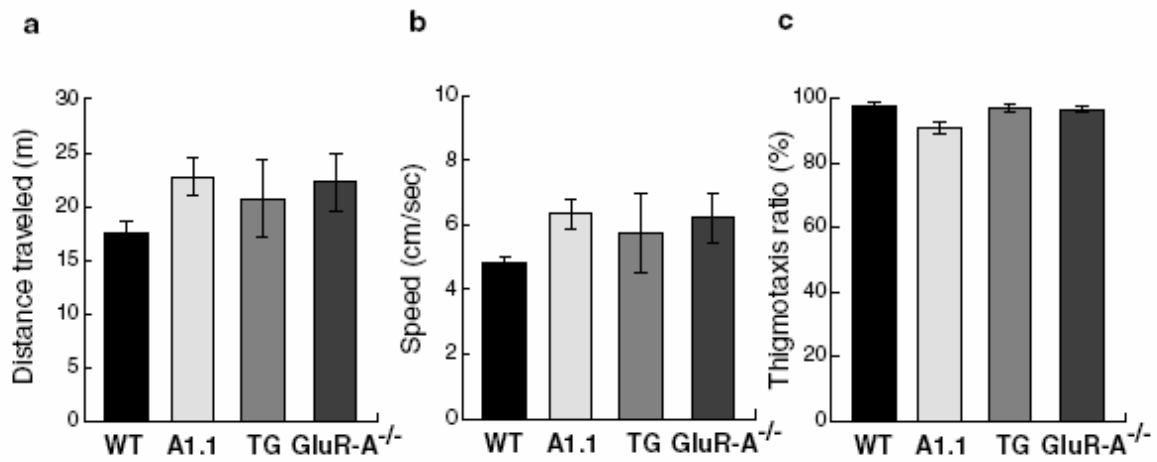
Figure 41. Motor activity as studied in an open field. Three variables, namely distance traveled (a), speed of movement (b) and Thigmotaxis ratio (c) were quantified to study the pattern of motor activity. Values are mean±STD.

Changes in the speed of movement across genotypes followed the pattern described for the distance travelled in the open field task (Figure 41b). WT mice showed the worst performance (4.8±0.6 cm/sec) among the genotypes studied. Compared to GluR-A^{-/-} (6.2±1.5 cm/sec) and A1.1 (6.3±1.3 cm/sec), WT mice travelled significantly slower (T-test, P<0.005). TG mice, once more, behaved statistically similar to the WT animals (5.7±2.4 cm/sec, T-test, P<0.15). There was no statistical interaction between any of the other pairwise comparisons.

Increased motor activity on the open field can be either due to reduced anxiety or, alternatively, because of hyperactivity. One variable that could potentially dissociate the source of the increased locomotor exploration is the thigmotaxis. Thigmotaxis is described as the natural tendency of the rodent to explore new environments while keeping in close contact with a wall. In the open field, mice therefore preferentially explore the periphery of the arena for prolonged periods of time before starting to visit the center portion. Most commonly, thigmotaxis ratio is described as the ratio between the duration of exploration at the periphery and duration of the experimental session. As shown in Figure 41c, independent from the genotype studied all mice overwhelmingly preferred to explore the periphery of the apparatus >90% of the time. Among the pairwise comparisons performed, WT mice differed only from the A1.1 (WT=97.2±1 vs A1.1=91±0.1, T-test, P<0.001) but not from GluR-A^{-/-} (WT=97.2±1 vs A1.1=96.4±0.02, T-test, P=0.3) or TG mice (WT=97.3±1 vs A1.1=91±0.1, T-test, P=0.63).

These results complement the findings in the swimming task and support the conclusion that alteration in GluR-A containing AMPA receptors results in hyperactivity.

4.2.1.10. T-maze

On the T-maze, a non-matching-to-place (NMTP) task, each trial consists of two runs: a sample run and a choice run. During the sample run the mouse is directed to one of the two arms; on the subsequent choice run, it is rewarded if it chooses the previously unsampled arm. TG and GluR-A$^{-/-}$ mice were profoundly impaired on this working memory paradigm relative to WT animals (Figure 42). WT mice reached to an asymptotic level of success rate (89% ± SEM), by the end of training, comparable to previously published results and other T-maze results presented in this thesis, whereas TG (49%) and GluR-A$^{-/-}$ mice (56%) were profoundly impaired even at the end of the training protocol after 48 trials. The chance level performance of the TG mice until the last day of testing, suggests that expression of this altered GluR-A subunit does not rescue the working memory deficit in the T-maze task.

Four sessions each consisting of 12 trials were conducted in this set of experiments. There was a difference between WT mice and the other groups from the first block of the testing phase on (WT=64.286%, GluR-A$^{-/-}$=43.750%, TG=50%). While the performance level of WT mice increased with training (difference of means=25, t=4.232, P=0) and learning took place within the first two sessions (difference of means=17.857, t=3.023, P=0.004), GluR-A$^{-/-}$ mice improved only 12.5% (difference of means=12.5, t=1.6, P=0.117) while TG mice even alternated less (1%) than at the beginning. TG and GluR-A$^{-/-}$ did not differ from each other (TG=48.511±2.414% (mean±SEM), GluR-A$^{-/-}$=48.437±3.194%) while both differed significantly from WT mice (WT=79.464 ±2.414%).

There was a significant difference between genotypes (F(2)=50.309, P<0.001; Normality Test , P<0,050 and Equal Variance Test, P=0,939) when training sessions are considered. However, no main effect of the training session (F(3)=4.313, P=0.009) or genotype by training session interaction was observed (F(6)=2.356, P=0.046).

Pairwise multiple comparisons (Holm-Sidak method) were conducted to pin-point which genotypes differ from each other. These comparisons revealed a significant difference for WT vs TG (difference of means=30.954, t=9.065, P<0.001) and WT vs GluR-A$^{-/-}$ (difference of means=31.027, t=7.749, P<0.001) but not for TG vs GluR-A$^{-/-}$ (difference of means=0.0732, t=0.0183, P=0.986). The comparison for the factor block within groups showed only a significant difference within the group of WT animals, which improved from

block to block significantly (All Pairwise Multiple Comparison Procedures (Holm-Sidak method).
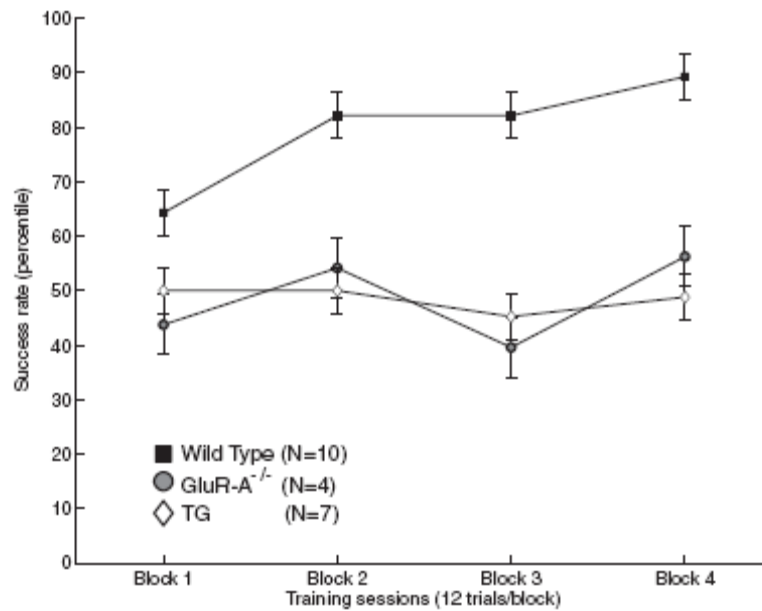
Figure 42. Success rates in the T-maze task showed that GluR-A$^{-/-}$ mice were impaired in the acquisition of this spatial working memory task and that expression of the GluR-A subunit with the mutation at the PDZ interaction domain did not rescue the memory deficit. Values are mean ±SEM

The comparison for the training sessions across genotypes revealed a significant difference only for block 1 versus block 4 (difference of means=12.103, t=3.174, P=0.00271).

The comparison of the different training sessions in the different groups themselves revealed for block 1 versus block 4 a significant difference in WT (difference of means=25, t=4.232, P<0.05), but not in TG (difference of means=1.19, t=0.202, P=0.841) or GluR-A$^{-/-}$ mice (difference of means=12.5, t=1.6, P=0.117).

Success rate in T-maze during the 1st block

From the first day on WT mice performed significantly better than GluR-A$^{-/-}$ and TG mice, which differed almost not at all and were therefore not significantly different from each other (Figure 43; WT=64.286±4.177%; GluR-A$^{-/-}$=43.750±5.525%, TG=50±4.177%), (Difference of means: WT vs GluR-A$^{-/-}$=20.536, t=2.848, P=0.006; WT vs TG=14.286, t=2.323, P=0.024; TG vs GluR-A$^{-/-}$=6.250, t=0.867, P=0.39).
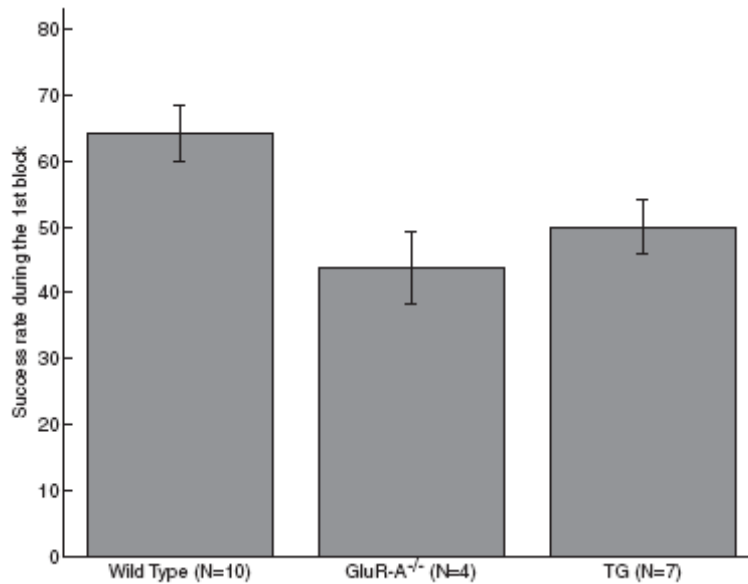
Figure 43. Alternation measured in the first training block of the T-maze was significantly different across genotypes. Values are mean±SEM.

Success rate in T-maze during the 4th block

Including the last block GluR-A$^{-/-}$ and TG animals did not improve significantly and their performance on the T-maze was impaired compared to WT mice (Figure 44). Neither GluR-A$^{-/-}$ mice (56%) nor TG mice (49%) performed better than chance level (TG=48.810±4.177% (mean±SEM), GluR-A$^{-/-}$=56.25±5.525%) whereas WT animals (89%) increased their level of performance significantly (WT=89.286±4.177%), (difference of means: WT vs TG=40.476, t=6.581, P<0.001; WT vs GluR-A$^{-/-}$=33.036, t=4.581, P<0.001; TG vs GluR-A$^{-/-}$ =7.44, t=1.032, P=0.306). This shows that GluR-A$^{-/-}$ mice have a deficit in spatial working memory on the rewarded T-maze (NMTP) task as shown before (McHugh et al, 2004; Reisel et al, 2002) and that the transgene with the mutated PDZ interaction domain cannot rescue the phenotype.
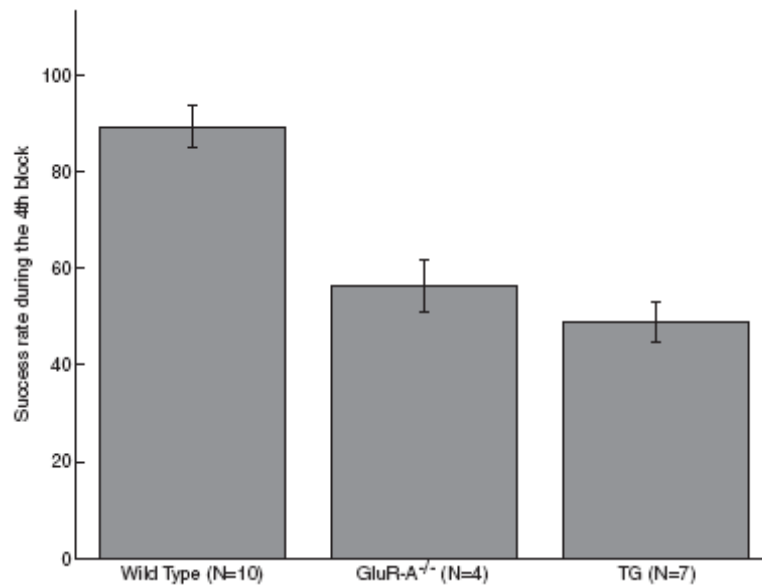
Figure 44. After training in the T-maze for 48 trials, the success rate of WT mice was still better than of the mutant mice. Values are mean±SEM.

4.2.2. WT | GluR-A$^{-/-}$ | SA

4.2.2.1. Accelarating rotarod

WT mice started already with a performance level of 277.5±17.431 (mean ±SEM) seconds (maximum=300 sec) so that a significant improvement over the sessions was not possible due to statistical ceiling effect. SA and GluR-A$^{-/-}$ mice started much lower and learned over the sessions and acquired the task until they did not differ significantly in performance from WT animals (block8: WT vs GluR-A$^{-/-}$: difference of mean=77.857, t=2.222, P=0.03; WT vs SA difference of means=61.125, t=1.805, P=0.076; SA vs GluR-A$^{-/-}$ difference of means =16.732, 0.477, P=0.635). Although the difference for SA and GluR-A$^{-/-}$ mice was not significant during the first day, they learned the task with a different speed. While SA mice show a learning effect from day four on, GluR-A$^{-/-}$ mice start to improve their performance from day four on. Looking at the whole test period they do differ significantly from each other. A pairwise multiple comparison (Holm-Sidak) for the factor genotype revealed the significant difference (difference of means: wt vs GluR-A$^{-/-}$=138.982, t=5.416, P=0.0000266; Wt vs SA=84.266, t=3.399, P=0.00285, SA vs GluR-A$^{-/-}$=54.717, t=2.132, P=0.0456) (Figure 45).
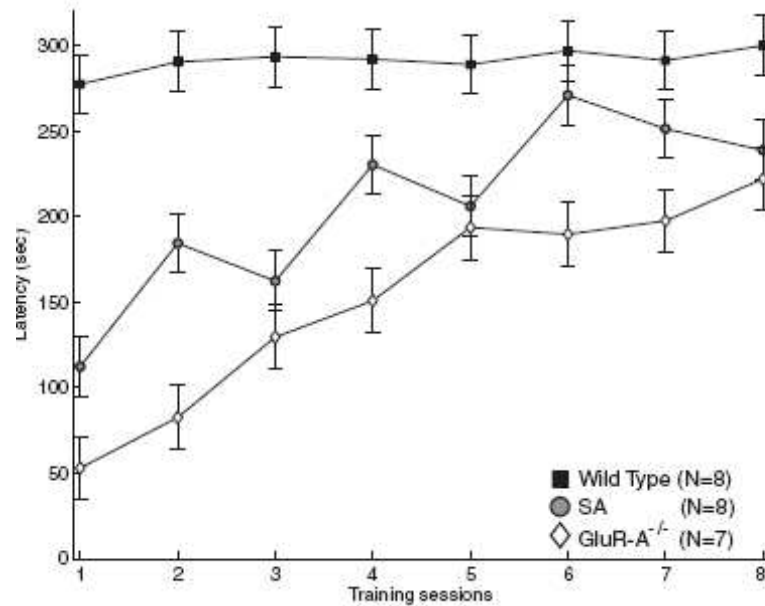
Figure 45. Motor learning performance is impaired in GluR-A mutants. Values are mean±SEM.

4.2.2.2. T-maze

GluR-A$^{-/-}$ mice started at chance level (51.786±6.818% (mean±SEM)) at the first block of the T-maze training. Although they reached their best performance on day four (62.5±6.818%), training in the task did not result in learning/performance improvements and ended with the last block at a performance level (53.571±6.818%) which was not better than chance. WT mice, however, started already over chance level with 67.188±6.378% and reached their best performance with the last block 82.031±6.378%. This test showed an over-all significance for genotypes (GluR-A$^{-/-}$=53.571±3.561% (mean±SEM), WT=75.938±3.3331%).

A Two Way Repeated Measures ANOVA (one factor repetition, general linear model) (normality test, P=0.073; equal variance test, P=0.428) showed a significant difference be-tween genotypes (Figure 46; F(2)=14.194, P<0.001). However, there was no main effect of block (F(4)=0.474, P=0.754) or group by block interaction (F(8)=1.629, P=0.130). Pairwise multiple comparisons (Holm-Sidak method) showed a significant difference for WT versus GluR-A$^{-/-}$ and WT versus SA but not for SA versus GluR-A$^{-/-}$ (WT=75.938±3.44%, SA=52.857±3.678%, GluR-A$^{-/-}$=53.594±3.44%), (difference of means: WT vs GluR-A$^{-/-}$ =22.344, t=4.593, P=0.000176; WT vs SA=23.08, t=4.583, P=0.00018; GluR-A$^{-/-}$ vs SA=0.737, t=0.146, P=0.885).
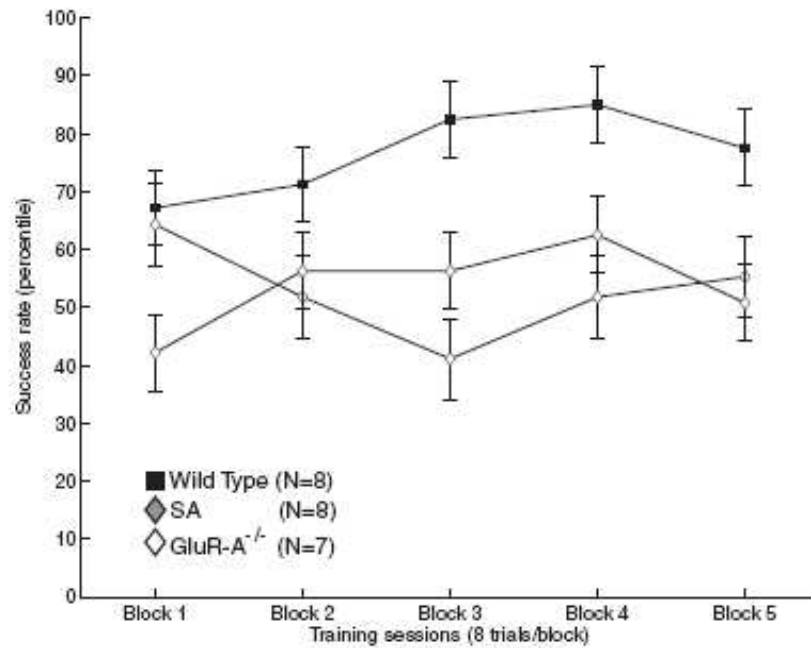
Figure 46. In SA mice the working memory impairment seen in GluR-A$^{-/-}$ is not rescued. Values are mean±SEM.

4.2.2.3. Spontaneous alternation

In order to exclude the possibility that the difference in the rewarded alternation (T-maze) task is due to the fact that the animals have preference to enter the same arm where they got a reward in the previous run, mice where tested in a spontaneous non rewarded alternation task on the elevated T-maze. Animals received ten consecutive trials on a T-maze. In the first and second run they were allowed to choose the arm freely. These results confirmed the previous finding in the rewarded task, which is impairment for GluR-A$^{-/-}$ mice (35.714±5.084% (% of correct choice), (mean±SEM)) and SA (31.429±4.809%) animals in comparison to WT mice (78.750±5.154).

Data distribution passed the normality test (P=0.141) and the equal variance test (P=0.556). One way repeated measures analysis of variance revealed a significant effect (Figure 47; $F_{(2)}$=30.273, P=<0.001). Hence, pairwise multiple comparisons (Holm-Sidak Method) was conducted, which discovered a difference between WT and GluR-A$^{-/-}$ mice (difference of means=42.857, t=6.396, P=0.000342) and between WT and SA animals (difference of means=47.143, t=7.036, P=0.0000136). There was not a significant difference between GluR-A$^{-/-}$ versus SA (difference of means=4.286, t=0.603, P=0.558).
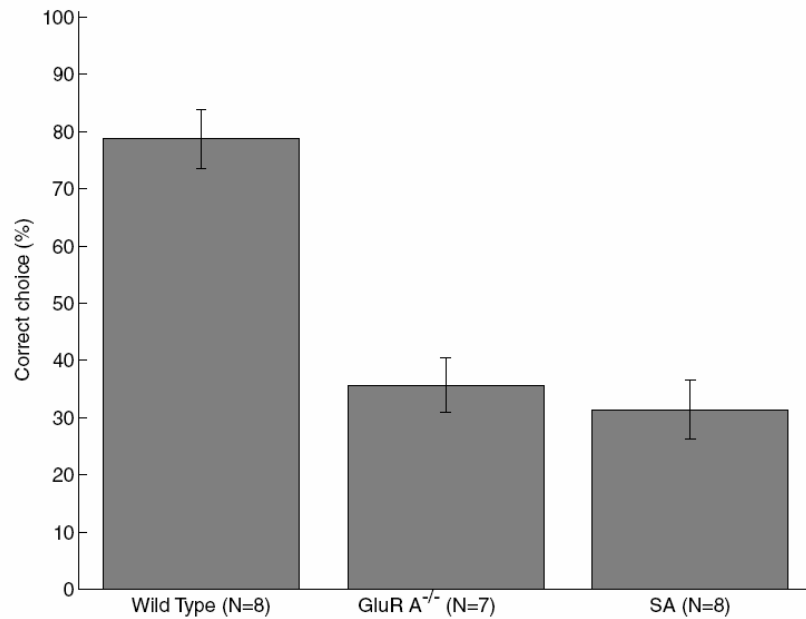
Figure 47. Number of successful alternations in the spontaneous alternation task differed across genotypes in a way that mutant animals were impaired compared to WT mice. Values are mean±SEM.

4.2.3. WT | GluR-B$^{\Delta Fb}$

4.2.3.1. T-maze

I quantified the role of GluR-B containing AMPA receptors in spatial working memory using the T-maze task.

The two groups, namely animals missing GluR-B containing AMPA receptors from the forebrain and WT mice, significantly differed from each other in terms of their overall performance in the task (Figure 48; F(4)=2.814; P<0.03; Two Way Repeated Measures ANOVA; Normality test, P=0.221 and equal variance test, P=0.309), despite the two groups had started the test with statistically similar success rates (difference of means=12.5, t=1.734, P=0.087; Holm-Sidak pairwise comparison). The first difference between the two groups was observed at the third block when WT mice reached to a success level of 82.5%±4.6 (mean±SEM) and GluR-B$^{\Delta Fb}$ mice still performed at chance level (51.3%±4.6) (difference of means=20, t=2.775, P=0.007). Although the GluR-B$^{\Delta Fb}$ mice performed worse than the group of WT animals on the next session (51.25±4.64 vs 85±4.6; difference of means=33.75, T=4.683, P<0.001), the two groups' success rates were not statistically different at the end of the training (66.25±4.64 vs 77.5±4.6; difference of means=11.25, t=1.561, P<0.122), although GluR-B$^{\Delta Fb}$ were still worse at performing the task.
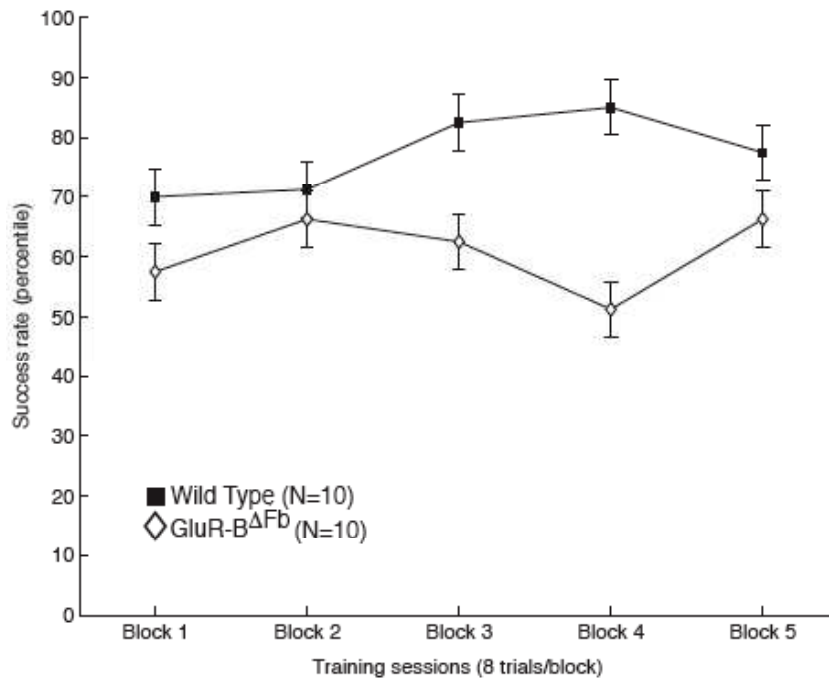
Figure 48. Spatial working memory performance on the T-maze is impaired after deletion of the GluR-B subunit. Values are mean±SEM.

4.2.3.2. Y-maze

As in the hippocampus dependent spatial working memory task, see above, GluR-B$^{\Delta Fb}$ mice showed an impairment in the Y-maze, a spatial reference memory task (Figure 49; $F(11)=2.426$; $P=0.007$; Two Way Repeated Measures ANOVA (balanced design); normality test=0.062 and equal variance test, $P<0.05$).

The two groups started the task with similar performances (difference of means=0.3, $t=0.3$, $P=0.690$; Holm-Sidak pairwise comparison). WT mice increased their performance and learned the task by the fourth session (session 1 vs session 4; difference of means=1.9, $t=3.454$, $P=0.001$). GluR-B$^{\Delta Fb}$ mice, however, took an additional 3 days and reached the statistical level of learning on session 7 (session 1 vs session 7; difference of means=2.3, $t=4.181$, $P<0.001$).

The difference between the two groups first started on the 5th session (difference of means=2.6, $t=3.468$, $P=0.001$) and continued until the 9th session (difference of means=, $t=1.334$, $P=0.187$). After the 9th session, GluR-B$^{\Delta Fb}$ mice had a tendency to under achieve in the task, however this trend did not reach statistical difference ($P>0.187$).
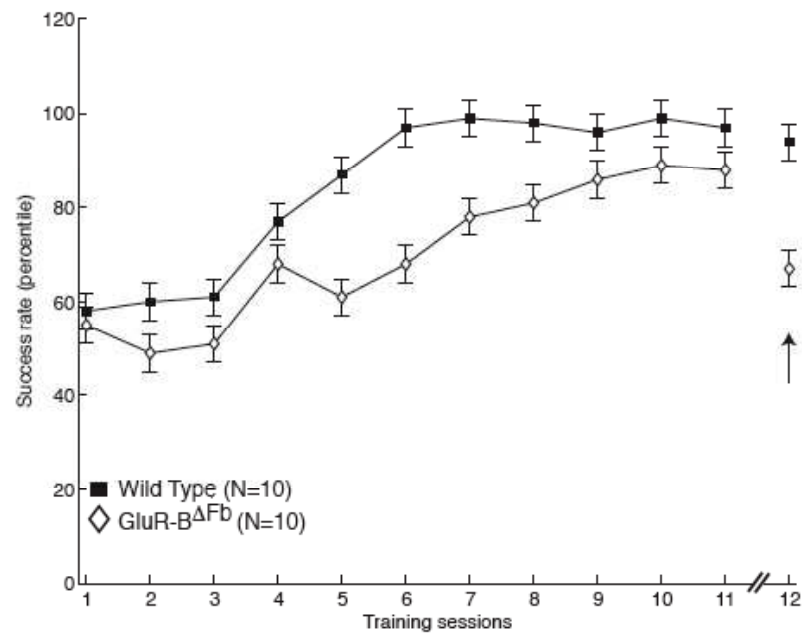
Figure 49. Spatial reference memory performance on the T-maze is impaired after deletion of the GluR-B subunit. Arrow shows the session with restricted sensory cues (see text below). Values are mean±SEM.

Before session 12 started, a curtain was placed around the Y-maze to reduce the spatial cues. When animals were run with this "reduced cues" conditions, the two groups, once more, showed a difference (difference of means=2.7, t=3.601, P=0.001). Success rate of the GluR-B$^{\Delta Fb}$ mice significantly dropped compared to the previous the session (difference of means=2.1, t=3.817, P<0.001), although WT mice had comparable success rate in respect to the session #11 (difference of means=0.3, t=0.545, P<0.586).

4.2.4. WT | GluR-A$^{-/-}$/B$^{\Delta Fb}$

4.2.4.1. T-maze

WT mice did perform better compared to the GluR-A$^{-/-}$/B$^{\Delta Fb}$ mice throughout the training (Figure 50). WT mice started the training already above chance level. GluR-A$^{-/-}$/B$^{\Delta Fb}$ animals, on the other hand, started the training with a success rate equal to chance level and continued performing the task at the chance level throughout the entire period of testing. None of the groups improved significantly during the test phase.

A Two Way Repeated Measures ANOVA (one factor repetition, general linear model) (normality test, P=0.248; equal variance test, P=0.538) showed a significant difference between genotypes (F(1)=21.044, P<0.001), but no main effect of block (F(4)=1.082, P=0.375) or group by block interaction (F(4)=0.586, P=0.674). GluR-A$^{-/-}$/B$^{\Delta Fb}$ mice started at the

chance level (51.786 ± 6.818% (mean ± SEM)), reached the best performance on day four (62.5±6.818%) and ended with the last block at a performance level (53.571 ± 6.818%), which was not better than the chance level. WT mice started already over chance level with 67.188±6.378% and reached their best performance with the last block 82.031±6.378%. This test showed an overall significance for genotypes (means for genotypes: GluR-A$^{-/-}$/B$^{\Delta Fb}$=053.571±3.561% (mean±SEM), WT=75.938±3.3331%). Pairwise multiple comparisons (Holm-Sidak method) showed as well that the difference observed between the genotypes is statistically significant (difference of means=22.366, t=4.587, P<0.001).
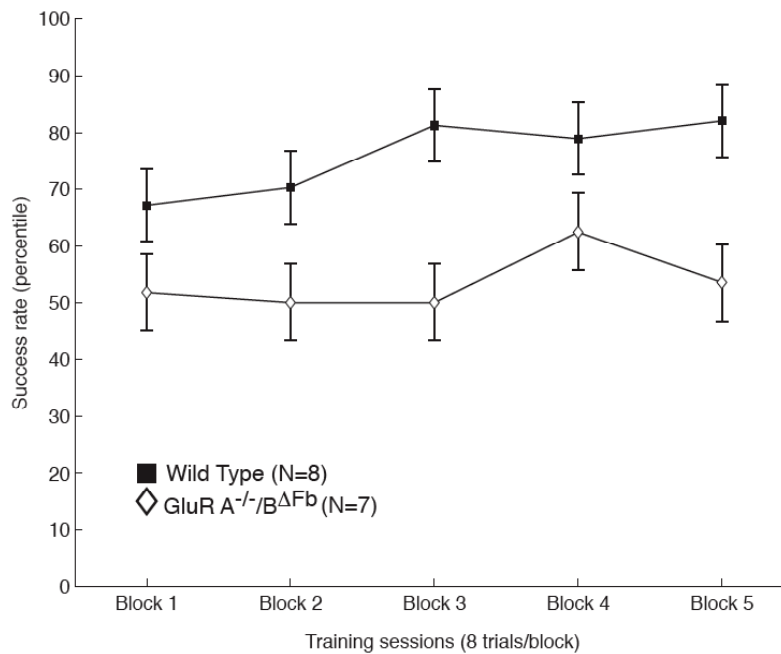
Figure 50. Working memory performance on the T-maze is impaired in mice with a double knock-out of GluR-A/B subunits. Values are mean±SEM.

4.2.4.2. Y-maze

In this paradigm, mice were trained to choose a target arm at a constant location with respect to spatial cues in the environment (see Materials and Methods). This task requires animals to use allocentric spatial information to locate the target arm. Hippocampal lesions alter this form of learning (Reisel et al, 2002; Schmitt et al, 2005).

GluR-A$^{-/-}$/B$^{\Delta Fb}$ started their performance at chance level (52.86±4.36%; (mean±SEM)) and showed the first significant improvement at the training block number seven (71.43±4.36%), (1 vs 7 difference of means=3, t=4.867, P=0). GluR-A$^{-/-}$/B$^{\Delta Fb}$ completed their training with a performance of 90±4.36%, which did not significantly differ from day seven (7 vs 10 diff of mean=0.714, t=1.159, P=0.249). WT mice in contrast began already higher than chance level (58±3.65%). Although they were not significantly different from GluR-A$^{-/-}$

/B$^{\Delta Fb}$ mice at the start, they displayed a significant learning effect already from day four on (77±3.65%) and acquired the task to an extent that they reached a performance level of 99%±3.65. Their first day of learning differs significantly from the last day of performance (difference of means=2.2, t=4.266, P=0.002). WT and GluR-A$^{-/-}$/B$^{\Delta Fb}$ mice acquired the task to a comparable extend until the last day (Figure 51). This shows that GluR-A$^{-/-}$/B$^{\Delta Fb}$ start to learn later, but once they learn, they reach to success rates statistically comparable to the performance of WT animals.
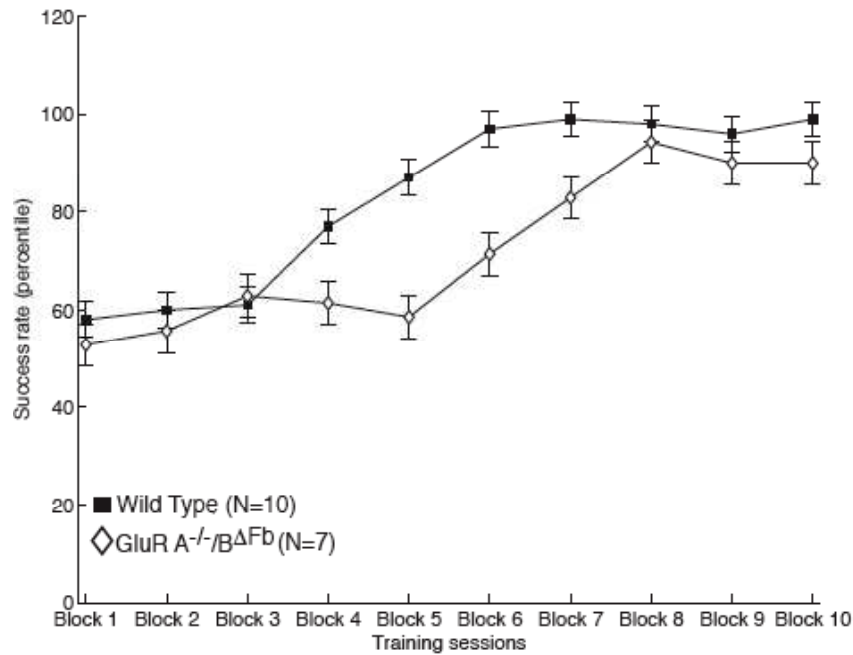
Figure 51. Acquisition of spatial reference memory is impaired after deletion of GluR-A/B AMPA receptor subunits. Values are mean±SEM.

A Two Way Repeated Measures ANOVA (one factor repetition, general linear model) (normality test, P=0.054; equal variance test, P=0.234) showed a significant difference between genotypes (F(1)=6.602, P=0.021), a main effect of block (F(9)=31.768, P<0.001) and group by block interaction (F(9)=3.061, P=0.002). Pairwise multiple comparisons (Holm-Sidak method) were conducted. This test showed a significance for genotypes (means for genotypes: GluR-A$^{-/-}$/B$^{\Delta Fb}$=72±3.34% (mean±SEM), WT=83.2±2.8%) (difference of means: Wt vs GluR-A$^{-/-}$/B$^{\Delta Fb}$=11.2, t=2.569, P=0.0214). The comparison for the groups within blocks discovered a significant difference for the fourth to seventh block (difference of means>1.557, t>0.028, P<0.028). These results indicate that GluR-A$^{-/-}$/B$^{\Delta Fb}$ mice are able to learn the task, but take three days longer to display a learning effect on the Y-maze.

4.2.5. WT | Homer 1a

4.2.5.1. T-maze

Mice have a natural tendency to visit previously unexplored areas. In this task, such innate behaviour translates as spontaneous alternation behaviour. Indeed, both WT and Homer1a mice performed the task better than chance level (50%) already during the first block (Chi-square, P<0.001; WT=76±6%; Homer1a=65±5%). The two genotypes did not differ from each other in this phase of the training (unpaired T-test, P=0.14; Figure 52). Training in the task for 5 sessions resulted in improved performance (Two Way Repeated ANOVA, $F_{(1,19)}$=21.205, P<0.001) of the WT mice (93±2%; paired T-test, P<0.05). Homer1a mice, however, did not improve in the T-maze task and concluded the training at the same success level it had started with (71±5%; paired T-test, P=0.27). At the end of the training, WT mice were significantly better than Homer1a mice (unpaired T-test, P<0.005) indicating that Homer1a expression impairs acquisition of spatial working memory on the T-maze.
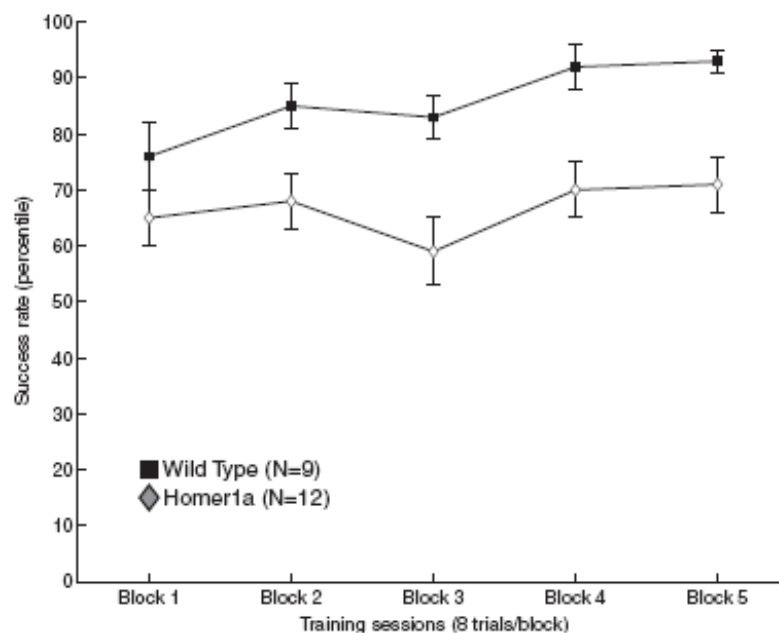
Figure 52. Sustained expression of Homer1a impairs spatial working memory on the T-maze. Values are mean±SEM.

4.2.5.2. Y-maze

Sustained over expression of the Homer1a had overall no effect on the spatial reference memory. A Two Way (genotype by session interaction) repeated measures ANOVA showed that although the two genotypes did not differ from each other (F(1)=1.692,

P=209; Normality Test, P=0.099 and equal variance test, P<0.05), the success rate in the task significantly modulated by experience (Figure 53; F(8)=30.423, P<0.001).

In order to discover when animals in each group learned the tasks, multiple comparisons (Holm-Sidak method) between training sessions within each group was performed. Analysis showed that for both groups learning occurred on the 5th day (WT; difference of means=21.1, t=3.527, P=0.01 and Homer1a; difference of means=20, t=3.858, P<0.001). After the 5th session, neither group showed any improvement in their performance (session 5 vs session 9: WT; difference of means=5.6, t=0.928, P=0.355 and Homer1a; difference of means=20, t=3.858, P<0.017 (Critical P=0.004 after being corrected for multiple comparisons)), suggesting that they reached the asymptotic level of performance already on the 5th day (Figure 53).
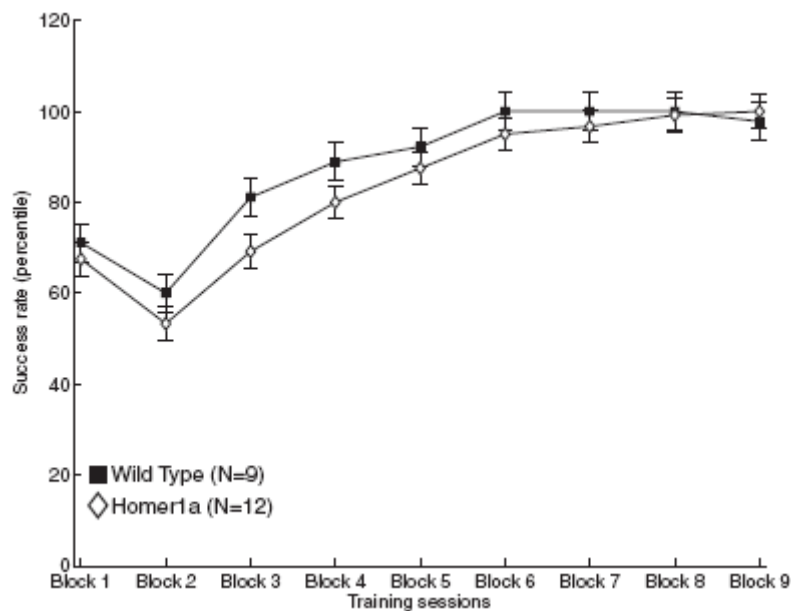
Figure 53. Sustained over expression of Homer1a does not interfere with the acquisition of spatial reference memory. Values are mean±SEM.

Homer1a is an immediate early gene and immediate early genes are believed to be involved in long-term storage of behavioral memories. Therefore, I further retested the two groups in the Y-maze after 5 weeks of no training.

Both groups had impaired levels of success compared to the last block of the acquisition training (WT=100±0% vs 78±7%; Homer =100±0% vs 70±8%; paired T-test, P<0.05). Similar to the acquisition phase of the training during this long-term retrieval there was no difference between the two genotypes' performance levels (F(1)=0.265, P=0.621). However there was significant session effect (F(4)=12.112, P=<0.001) supporting the

conclusion that after 5 weeks of no training both groups forgot the task, though they regained it during the 5th sessions long retesting.

After animals reached to the asymptotic level of success rate during the retrieval phase, to control for the use of spatial cues to solve the task, I first placed a curtain around the Y-maze, then placed the Y-maze in an entirely new room with new spatial cues and retested both groups. Homer1a did not differ from the WT mice, neither after curtain placement (difference of means=10, $t=1.336$, $P=0.194$), nor in the new room (difference of means=2; $t=0.267$, $P=0.792$), although being run in a new room impaired both groups' performance significantly (WT; difference of means=60, $t=7.725$, $P<0.001$ and Homer; difference of means=62, $t=7.982$, $P<0.001$).

5. Discussion

This thesis aimed at studying molecular mechanisms of hippocampal function. Doing so not only required administering a large number of behavioral paradigms covering the wide range of behavioral functions associated with hippocampal formation, but also necessitated breeding lines of genetically engineered animals. I have used >10 behavioral paradigms to study 8 distinct genotypes. These experiments showed that glutamatergic excitatory neurotransmission has a critical role in the expression of the emotional responses, emotional and motor learning as well as spatial working and reference memory. Principal conclusions from the experiments are:

5.1. Sensory-motor coordination does not require interaction with the PDZ domain, but might involve phosphorylation of GluR-A

Experiments measuring sensory-motor coordination showed that deletion of the GluR-A containing AMPA receptors (GluR-A$^{-/-}$) results in an impairment in motor coordination, as tested in the initial phase of the rotarod task (Figure 54). Expression of this deficit in the GluR-A$^{-/-}$ mice did not result in a reduction of the spontaneous exploration, as studied in the open field and swimming tasks (Figure 54).

The stimulus to act upon, coding sensory information and the phases of decision-making lead to the execution of a movement. During this process, cortical and subcortical areas become active before they finally activate or inhibit the motor neurons of the spinal cord (no GluR-A in the spinal cord). The sensory feedback, whose transfer is controlled actively, is important for the success of most of the movements.

Motor cortices send corticospinal projections originated from primary and secondary motor cortices. Primary motor cortical projections are involved in execution, secondary projections contribute mainly in planning and initiation of movements (Kandel et al, 2000; Schmidt and Schaible, 2006). All motor cortices project into the subcortical areas and the spinal cord. Most of the projections end in the supra spinal areas which are among others basal ganglia and thalamus.

Basal ganglia get their input from cerebral cortex and project via the thalamus back to it. The location for the input is the striatum. The exit nuclei, namely globus pallidus, pars interna and substantia nigra, pars reticulata, send their inhibitory projections to the thalamus, which in turn sends excitatory projections to the four motor cortices and the prefrontal cortex. Considering the negative feed-forward control of these exit nuclei, it is suggested that they

control the thalamocortical transmission. The activity of the exit nuclei is controlled by the striatum via the direct and the indirect pathway. The direct pathway is the inhibitory projection from the striatum onto globus pallidus, pars interna and the substantia nigra, pars reticulata (primary transmitter: GABA, cotransmitter: subtance P). The indirect pathway consists out of three series of connected systems. It starts with the inhibitory projections of the striatum to the globus pallidus, pars externer (primary transmitter: GABA, cotransmitter: enkephalin). Latter inhibits nucleus subthalamicus (transmitter: GABA), which inhibits globus pallidus, pars interna and substantia nigra, pars reticulata (transmitter: glutamate). The indirect projection pathway inhibits the thalamocortical transmission. Hyperkinetic motor impairment is a result of reduced inhibition of the thalamocortical transmission. Unintended activation of motor programs leads to disturbances, which enter the normal movement uncontrolled (like in Chorea Huntington).

The cerebellum plays an important role in planning, execution and control of movements (Kandel et al, 2000; Schmidt and Schaible, 2006). It regulates the coordination of the directed motility and the postural motor system and the fine tuning of movement by coordinating the precise spatiotemporal exertion of muscles. Its activity is shown to be important for motor learning, stabilizing of the posture and balance as well as the control of eye movement. The cerebellum compares the afferent feedback with the planned movement and calculates signals for the correction in order to optimize the movement. Axons and neurons of the brain stem and the spinal cord transfer information out of the periphery, different sense systems (vestibular, visual, acoustic) and out of the cerebral cortex. Others help to measure the correct procedure of the planned movement. The purkinje cells are the only area where efferent connections are going out of the cerebellum. Their signals are inhibitory. The motor learning is impaired after lesion of the cerebellum. The preservation and adaptation of acquired movements and the creation of new strategies of movement (motor learning) is one of the main functions of the cerebellum.

In the case of AMPA subunit GluR-A alterations the motor cortices and basal ganglia, which lie in the forebrain, are more likely to be involved in impaired motor coordination as it occurs in SA and GluR-A$^{-/-}$ mice, than the cerebellum. In the accelerating rotarod task, carried out with an extensive training schedule, they both improve their performance over time. Mice with a mutated GluR-A subunit at the phosphorylation sites S831 and S845 do start better from the beginning and keep that until the end even though if one compares only genotypes within days, a statistically significant difference between these two genotypes is only seen on day two. SA mice reach a level of insignificant difference on day four where as

GluR-A$^{-/-}$ mice reach that level on day eight. Because of the ceiling effect WT mice do not have the chance to improve. Nonetheless this test showed that GluR-A$^{-/-}$ mice and SA mice have an impaired motor coordination (Figure 45), but are still capable of motor learning (Figure 45). This implicates that GluR-A and its phosphorylation sites are important for the function of motor coordination. The fact that SA mice do perform better than GluR-A$^{-/-}$ mice could be a hint that the expression of the GluR-A subunit without phosphorylation sites could already support motor learning or the maintenance of acquired movements. TG mice on the other hand are comparable to WT mice from the initial phase of the rotarod task on, which suggests that the transgene expressed in these mice can rescue the motor coordination impairment. Although the transgene is also expressed in the cerebellum it is highly unlikely that this fact contributes to the rescue because there dominate GluR-B/C heteromeres and because of the earlier mentioned role of the cerebellum (see above).

The fact that SA and GluR-A mice are both hyperactive in the open field (Figure 54, for SA data not shown), but TG mice are not, supports the hypothesis that the indirect pathway is inhibited in SA and GluR-A$^{-/-}$ mice, which causes the sensory-motor impairment. The transgene in the TG mice is expressed all over the brain, that is why it can not be excluded that brain regions like the mesencephalon or the pons play a role in the rescue seen in this mice. Mesencephalon and pons send signals to the spinal generator of locomotion. Locomotion is a rhythmic walking. It is a coordinated operation where spinal reflex, posture and descendent control work together. It is organized by the spinal generator of locomotion.

The anatomical pathways of the sensory-motor impairment observed in the current study remain to be shown. This could be supported by testing mice expressing the GluR-A subunit with the mutated phosphorylation sides in a GluR-A$^{-/-}$ background also in other brain regions.

5.2. Lack of GluR-A containing AMPA receptors results in hyperactivity

Measurement of mobility on the behavioral tasks administered on land (i.e. open field) or in water (i.e. 1st day of the forced swimming test) showed that GluR-A containing AMPA receptors have a critical role in determining the degree of motor execution during spontaneous exploration. GluR-A$^{-/-}$ mice were hyperactive in all exploration tasks (including open field test and forced swimming task) conducted. Molecular mechanisms responsible for the regulation of the motor execution seem to differ across land (i.e. walking) and water (i.e. swimming) tasks. In the forced swimming task, the hyperactivity associated with GluR-A deletion persists even after the expression of a transgene with a point mutation in the PDZ

interaction domain. Hyperactivity associated with lack of GluR-A or inability to bind PSD95 is rescued, if a copy of the native GluR-A subunit is expressed (Figure 54). These results identify the PSD interaction and/or amount of GluR-A containing AMPA receptors as a mechanism for glutamate dependent modulation of the exploration in the swim task.

Regulation of the motor execution to explore of an open field, however, does not require PSD binding. Hyperactivity in the GluR-A$^{-/-}$ is abolished after expressing GluR-A with a point mutation in the PDZ interaction domain. Although the hyperactivity persists after the native GluR-A subunit is transgenically expressed, a conclusion about the role of PDZ domain interaction in regulation of the motor exploration in the open field is premature. This is mainly because of the weaker transgene expression in A1.1 mice compared to TG animals.
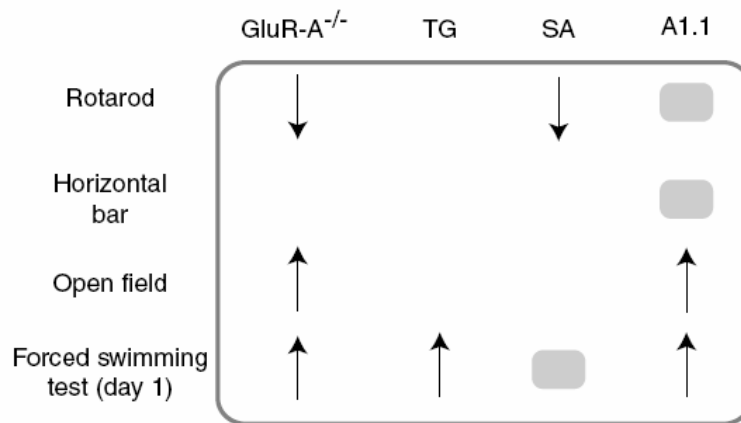
Figure 54. Summary of the findings of the tasks measuring sensory-motor coordination and motor abilities. Genotypes studied: GluR-A$^{-/-}$, TG, SA and A1.1. Downward arrows depict impaired performance compared to WT controls. Grey squares signify lack of data from a particular genotype in the behavioral task of interest.

Because of the different integration sites of the transgenes there are several uncontrollable factors which need to be taken in account while thinking about further experiments building up on these discoveries. The tTA system as a tool for controlling time and location of expression is based on the fact that the promoter that drives the tTA transgene, is only expressed in the neocortex of the brain. This is also very useful, because a rescue of the behavioral phenotype of GluR-A$^{-/-}$ mice (which is a global knockout) by the expression of a GluR-A transgene can help to locate the brain regions responsible for the behavioral impairment. The different integration sites of the GFP-GluR-A fusion proteins resulted in different expression patterns and different expression levels. This shows that there are uncontrollable factors, which influence the expression (time and location) of these genes

depending on, for example, if the genomic region they are integrated is normally strongly expressed. It also depends on the number of copies, which are integrated. Furthermore, the transgene could also be integrated into genes, which help to regulate the activity of an animal. For example the increased mobility of the TG mice after facing a stressor could also be a result of the integration site and not only result from the mutation at the PDZ interaction domain or the expression pattern. A next step, in order to find out the role of the different mutations in the GluR-A subunit, one could try to create mice, which carry the differentially mutated GluR-A subunits at the same location of the genome. This would result in homogeneous expression levels and patterns and could also exclude different behaviors caused by different disturbance of genes.

5.3. GluR-A deletion does not alter affective behavior

Hyperactivity quantified in the open field and forced swimming test was not due to changes in the affective state/behaviors of the GluR-A$^{-/-}$ mice. In this study, the level of anxiety is studied in several tasks, including neophobia, succesive alleys, black-white-alley and light-dark-box. In the majority of these studies GluR-A$^{-/-}$ mice behaved statistically similar to the WT mice (Figure 55). Exceptions to the similarity between WT and GluR-A$^{-/-}$ existed only in the light-dark-box where animals displayed less anxiety and readily entered the brightly colored arena WT mice hesitate to enter. The discrepancy between the light-dark-box and other test could be explained by the increased mobility (i.e. hyperactivity) of the GluR-A$^{-/-}$ mice as shown in the open field test and forced swimming test (Figure 54-55).

## 5.4. GluR-A deletion impairs "emotional learning"

When animals (like humans) are faced with emotionally challenging situations they learn from their experience and modify their behavior next time they are in a similar position to the one they experienced. This context dependent expression of learned behavior includes hippocampal activity, not only because ventral hippocampus takes a role in the modulation of anxiety related responses, but also the ventral hippocampus is enriched with receptors for hormones released in response to stress. Therefore, it is widely supported that stress-induced modifications in the hippocampal circuitry mediate memory storage associated with uncontrollable events happening in life (Kim and Yoon, 1998; Son et al, 2006; Kim et al, 2006).

In this study, the mechanism of this "emotional learning" was studied in the forced (Porsolt) swimming test. The swimming task creates an experience (i.e. forced swimming) as

an <u>uncontrollable</u> event happening at a time <u>unpredictable</u> to the animal under <u>inescapable</u> conditions. When WT mice are put back in the forced swimming test apparatus 24 h after their first forced swimming experience, they display learned-helplessness, as they become immobilized earlier and stay immobile longer. The learning component in this task allows animals to economically manage their mobility in the environment and escape a probable fatigue-induced drowning before they are removed from the pool.

Deletion of the GluR-A containing AMPA receptors, as shown in this study, impairs this form of learning. GluR-A$^{-/-}$ mice become immobile significantly later than WT mice and stay immobile significantly shorter than WT mice in both sessions. Interestingly, while WT mice learn the task with one trial and reduce their latency to become immobile and increase the duration that they stay immobile, GluR-A$^{-/-}$ mice do not learn from their experience (impaired emotional learning), as shown by statistically comparable swimming and immobility patterns of the GluR-A$^{-/-}$ mice across sessions (Figure 55).

The mechanisms involved in this form of emotional learning include post-synaptic density proteins binding to GluR-A and stabilizing the AMPA receptors in the synapse. This conclusion is supported by those findings, that TG mice behave comparable to the

GluR-A$^{-/-}$ mice in both sessions of the swimming test. Unlike the motor exploration results in the open field, the extent of the transgene expression does not confound these conclusions considering that animals expressing a native version of the GluR-A do successfully learn the task even with a protein expression level significantly smaller than the level expressed in TG mice.
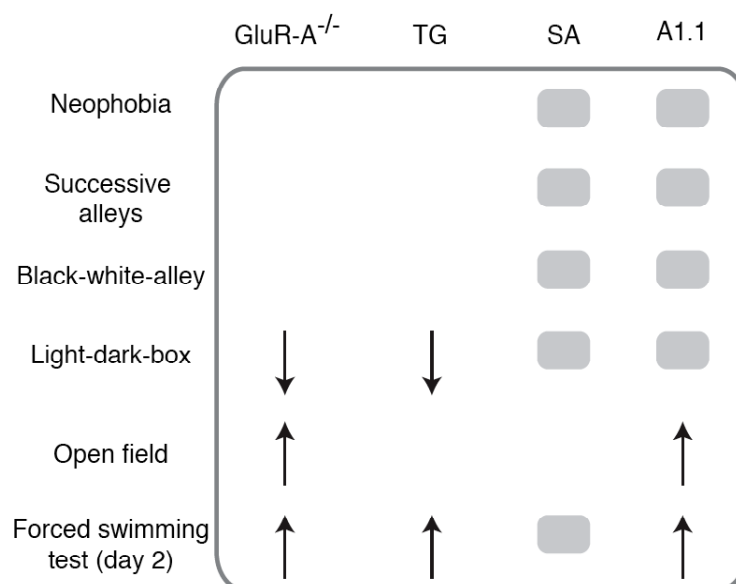
Figure 55. Summary of findings of those tasks measuring anxiety and behavioral despair. Downward arrows depict impaired performance compared to WT controls. Grey squares signify lack of data from a particular genotype in the behavioral task of interest.

5.5. GluR-A containing AMPA receptors are required for spatial working memory

One of the chief functions of hippocampus is to integrate multi-sensory information across time and contribute to act upon the changes in the environment (OKeefe and Nadel, 1978). Therefore, it is not surprising that numerous studies examined the role of hippocampal formation in encoding spatial working memory. Among these studies, Bannerman, Rawlins and their colleagues were first to show that GluR-A containing AMPA receptors are required for acquisition of spatial working memory on the T-maze (Reisel et al, 2002; Schmitt et al, 2003; Schmitt et al, 2005).

Results of the current study expand these findings and show that the way that the GluR-A containing AMPA receptors mediate the spatial working memory is through post-synaptic density protein binding and phosphorylation of the subunit by αCaMKII/PKC and/or PKA (Figure 56). These results suggest that synaptic insertion/localization of the GluR-A containing AMPA receptors is critically involved in encoding spatial working memory. The amount of the expression of the transgenes with the mutation in the TG and SA mice can not be the reason for the lack of abolishment of the GluR-A$^{-/-}$ phenotype, because it was already shown that the native GluR-A subunit expressed as a transgene in a lower amount than the gene in the TG and SA mice, can partially revert the phenotype of the GluR-A$^{-/-}$ mice (Schmitt et al. 2005).

Although this study can narrow down the kinases responsible for acquisition of spatial working memory to αCaMKII, PKC and PKA, one cannot further speculate whether all of them contribute equally to the spatial working memory. The genotype studied to question the involvement of the kinase-meditated phosphorylation in GluR-A receptor function expresses a copy of the GluR-A subunit with point mutations in the two phosphorylation sites close to the C-terminus in a GluR-A$^{-/-}$ mouse. Between these two sites, S831 is the binding site for αCaMKII and PKC and S845 is phosphorylated by PKA. Because the transgene has point mutations in both phosphorylation sites, the difference between the action of the different kinases is obscured. Further studies specifically targeting S831 and S845 individually and kinases selectively will be required to examine if there is any differential contribution to the spatial working memory across these kinases.
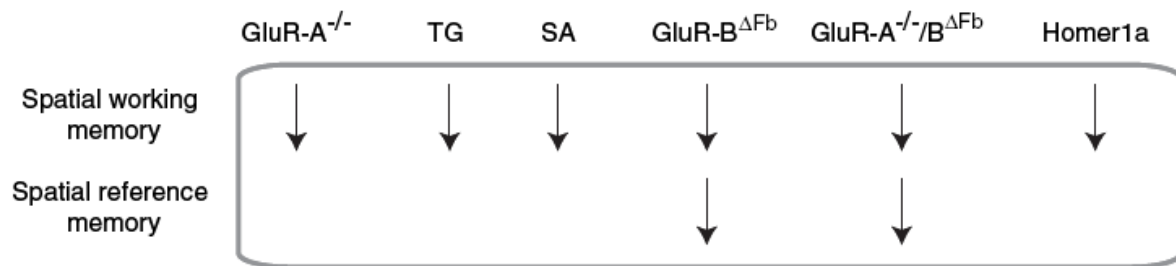
Figure 56. Summary of the findings in hippocampus dependent learning tasks. Spatial working memory is studied on the T-maze and spatial reference memory on the Y-maze. Genotypes studies include, GluR-A$^{-/-}$, TG, SA as well as GluR-B$^{\Delta Fb}$, GluR-A$^{-/-}$/B$^{\Delta Fb}$ and Homer1a (all described previously). Downward arrows depict impaired performance compared to WT controls. White areas show those comparisons where genetically engineered animals were statistically similar to the WT counterparts.

5.6. GluR-B containing AMPA receptors are required for spatial reference memory

Hippocampal formation is best known for its contribution to encoding space and is commonly referred to as the neural structure, which builds a cognitive map of the sensory world (O'Keefe and Nadel, 1978). Experimental support for hippocampus encoding space is abundant. Functional imaging studies in humans, for example, showed that London taxi drivers whose job heavily depends on spatial navigational skills have enlarged posterior hippocampi (corresponds to the dorsal hippocampus in mice) (Maguire et al, 2000). Moreover, with increasing experience in spatial navigation, the volume of the hippocampus increases, suggesting that even in adulthood hippocampus undergoes anatomical changes as a function of spatial encoding of the environment.

Molecular mechanisms of such spatial learning are unknown. The current study, however, proposes that GluR-B containing AMPA receptors are significantly involved in

acquisition of the spatial relationship in the environment and learning to associate spatial cues with sensory information. This conclusion is supported by studies performed on the Y-maze, a spatial reference memory task. In this task, animals are required to establish a "spatial map" of the environment and locate the location of food in respect to sensory cues in their immediate environment. Mice lacking GluR-A containing AMPA receptors can readily learn this task at a rate comparable to WT mice (Reisel et al, 2002 and the current study), suggesting that GluR-A containing AMPA receptors are <u>not</u> required for acquisition of this spatial reference memory paradigm. This finding is further supported by those observations that manipulations (point mutations in the PDZ interaction site and phosphorylation sites) that impair hippocampus dependent working memory do not contribute to the encoding of spatial reference memory (Figure 56).

When GluR-B containing AMPA receptors are deleted, however, the spatial reference memory as studied on the Y-maze is impaired. GluR-B$^{\Delta Fb}$ mice require significantly more training to reach an asymptotic level of performance similar to that of WT mice trained on the task. This conclusion is further supported by the identical results obtained from GluR-A$^{-/-}$/B$^{\Delta Fb}$ mice. These results support dissociation in terms of molecular mechanisms of the spatial memory: GluR-A containing AMPA receptors are selectively involved in encoding temporal features and GluR-B containing receptors take a role in encoding spatial relationships in the sensory world.

5.7. Metabotropic glutamate receptors differentially contribute to spatial memory

The majority of the studies examining the role of glutamatergic neurotransmission in behavioral function focused on ionotropic, especially AMPA and NMDA, receptors due to their rapid and prominent activation pattern. A second class of glutamate receptors, which are G-protein receptores, coupled to ion channels also operate on excitatory synapses and their activation modulate synaptic efficacy and plasticity. Therefore, it is likely that they modulate behavior (Pin et al, 1995; Conn and Pin, 1997; Manahan-Vaughan et al, 2005; Poschel et al, 2005). Here, I studied one of the metabotropic glutamate receptor associated pathway (for details of the contribution of Homer proteins to cellular function please see introduction) in terms of its contribution to spatial reference and working memory.

Constitutive neocortical expression of the Homer1a protein caused a behavioral phenotype similar to GluR-A$^{-/-}$ mice, as Homer1a mice displayed intact spatial reference memory but impaired spatial working memory. These results strongly support the conclusion that glutamatergic neural transmission carries out its function in behavior through not only

rapid excitation but also slower acting second messenger-mediated excitation in the rodent nervous system.

These results allow the conclusion that functions of the hippocampus are mediated by different molecular pathways. Phosphorylation of receptor subunits and their localization to the synapses might be two of the underlying principle of the receptors' contribution to the behavioral outcome, the regulated splicing of G-protein coupled immediate early genes might be another one.

6. Abbreviations

II-V	Layers of the entorhinal cortex
A1.1	Mice which express the GFP-tagged GluR-A subunit in the forebrain in the GluR-A knock-out background
αCaMKII	Alpha cacium/ calmodulin protein kinase II
ANOVA	Analysis of variance
AC	Association commissural pathway
AMPA	2-amino-3-(3-hydroxy-5-methylisoxazol-4-yl) propionic acid
BSA	Bovine serum albumin
Ca^{2+}	Calcium
cDNA	complementary DNA
DNA	Desoxyribonucleic acid
DG	Dentate gyrus
EC	Entorhinal cortex
EDTA	Ethylenediaminetetraacetic acid
ES cells	Embryonic stem cells
GFP	Green fluorescent protein
$GluR\text{-}A^{-/-}$	Mouse in which the GluR-A subunit is knocked out in the whole brain
$GluR\text{-}A^{-/-}/B^{\Delta Fb}$	Mouse in which the GluR-A subunit is knocked out in the whole brain and the GluR-B subunit in the forebrain
$GluR\text{-}B^{\Delta Fb}$	Mouse in which the GluR-B subunit is knocked out in the forebrain
h	hour(s)
HEPES	4-(2-hydroxyethyl)-1-piperazineethanesulfonic acid
Homer1a	Mouse in which venus-tagged Homer1a is expressed
iGluR	Ionotropic glutamate receptors
IP3R	Inositol 1,4,5-trisphosphate receptor
IQR	Inter quartile range
LEC	Lateral entorhinal cortex
LPP	Lateral perforant pathway
LTD	Long-term depression
LTP	Long-term potentiation
mGluR	Metabotropic glutamate receptors
MEC	Medial entorhinal cortex

MF	Mossy fibers
MPP	Medial perforant pathway
NMDA	N-methyl-D-aspartate
NTD	N-terminal domain
PBS	Phosphate based buffer solution
PFA	Paraformaldehyde
PKA	Protein-Kinase A
PKC	Protein-Kinase C
PLC	Phospholipase C
PP	Perforant pathway
RT	Room temperature
RyR	Ryanodine receptor
S	Serine
SA	Mouse line which expresses the GFP-tagged GluR-A subunit with point mutations at the phosphorylation sites S831 and S845 in the GluR-A knock-out background
SDS	Sodium dodecyl sulfate
SEM	Standard error of the mean
TMD	Trans-membrane domain
Sb	Subiculum
SC	Schaffer collaterals
TG	Mouse line which expresses the GFP-tagged GluR-A subunit with point a mutation at the PDZ domain in the GluR-A knock-out background
vs	Versus
WT	Wild type (control group with out the gene manipulations, which are either littermates or pure C57/BL6)

7. References

Abbott, M. L., Walsh, C. J., Storey, A. E., Stenhouse, I. J., and Harley, C. W. (1999). Hippocampal volume is related to complexity of nesting habitat in Leach's storm-petrel, a nocturnal procellariiform seabird. Brain Behav Evol *53*, 271-276.

Abe, T., Sugihara, H., Nawa, H., Shigemoto, R., Mizuno, N., and Nakanishi, S. (1992). Molecular characterization of a novel metabotropic glutamate receptor mGluR5 coupled to inositol phosphate/Ca2+ signal transduction. J Biol Chem *267*, 13361-13368.

Alonso, S. J., Castellano, M. A., Afonso, D., and Rodriguez, M. (1991). Sex differences in behavioral despair: relationships between behavioral despair and open field activity. Physiol Behav *49*, 69-72.

Amaral, D. G., and Witter, M. P. (1989). The three-dimensional organization of the hippocampal formation: a review of anatomical data. Neuroscience *31*, 571-591.

Antonawich, F. J., Melton, C. S., Wu, P., and Davis, J. N. (1997). Nesting and shredding behavior as an indicator of hippocampal ischemic damage. Brain Res *764*, 249-252.

Anwyl, R. (1999). Metabotropic glutamate receptors: electrophysiological properties and role in plasticity. Brain Research Reviews *29*, 83-120.

Bahn, S., Volk, B., and Wisden, W. (1994). Kainate receptor gene expression in the developing rat brain. J Neurosci *14*, 5525-5547.

Bannerman, D. M., Deacon, R. M., Brady, S., Bruce, A., Sprengel, R., Seeburg, P. H., and Rawlins, J. N. (2004a). A comparison of GluR-A-deficient and wild-type mice on a test battery assessing sensorimotor, affective, and cognitive behaviors. Behav Neurosci *118*, 643-647.

Bannerman, D. M., Deacon, R. M., Offen, S., Friswell, J., Grubb, M., and Rawlins, J. N. (2002). Double dissociation of function within the hippocampus: spatial memory and Neophobia. Behav Neurosci *116*, 884-901.

Bannerman, D. M., Grubb, M., Deacon, R. M., Yee, B. K., Feldon, J., and Rawlins, J. N. (2003). Ventral hippocampal lesions affect anxiety but not spatial learning. Behav Brain Res *139*, 197-213.

Bannerman, D. M., Rawlins, J. N., McHugh, S. B., Deacon, R. M., Yee, B. K., Bast, T., Zhang, W. N., Pothuizen, H. H., and Feldon, J. (2004b). Regional dissociations within the hippocampus--memory and anxiety. Neurosci Biobehav Rev *28*, 273-283.

Barria, A., Derkach, V., and Soderling, T. (1997a). Identification of the Ca2+/calmodulin-dependent protein kinase II regulatory phosphorylation site in the alpha-amino-3-hydroxyl-5-methyl-4-isoxazole-propionate-type glutamate receptor. J Biol Chem *272*, 32727-32730.

Barria, A., Muller, D., Derkach, V., Griffith, L. C., and Soderling, T. R. (1997b). Regulatory phosphorylation of AMPA-type glutamate receptors by CaM-KII during long-term potentiation. Science *276*, 2042-2045.

Bettler, B., Boulter, J., Hermans-Borgmeyer, I., O'Shea-Greenfield, A., Deneris, E. S., Moll, C., Borgmeyer, U., Hollmann, M., and Heinemann, S. (1990). Cloning of a novel glutamate receptor subunit, GluR5: expression in the nervous system during development. Neuron *5*, 583-595.

Black, M. D. (2005). Therapeutic potential of positive AMPA modulators and their relationship to AMPA receptor subunits. A review of preclinical data. Psychopharmacology (Berl) *179*, 154-163.

Boulter, J., Hollmann, M., O'Shea-Greenfield, A., Hartley, M., Deneris, E., Maron, C., and Heinemann, S. (1990). Molecular cloning and functional expression of glutamate receptor subunit genes. Science *249*, 1033-1037.

Burwell, R. D., and Amaral, D. G. (1998a). Cortical afferents of the perirhinal, postrhinal, and entorhinal cortices of the rat. J Comp Neurol *398*, 179-205.

Burwell, R. D., and Amaral, D. G. (1998b). Perirhinal and postrhinal cortices of the rat:

interconnectivity and connections with the entorhinal cortex. J Comp Neurol *391*, 293-321.

Carvalho, A. L., Duarte, C. B., and Carvalho, A. P. (2000). Regulation of AMPA receptors by phosphorylation. Neurochem Res *25*, 1245-1255.

Catania, M. V., Bellomo, M., Giuffrida, R., Giuffrida, R., Stella, A. M., and Albanese, V. (1998). AMPA receptor subunits are differentially expressed in parvalbumin- and calretinin-positive neurons of the rat hippocampus. Eur J Neurosci *10*, 3479-3490.

Celikel, T., Marx, V., Zivkovic, A., Hasan, M. T., Licznerski, P., Osten, P., Rozov, A., Seeburg, P. H., and Schwarz, M. K. (submitted). Sustained Homer1a expression imprais LTP, spatial working memory but not spatial reference memory.

Chenu, F., Guiard, B. P., Bourin, M., and Gardier, A. M. (2006). Antidepressant-like activity of selective serotonin reuptake inhibitors combined with a NK1 receptor antagonist in the mouse forced swimming test. Behav Brain Res *172*, 256-263.

Colledge, M., Snyder, E. M., Crozier, R. A., Soderling, J. A., Jin, Y., Langeberg, L. K., Lu, H., Bear, M. F., and Scott, J. D. (2003). Ubiquitination regulates PSD-95 degradation and AMPA receptor surface expression. Neuron *40*, 595-607.

Cryan, J. F., and Holmes, A. (2005). The ascent of mouse: advances in modelling human depression and anxiety. Nat Rev Drug Discov *4*, 775-790.

Cryan, J. F., Valentino, R. J., and Lucki, I. (2005). Assessing substrates underlying the behavioral effects of antidepressants using the modified rat forced swimming test. Neurosci Biobehav Rev *29*, 547-569.

Deacon, R. M., Bannerman, D. M., Kirby, B. P., Croucher, A., and Rawlins, J. N. (2002). Effects of cytotoxic hippocampal lesions in mice on a cognitive test battery. Behav Brain Res *133*, 57-68.

do-Rego, J.-C., Viana, A. F., Le Maitre, E., Deniel, A., Rates, S. M. K., Leroux-Nicollet, I., and Costentin, J. (2006). Comparisons between anxiety tests for selection of anxious and non

anxious mice. Behavioural Brain Research *169*, 282-288.

Dolorfo, C. L., and Amaral, D. G. (1998a). Entorhinal cortex of the rat: organization of intrinsic connections. J Comp Neurol *398*, 49-82.

Dolorfo, C. L., and Amaral, D. G. (1998b). Entorhinal cortex of the rat: topographic organization of the cells of origin of the perforant path projection to the dentate gyrus. J Comp Neurol *398*, 25-48.

El-Husseini Ael, D., Schnell, E., Dakoji, S., Sweeney, N., Zhou, Q., Prange, O., Gauthier-Campbell, C., Aguilera-Moreno, A., Nicoll, R. A., and Bredt, D. S. (2002). Synaptic strength regulated by palmitate cycling on PSD-95. Cell *108*, 849-863.

Esteban, J. A. (2003). AMPA receptor trafficking: a road map for synaptic plasticity. Mol Interv *3*, 375-385.

Esteban, J. A., Shi, S. H., Wilson, C., Nuriya, M., Huganir, R. L., and Malinow, R. (2003). PKA phosphorylation of AMPA receptor subunits controls synaptic trafficking underlying plasticity. Nat Neurosci *6*, 136-143.

Good, M., and Honey, R. C. (1997). Dissociable effects of selective lesions to hippocampal subsystems on exploratory behavior, contextual learning, and spatial learning. Behav Neurosci *111*, 487-493.

Gossen, M., and Bujard, H. (1993). Anhydrotetracycline, a novel effector for tetracycline controlled gene expression systems in eukaryotic cells. Nucleic Acids Res *21*, 4411-4412.

Herb, A., Burnashev, N., Werner, P., Sakmann, B., Wisden, W., and Seeburg, P. H. (1992). The KA-2 subunit of excitatory amino acid receptors shows widespread expression in brain and forms ion channels with distantly related subunits. Neuron *8*, 775-785.

Hinojosa, F. R., Spricigo, L., Jr., Izidio, G. S., Bruske, G. R., Lopes, D. M., and Ramos, A. (2006). Evaluation of two genetic animal models in behavioral tests of anxiety and depression. Behav Brain Res *168*, 127-136.

Ito, M. (2001). Cerebellar long-term depression: characterization, signal transduction and functional roles. Physiol Rev *81*, 1143-95

Kandel, E.R., Schwartz, J.H., and Jessell, T.M. (2000). Principles of neural science. New York: McGraw-Hill

Katz, L. C., and Shatz, C. J. (1996). Synaptic Activity and the Construction of Cortical Circuits. Science *274*, 1133-1138.

Keinanen, K., Wisden, W., Sommer, B., Werner, P., Herb, A., Verdoorn, T. A., Sakmann, B., and Seeburg, P. H. (1990). A family of AMPA-selective glutamate receptors. Science *249*, 556-560.

Kim, E., and Sheng, M. (2004). PDZ domain proteins of synapses. Nat Rev Neurosci *5*, 771-781.

Koerner, J. F., and Cotman, C. W. (1981). Micromolar L-2-amino-4-phosphonobutyric acid selectively inhibits perforant path synapses from lateral entorhinal cortex. Brain Res *216*, 192-198.

Kristensen, P., Suzdak, P. D., and Thomsen, C. (1993). Expression pattern and pharmacology of the rat type IV metabotropic glutamate receptor. Neurosci Lett *155*, 159-162.

Kritchevsky, M., Chang, J., and Squire, L. R. (2004). Functional Amnesia: Clinical Description and Neuropsychological Profile of 10 Cases. Learn Mem *11*, 213-226.

Layer, L. E. (2003) Funktioneller Austausch der endogenen GluR-A-Untereinheit durch GluR-A-Varianten im Hippokampus der Maus, Ruprecht-Karls-Universitaet Heidelberg.

Lomeli, H., Wisden, W., Kohler, M., Keinanen, K., Sommer, B., and Seeburg, P. H. (1992). High-affinity kainate and domoate receptors in rat brain. FEBS Lett *307*, 139-143.

Mack, V. (2001) Regulation hippocampaler synaptischer Plastizitaet durch konditionale Expression der AMPA-Rezeptor Untereinheit GluR-A, Ruprecht-Karls-Universitaet,

Heidelberg.

Mack, V., Burnashev, N., Kaiser, K. M., Rozov, A., Jensen, V., Hvalby, O., Seeburg, P. H., Sakmann, B., and Sprengel, R. (2001). Conditional restoration of hippocampal synaptic potentiation in Glur-A-deficient mice. Science *292*, 2501-2504.

Maren, S., Tocco, G., Chavanne, F., Baudry, M., Thompson, R. F., and Mitchell, D. (1994). Emergence neophobia correlates with hippocampal and cortical glutamate receptor binding in rats. Behav Neural Biol *62*, 68-72.

Maren, S. (2005). Synaptic mechanisms of associative memory in the amygdala. Neuron *47*, 783-786.

Martin, L. J., Blackstone, C. D., Huganir, R. L., and Price, D. L. (1992). Cellular localization of a metabotropic glutamate receptor in rat brain. Neuron *9*, 259-270.

McHugh, S. B., Deacon, R. M., Rawlins, J. N., and Bannerman, D. M. (2004). Amygdala and ventral hippocampus contribute differentially to mechanisms of fear and anxiety. Behav Neurosci *118*, 63-78.

McNish, K. A., Gewirtz, J. C., and Davis, M. (1997). Evidence of contextual fear after lesions of the hippocampus: a disruption of freezing but not fear-potentiated startle. J Neurosci *17*, 9353-9360.

Miller, J. S., Nonneman, A. J., Kelly, K. S., Neisewander, J. L., and Isaac, W. L. (1986). Disruption of neophobia, conditioned odor aversion, and conditioned taste aversion in rats with hippocampal lesions. Behav Neural Biol *45*, 240-253.

Monyer, H., Burnashev, N., Laurie, D. J., Sakmann, B., and Seeburg, P. H. (1994). Developmental and regional expression in the rat brain and functional properties of four NMDA receptors. Neuron *12*, 529-540.

Monyer, H., Sprengel, R., Schoepfer, R., Herb, A., Higuchi, M., Lomeli, H., Burnashev, N., Sakmann, B., and Seeburg, P. H. (1992). Heteromeric NMDA receptors: molecular and

functional distinction of subtypes. Science *256*, 1217-1221.

Moser, E., Moser, M. B., and Andersen, P. (1993). Spatial learning impairment parallels the magnitude of dorsal hippocampal lesions, but is hardly present following ventral lesions. J Neurosci *13*, 3916-3925.

Moser, M. B., and Moser, E. I. (1998). Distributed encoding and retrieval of spatial memory in the hippocampus. J Neurosci *18*, 7535-7542.

Nadel, L. (1968). Dorsal and ventral hippocampal lesions and behavior. Physiol Behav *3*, 891-900.

Nase, G., Weishaupt, J., Stern, P., Singer, W., and Monyer, H. (1999). Genetic and epigenetic regulation of NMDA receptor expression in the rat visual cortex. Eur J Neurosci *11*, 4320-4326.

Nicoll, R. A., Tomita, S., and Bredt, D. S. (2006). Auxiliary Subunits Assist AMPA-Type Glutamate Receptors. Science *311*, 1253-1256.

O'Brien, R. J., Lau, L. F., and Huganir, R. L. (1998). Molecular mechanisms of glutamate receptor clustering at excitatory synapses. Curr Opin Neurobiol *8*, 364-369.

O'Keefe, J., and Nadel, L. (1978). The hippocampus as a cognitive map (London, Oxford University Press).

Passafaro, M., Piech, V., and Sheng, M. (2001). Subunit-specific temporal and spatial patterns of AMPA receptor exocytosis in hippocampal neurons. Nat Neurosci *4*, 917-926.

Petit-Demouliere, B., Chenu, F., and Bourin, M. (2005). Forced swimming test in mice: a review of antidepressant activity. Psychopharmacology (Berl) *177*, 245-255.

Petrovich, G. D., Canteras, N. S., and Swanson, L. W. (2001). Combinatorial amygdalar inputs to hippocampal domains and hypothalamic behavior systems. Brain Res Brain Res Rev *38*, 247-289.

Pin, J. P., Waeber, C., Prezeau, L., Bockaert, J., and Heinemann, S. F. (1992). Alternative splicing generates metabotropic glutamate receptors inducing different patterns of calcium release in Xenopus oocytes. Proc Natl Acad Sci U S A *89*, 10331-10335.

Poleszak, E., Wlaz, P., Szewczyk, B., Kedzierska, E., Wyska, E., Librowski, T., Szymura-Oleksiak, J., Fidecka, S., Pilc, A., and Nowak, G. (2005). Enhancement of antidepressant-like activity by joint administration of imipramine and magnesium in the forced swim test: Behavioral and pharmacokinetic studies in mice. Pharmacol Biochem Behav *81*, 524-529.

Ramboz, S., Oosting, R., Amara, D. A., Kung, H. F., Blier, P., Mendelsohn, M., Mann, J. J., Brunner, D., and Hen, R. (1998). Serotonin receptor 1A knockout: an animal model of anxiety-related disorder. Proc Natl Acad Sci U S A *95*, 14476-14481.

Raymond, J.L., Lisberger, S.G., and Mauk, M.D. (1996). The cerebellum: A neuronal learning machine. Science *272*, 1126-1131.

Redish, A. D. (2001). The hippocampal debate: are we asking the right questions? Behav Brain Res *127*, 81-98.

Reisel, D., Bannerman, D. M., Schmitt, W. B., Deacon, R. M., Flint, J., Borchardt, T., Seeburg, P. H., and Rawlins, J. N. (2002). Spatial memory dissociations in mice lacking GluR1. Nat Neurosci *5*, 868-873.

Richmond, M. A., Yee, B. K., Pouzet, B., Veenman, L., Rawlins, J. N., Feldon, J., and Bannerman, D. M. (1999). Dissociating context and space within the hippocampus: effects of complete, dorsal, and ventral excitotoxic hippocampal lesions on conditioned freezing and spatial learning. Behav Neurosci *113*, 1189-1203.

Roche, K. W., O'Brien, R. J., Mammen, A. L., Bernhardt, J., and Huganir, R. L. (1996). Characterization of multiple phosphorylation sites on the AMPA receptor GluR1 subunit. Neuron *16*, 1179-1188.

Schmidt, R.F., and Schaible, H.G. (2006). Neuro- und Sinnesphysiologie. Springer Medizin Verlag, Heidelberg.

Schmitt, W. B., Deacon, R. M., Seeburg, P. H., Rawlins, J. N., and Bannerman, D. M. (2003). A within-subjects, within-task demonstration of intact spatial reference memory and impaired spatial working memory in glutamate receptor-A-deficient mice. J Neurosci *23*, 3953-3959.

Schmitt, W. B., Sprengel, R., Mack, V., Draft, R. W., Seeburg, P. H., Deacon, R. M., Rawlins, J. N., and Bannerman, D. M. (2005). Restoration of spatial working memory by genetic rescue of GluR-A-deficient mice. Nat Neurosci *8*, 270-272.

Shi, S., Hayashi, Y., Esteban, J. A., and Malinow, R. (2001). Subunit-specific rules governing AMPA receptor trafficking to synapses in hippocampal pyramidal neurons. Cell *105*, 331-343.

Shigemoto, R., and Mizuno, N. (2000). Metabotropic glutamate receptors - immunocytochemical and in situ hybridization analysis (New York, Elsevier).

Shigemoto, R., Nakanishi, S., and Mizuno, N. (1992). Distribution of the mRNA for a metabotropic glutamate receptor (mGluR1) in the central nervous system: an in situ hybridization study in adult and developing rat. J Comp Neurol *322*, 121-135.

Shigemoto, R., Nomura, S., Ohishi, H., Sugihara, H., Nakanishi, S., and Mizuno, N. (1993). Immunohistochemical localization of a metabotropic glutamate receptor, mGluR5, in the rat brain. Neurosci Lett *163*, 53-57.

Shimshek, D. R., Jensen, V., Celikel, T., Geng, Y., Schupp, B., Bus, T., Mack, V., Marx, V., Hvalby, O., Seeburg, P. H., and Sprengel, R. (2006). Forebrain-Specific Glutamate Receptor B Deletion Impairs Spatial Memory But Not Hippocampal Field Long-Term Potentiation. J Neurosci *26*, 8428-8440.

Standaert, D. G. (1999). NMDA receptors and nitric oxide synthase. Mol Psychiatry *4*, 13-14.

Standaert, D. G., Testa, C. M., Rudolf, G. D., and Hollingsworth, Z. R. (1996). Inhibition of N-methyl-D-aspartate glutamate receptor subunit expression by antisense oligonucleotides reveals their role in striatal motor regulation. J Pharmacol Exp Ther *276*, 342-352.

Stupien, G., Florian, C., and Roullet, P. (2003). Involvement of the hippocampal CA3-region in acquisition and in memory consolidation of spatial but not in object information in mice.

Neurobiol Learn Mem *80*, 32-41.

Tanabe, Y., Nomura, A., Masu, M., Shigemoto, R., Mizuno, N., and Nakanishi, S. (1993). Signal transduction, pharmacological properties, and expression patterns of two rat metabotropic glutamate receptors, mGluR3 and mGluR4. J Neurosci *13*, 1372-1378.

Thinus-Blanc, C., Save, E., Rossi-Arnaud, C., Tozzi, A., and Ammassari-Teule, M. (1996). The differences shown by C57BL/6 and DBA/2 inbred mice in detecting spatial novelty are subserved by a different hippocampal and parietal cortex interplay. Behav Brain Res *80*, 33-40.

Thomsen, C., Kristensen, P., Mulvihill, E., Haldeman, B., and Suzdak, P. D. (1992). L-2-amino-4-phosphonobutyrate (L-AP4) is an agonist at the type IV metabotropic glutamate receptor which is negatively coupled to adenylate cyclase. Eur J Pharmacol *227*, 361-362.

Tomita, S., Nicoll, R. A., and Bredt, D. S. (2001). PDZ protein interactions regulating glutamate receptor function and plasticity. J Cell Biol *153*, F19-24.

van Groen, T., and Wyss, J. M. (1990). The connections of presubiculum and parasubiculum in the rat. Brain Res *518*, 227-243.

Wang, J. Q., Arora, A., Yang, L., Parelkar, N. K., Zhang, G., Liu, X., Choe, E. S., and Mao, L. (2005). Phosphorylation of AMPA receptors: mechanisms and synaptic plasticity. Mol Neurobiol *32*, 237-249.

Wenthold, R. J., Petralia, R. S., Blahos, J., II, and Niedzielski, A. S. (1996). Evidence for multiple AMPA receptor complexes in hippocampal CA1/CA2 neurons. J Neurosci *16*, 1982-1989.

Werner, P., Voigt, M., Keinanen, K., Wisden, W., and Seeburg, P. H. (1991). Cloning of a putative high-affinity kainate receptor expressed predominantly in hippocampal CA3 cells. Nature *351*, 742-744.

Wisden, W., and Seeburg, P. H. (1993). A complex mosaic of high-affinity kainate receptors in rat brain. J Neurosci *13*, 3582-3598.

Wisden, W., and Seeburg, P. H. (1993). Mammalian ionotropic glutamate receptors. Curr Opin Neurobiol *3*, 291-298.

Wisden, W., Seeburg, P.H., and Monyer, H. (2000). AMPA, kainate and NMDA ionotropic glutamate receptor expression - an in situ hybridization atlas, Vol 18 (New York, Elsevier).

Wood, E. R., and Dudchenko, P. A. (2003). Aging, spatial behavior and the cognitive map. Nat Neurosci *6*, 546-548.

Yakel, J. L., Vissavajjhala, P., Derkach, V. A., Brickey, D. A., and Soderling, T. R. (1995). Identification of a Ca2+/calmodulin-dependent protein kinase II regulatory phosphorylation site in non-N-methyl-D-aspartate glutamate receptors. Proc Natl Acad Sci U S A *92*, 1376-1380.

Zamanillo, D., Sprengel, R., Hvalby, O., Jensen, V., Burnashev, N., Rozov, A., Kaiser, K. M., Koster, H. J., Borchardt, T., Worley, P.*, et al.* (1999). Importance of AMPA receptors for hippocampal synaptic plasticity but not for spatial learning. Science *284*, 1805-1811.

Zhu, J. J., Esteban, J. A., Hayashi, Y., and Malinow, R. (2000). Postnatal synaptic potentiation: delivery of GluR4-containing AMPA receptors by spontaneous activity. Nat Neurosci *3*, 1098-1106.

Zola, S. M., Squire, L. R., Teng, E., Stefanacci, L., Buffalo, E. A., and Clark, R. E. (2000). Impaired recognition memory in monkeys after damage limited to the hippocampal region. J Neurosci *20*, 451-463.